

Best-In-Class Global Bumper Reinforcement Beam

by

Garret Bautista Student
Chad Hardin Student
Ben Taylor Student

Mechanical Engineering Department

California Polytechnic State University

San Luis Obispo

2009

Statement of Disclaimer

Since this project is a result of a class assignment, it has been graded and accepted as fulfillment of the course requirements. Acceptance does not imply technical accuracy or reliability. Any use of information in this report is done at the risk of the user. These risks may include catastrophic failure of the device or infringement of patent or copyright laws. California Polytechnic State University at San Luis Obispo and its staff cannot be held liable for any use or misuse of the project.

BEST-IN-CLASS GLOBAL BUMPER FINAL DESIGN REPORT

Submitted to:

American Iron and Steel Institute

Prepared by:

Garret Bautista gbautist@calpoly.edu

Chad Hardin chardin@calpoly.edu

Ben Taylor btaylor@calpoly.edu



December 4, 2009

TABLE OF CONTENTS

| | |
|--|----|
| ABSTRACT..... | 7 |
| CHAPTER 1: INTRODUCTION | 8 |
| Objectives..... | 8 |
| CHAPTER 2: BACKGROUND | 10 |
| CHAPTER 3: DESIGN DEVELOPMENT | 13 |
| Conceptual Designs..... | 13 |
| Analysis Tools..... | 15 |
| Preliminary Analysis..... | 15 |
| B-MAC 3000 - Excel spreadsheet to analyze simplified beams | 16 |
| 2-D Static FEA..... | 17 |
| 3-D Dynamic FEA..... | 18 |
| Design Plan..... | 19 |
| Selecting a Plug-n-Play Type | 20 |
| Selecting a Cross Section | 25 |
| Selecting a Cross Section Shape..... | 25 |
| Matchbooking Study | 28 |
| Selecting a Beam Material | 30 |
| Beam Impact Analysis | 31 |
| Energy Absorber..... | 32 |
| Introduction | 32 |
| Preliminary Analysis..... | 33 |
| SEA Impact Analysis | 35 |
| Advanced Impact Analysis | 36 |
| CHAPTER 4: FINAL DESIGN | 37 |
| Packaging space | 37 |
| Base Beam – B-shape..... | 38 |
| Steel Energy Absorber (SEA)..... | 39 |
| Analysis Results..... | 41 |
| CHAPTER 5: PRODUCT REALIZATION | 42 |
| CHAPTER 6: DESIGN VERIFICATION | 42 |



| | |
|------------------------------|----|
| Pendulum Impact Test | 43 |
| Pedestrian Impact Test | 46 |
| CHAPTER 7: CONCLUSIONS | 49 |
| REFERENCES | 51 |
| APPENDICES | 52 |

LIST OF FIGURES

| | |
|---|----|
| Figure 1. Package space dimensions..... | 9 |
| Figure 2. The Volkswagen Jetta (1993) has a hot stamped bumper beam. | 11 |
| Figure 3. The Ford F150 Pick-up (1996) has a cold stamped bumper beam. | 11 |
| Figure 4. The Ford Taurus/Mercury Sable (1995) has a roll formed bumper beam. | 12 |
| Figure 5. Alternative bumper designs..... | 13 |
| Figure 6. Cross section examples..... | 14 |
| Figure 7. Plug-n-Play concepts..... | 14 |
| Figure 8. 2D Static FEA cross section models and force-displacement data..... | 17 |
| Figure 9. 3-D dynamic FEA model to simulate a RCAR 40% offset test..... | 18 |
| Figure 10. Design plan layout..... | 19 |
| Figure 11. Horizontal stacking a common B-section and manufacturer reinforcements. | 20 |
| Figure 12. Comparison of normalized moment of inertia for bumpers. | 21 |
| Figure 13. Normalized moments of inertia for several Plug-n-Play designs. | 21 |
| Figure 14. Plug-n-Play force-deflection curves for an external reinforcement design. | 22 |
| Figure 15. Decision matrix for Plug-n-Play types..... | 23 |
| Figure 16. Best Plug-n-Play design: Flat plate with reinforcements..... | 24 |
| Figure 17. Various geometries for the bar attachments of the Reinforced Plate design..... | 25 |
| Figure 18. Plug-n-Play attachment shapes with normalized moments of inertia..... | 26 |
| Figure 19. Plug-n-Play attachment shapes are compared by their energy absorption..... | 26 |
| Figure 20. Decision matrix to determine the optimal Plug-n-Play shape..... | 27 |
| Figure 21. Example FEA model for matchbooking..... | 28 |
| Figure 22. Geometric parameters considered in the matchbooking study..... | 29 |
| Figure 23. Force-displacement plots at various α values | 29 |
| Figure 24. Material Trends relating to stress-strain curves..... | 30 |
| Figure 25. Uniaxial compression tests for different densities of EPP..... | 33 |
| Figure 26. Preliminary Steel Energy Absorber design for SEA “Susie”. | 34 |
| Figure 27. Static 3-D FEA test comparison of beam with and without SEA..... | 34 |
| Figure 28. 3D dynamic impact of SEA prototypes provided acceleration data of the leg..... | 35 |
| Figure 29. FEA acceleration results of a successful SEA design..... | 36 |
| Figure 30. Final beam designs for Chinese, North American, and European markets..... | 37 |
| Figure 31. Average D-segment packaging space with dimensions..... | 38 |
| Figure 32. Cal Poly bumper beam fit to packaging space..... | 38 |
| Figure 33. Base Beam for bumper system..... | 38 |
| Figure 34. Steel energy absorber for bumper system | 39 |
| Figure 35. Enlarged view of the SEA tabs and cuts..... | 39 |
| Figure 36. Assembly layout for Bumper Beam system..... | 40 |
| Figure 37. Crush Can provide by SHAPE CORP..... | 40 |
| Figure 38. Fabricated SEA from two pieces of sheet metal..... | 42 |
| Figure 39. Pendulum Impact Test Setup..... | 43 |
| Figure 40. FEA was conservative in deflection predictions | 44 |
| Figure 41. Compared to testing, simulated results depicted a nearly identical peak force..... | 45 |

Figure 42. Deflection-Time comparison 45

Figure 43. Legform Drop Test. 46

Figure 44. Plywood test platform. 47

Figure 45. Legform used for drop testing 47

Figure 46. Pedestrian Leg Drop Test Comparison..... 48

Figure 47. SEA deformation comparison between test and FEA data. 49

Figure 48. BMAC 3000. 61

Figure 49. FEA Barrier Models. 62

Figure 50. Extruded cross section sketch..... 63

Figure 51. Assembly of the base beam with D6080-1.1 SEA and RCAR 40% Offset barrier..... 63

Figure 52. Crush can static force-deflection data..... 64

Figure 53. Left crush can constrained to move with the back of the bumper beam. 64

Figure 54. Typical meshed beam. 65

Figure 55. Full bumper (left) and section view (right) of stress contours during impact..... 65

Figure 56. Beam geometry..... 66

Figure 57. Test requirements and results..... 67

Figure 58. FEA model description. 67

Figure 59. FEA comparison and validation 69

Figure 60. Plug-n-Play force-deflection curves for a flat plate with reinforcement bars design. 70

Figure 61. Plug-n-Play force-deflection curves for an external reinforcement design. 71

Figure 62. Plug-n-Play force-deflection curves for an internal reinforcement design. 72

Figure 63. Plug-n-Play force-deflection curves for a B-shape with reinforcing plate design 73

Figure 64. Effect of cross section width variation on energy absorption..... 74

Figure 65. Reinforcement height effects on energy absorption. 75

Figure 66. Effect of cross section taper orientation on energy absorption 76

Figure 67. Strain Energy approximation 78

Figure 63. Stress-strain data for HF 60 high strength steel. 79

Figure 64. Stress-strain data for M220 Ultra High Strength Steel 79

LIST OF TABLES

| | |
|---|----|
| Table 1. Best-in-Class Global Bumper project engineering requirements | 9 |
| Table 2. Cross section comparison spreadsheet | 15 |
| Table 3. Conclusions drawn from the match booking parameter study..... | 30 |
| Table 4. Test summary for final bumper designs. | 41 |
| Table 5. Summary of comparison between testing and FEA data..... | 44 |
| Table 6. Comparison between different Plug-n-Play methods. | 59 |
| Table 7. Conceptual Spreadsheet comparing cross section properties. | 60 |
| Table 8. List of AISI recommended materials | 77 |

ABSTRACT

Modern bumper systems are governed by laws and regulations imposed separately by various countries. Today, the regulations in China, North America, and Europe are becoming more similar, but there is not a widely accepted bumper reinforcement that meets the requirements of all markets around the globe.

A universal bumper reinforcement beam incorporating Plug-n-Play techniques was developed to meet and exceed all testing requirements and performance standards of each country. These Plug-n-Play techniques consist of adding energy absorbing attachments to the front of a base bumper beam. Simple beam analysis and FEA were the primary analysis tools in the development of the bumper beam system. Plug & Play techniques were utilized to increase the performance of the universal bumper across all markets.

CHAPTER 1: INTRODUCTION

The Best-in-Class Bumper Reinforcement project provides the opportunity to design and test a bumper reinforcement beam that is marketable in a global setting. The beam was designed to fit an average D segment package space and meet low speed impact requirements found in Chinese, North American, and European markets. In addition, weight should be reduced while improving performance compared to current systems. To accomplish this, a base beam can be fitted with simple attachments (Plug-n-Play attachments), allowing for variable performance levels to meet varying requirements. The American Iron and Steel Institute (AISI) sponsored the project. Tom Johnson and Brian Malkowski of Shape Corp. were the project's formal advisors, and Peter Schuster provided local technical support.

Objectives

The goal for this project is to design, prototype, and test a new front bumper reinforcement beam. The bumper beam shall meet the following requirements:

- Meet global government low speed requirements in North American, European, and Chinese markets
- Include Plug-n-Play reinforcements to allow the bumper to meet performance requirements in different markets
- Perform competitively in global markets
- Can be fabricated using known manufacturing equipment/processes

The Quality Function Deployment (QFD) method was used to translate the above requirements into engineering specifications. This approach involves assigning a numerical weighting to the customer's requirements. These requirements are compared against engineering specifications using a numerical system to indicate the strength of the relation between the requirement and the specification. Finally the relative importance of the engineering specifications can be determined. The QFD table used to determine the engineering specification for this project is attached in Appendix A. Based on this table, intrusion limit and maximum force applied to each rail were identified as the most important requirements.

Table 1 contains the formal design specifications for this project. The table includes a description of each parameter, the parameter targets and tolerances, the risk of meeting each target, and the compliance (how the target will be met). The package space dimensions included in the table are displayed in Figure 1.

The mass requirements will be difficult to achieve because there is a tradeoff between strength and weight of the bumper beam. The intrusion limit and max force requirements will be the most challenging. Deflection past the intrusion limit may result in damage to critical engine components. In order to minimize this, a stiffer beam can be designed. However a stiff beam may result in more force transmitted to the frame rails of the car. Again, a compromise is required between these two criteria.

Table 1. Best-in-Class Global Bumper project engineering requirements

| Spec. No. | Parameter Description | Requirement or Target | Tolerance | Risk ^[a] | Compliance ^[b] |
|-----------|--|-----------------------|-----------|---------------------|---------------------------|
| 1 | Chinese cross beam mass | 4 kg | Max | H | A,S,I |
| 2 | North American cross beam mass | 5 kg | Max | H | A,S,I |
| 3 | European cross beam mass | 6 kg | Max | H | A,S,I |
| 4 | Package space width | 1429.6 mm | Max | L | A,S,I |
| 5 | Package space height | 119.9 mm | Max | L | A,S,I |
| 6 | Package space depth | 144.3 mm | Max | L | A,S,I |
| 7 | Package space depth | 106.8 mm | Max | L | A,S,I |
| 8 | Beam set-up from ground | 420 mm | Max | L | A,S,I |
| 9 | Towing/recovery hook | Include | n/a | L | S,I |
| 10 | Full frontal intrusion limit at centerline | 55 mm | Max | H | A,T |
| 11 | Front offset intrusion limit at corner | 10 mm | Max | M | A,T |
| 12 | Peak force per rail | 80 kN | Max | H | A,T |
| 13 | Pedestrian max acceleration | 150g | Max | H | A,T |

^[a] High (H), Medium (M), Low (L)

^[b] Analysis (A), Test (T), Similarity to existing Designs (S), Inspection (I)

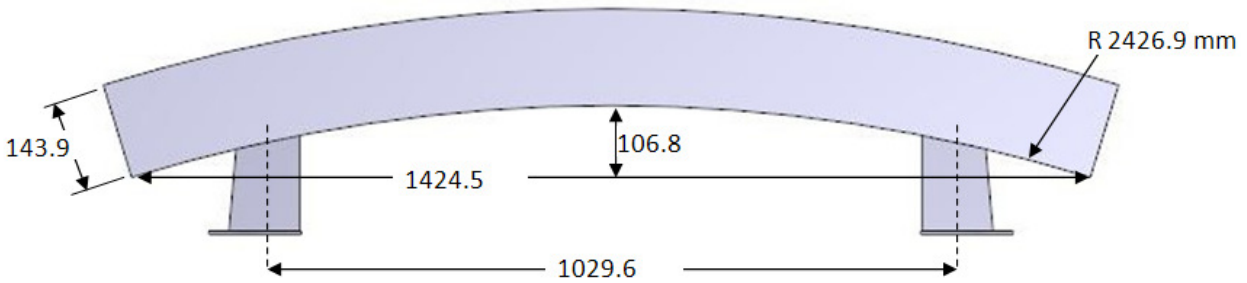


Figure 1. Package space dimensions.

CHAPTER 2: BACKGROUND

Laws and regulations imposed separately by various countries govern modern bumper systems. These regulations specify the conditions for testing and the criteria for passing those tests. For example, the US Department of Transportation [7] describes pendulum impacts at 2.5 mph between heights of 16” and 20”, while the China National Standard [1] describes 4 km/h pendulum impacts at a height of 445 mm. There are several similarities in the criteria for passing these tests. In general, the vehicle must be able to operate in a “normal” manner after the collision. This means that lighting and signaling devices have to be functional, all doors must be able to open and latch shut, there can be no fuel leaks, and the steering system must be functional. Today, the regulations in each country are becoming more similar, but there is not a widely accepted bumper reinforcement that meets the requirements of all markets around the globe.

Pedestrian safety is a prominent consideration when designing bumper systems. Requirements for pedestrian safety add a level of complexity to the design process because bumpers must be flexible enough to reduce the chance of injury of the passengers but stiff enough to protect vehicle components. Energy absorbers help accomplish this goal by dissipating energy from the collision. Injection molded or expanded polypropylene (EPP) foam are the most common materials used. Injection molded energy absorbers load through shear walls, so the impact force acts through a shear wall of the reinforcement beam. The load is carried beyond the impact area through the continuous shear walls, increasing the energy absorption capacity. EPP foam behaves like a pressure load and confines energy absorption to material directly compressed by the impact [2]. Steel energy absorbers are used by some manufacturers as well.

Extensive research has gone into finding the best materials and manufacturing methods for bumper reinforcement systems. Sindrey [3] found that the vast majority of bumper reinforcement systems today are made from steel. Steel beams have a low unit material cost, and have a greater strength to weight ratio than most aluminum beams.

The three major manufacturing methods of bumpers are hot stamping, cold stamping and roll forming [6]. In hot forming, preheated metal is placed between two metal dies. The dies can either be in open configuration where one die is pressed into the other, or in closed configuration where the two dies are initially face to face and a third die presses the metal into place [3]. The main advantages of hot forming are that it gives near-net-shape, has consistent tolerances and has a smooth finish.

Figure 2 is a bumper made using hot stamping method. The bumper has intricate features which is unique to this method. The main advantage the bumper has is styling [6].



Figure 2. The Volkswagen Jetta (1993) has a hot stamped bumper beam [6].

Cold stamping shapes metal by displacing it at room temperature through a series of dies to the desired shape. The main advantage to cold stamping, which is a type of cold working, is that it requires no heat and increases the yield strength of the material.

Figure 3 is a bumper made with the cold stamping method. The main advantage of this bumper is styling [6].

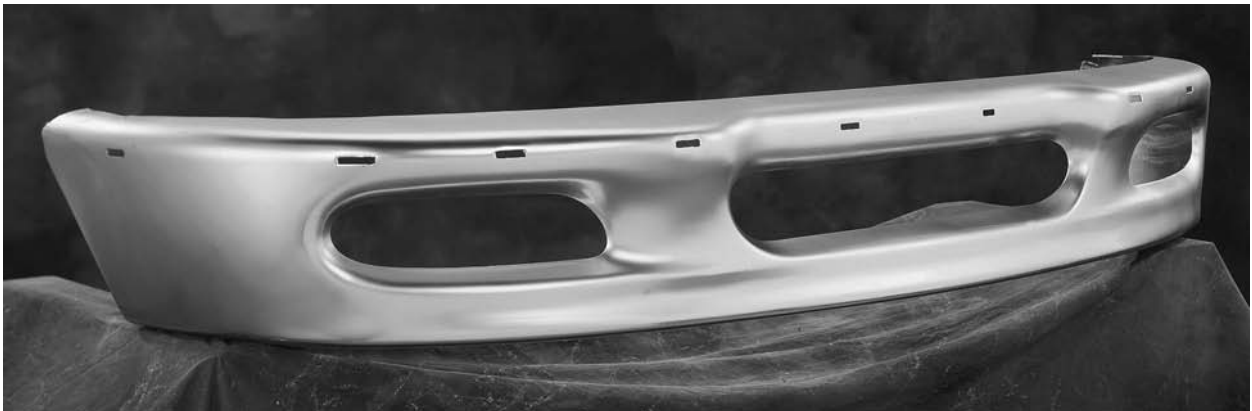


Figure 3. The Ford F150 Pick-up (1996) has a cold stamped bumper beam [6].

Roll forming continuously shapes a strip of steel using sets of roller dies called a flowering pattern. It lends itself to punching and sweeping before cutoff [4]. Compared to the other methods, it can shape higher strength steels. However, the process requires a constant cross-section.

Figure 4 depicts a bumper formed using roll forming. The major advantage is cost savings through higher throughput [6].



Figure 4. The Ford Taurus/Mercury Sable (1995) has a roll formed bumper beam [6].

To date, hydroforming has not been used to produce bumper reinforcement beams, but there is potential for future use.

Because bumper reinforcements play such a vital role in safety, validation through testing is a crucial part of the design process. Simple beam analysis gives a basis for beam deflection and simple stress analysis comparisons. Finite element models are common in the mid stages of design, but actual impact tests provide a high level of confidence in the product. There are two common impact test methods. The first consists of a universal test vehicle that can be outfitted with different bumpers and modified to simulate characteristics of several different vehicles. The vehicle impacts a stationary barrier at a controlled speed. The second involves a weighted pendulum which is elevated and swung into the bumper which is mounted to a stationary base. The latter method will be used in the testing phase of this project.

CHAPTER 3: DESIGN DEVELOPMENT

Conceptual Designs

Through brainstorming, many bumper beam concepts were ideated. Concepts of the beam include various cross sectional shapes, overall beam shapes, and ideas for Plug-n-Play attachments.

Ideas for bumper beams incorporated alternative methods of absorbing energy as opposed to the conventional foam energy absorbers and deformation of the beam itself. This is accomplished via springs, viscous dampers, crush elements, etc. Also, ideas for minimizing mass were conceptualized by decreasing the height of the beam at non-critical areas and replacing unnecessary solid plates with a wire mesh, honeycomb cores, or thin corrugated plates. Sketches of these concepts are shown in Figure 5.

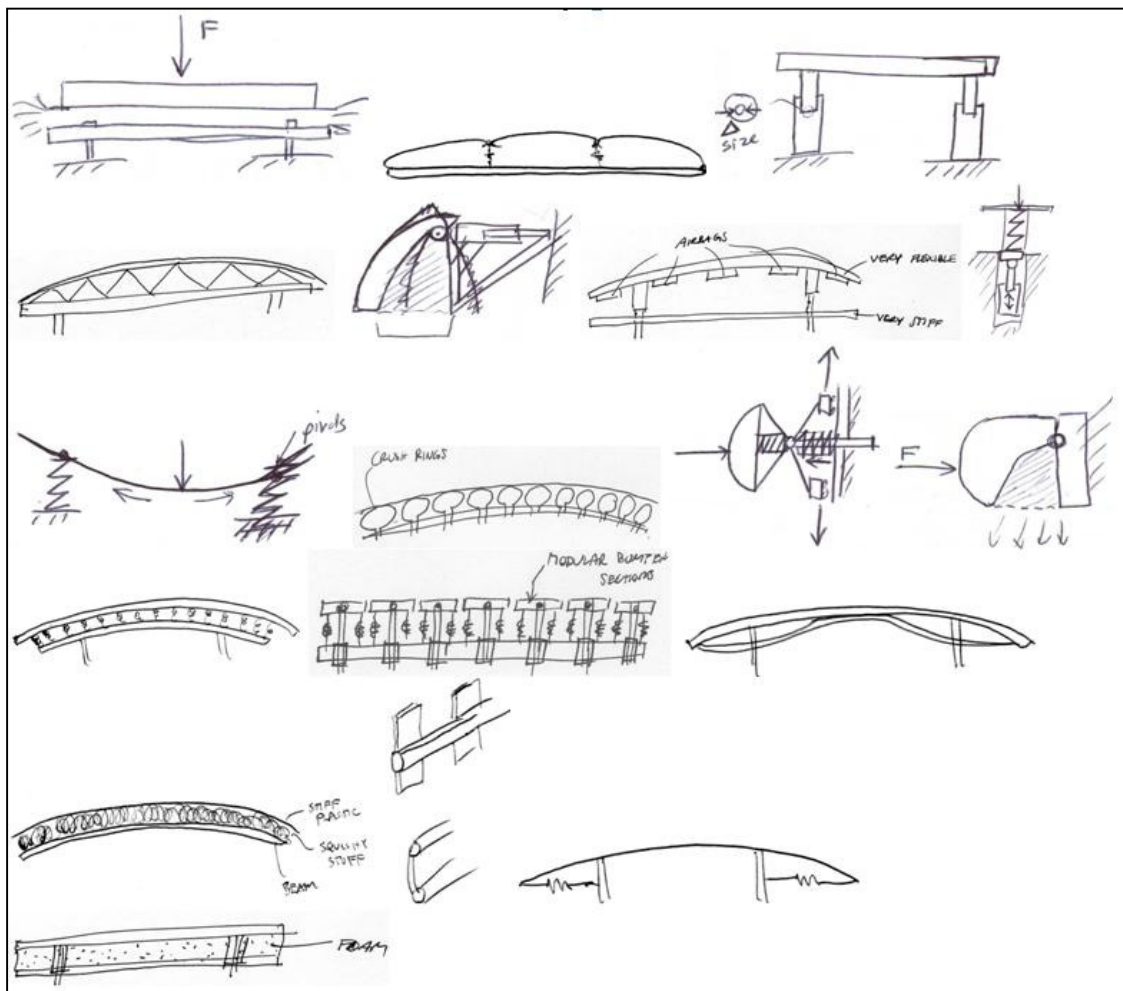


Figure 5. Alternative bumper designs

Concepts for cross sectional shapes ranged from open and closed thin-walled shapes to thick-walled and solid shapes. These include shapes that resemble I-beams, B shapes, C channels, and boxes. A few sketches of cross sections are provided in Figure 6.

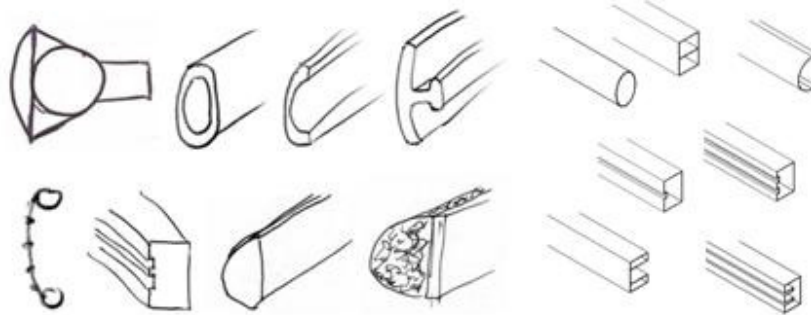


Figure 6. Cross section examples

Ideas for Plug-n-Play attachments included reinforcement plates, beams, and inserts that are added onto a beam; stackable beams; and interchangeable stiffeners and dampers. These attachments could assemble via snapping or bending components, screws, welds, adhesives, interference fits, rivets, etc. Sketches of Plug-n-Play concepts are provided in Figure 7. Another idea involved adding steps in the manufacturing process. For example, a set of optional machinery can be used to bend additional stiffeners into a thin walled beam.

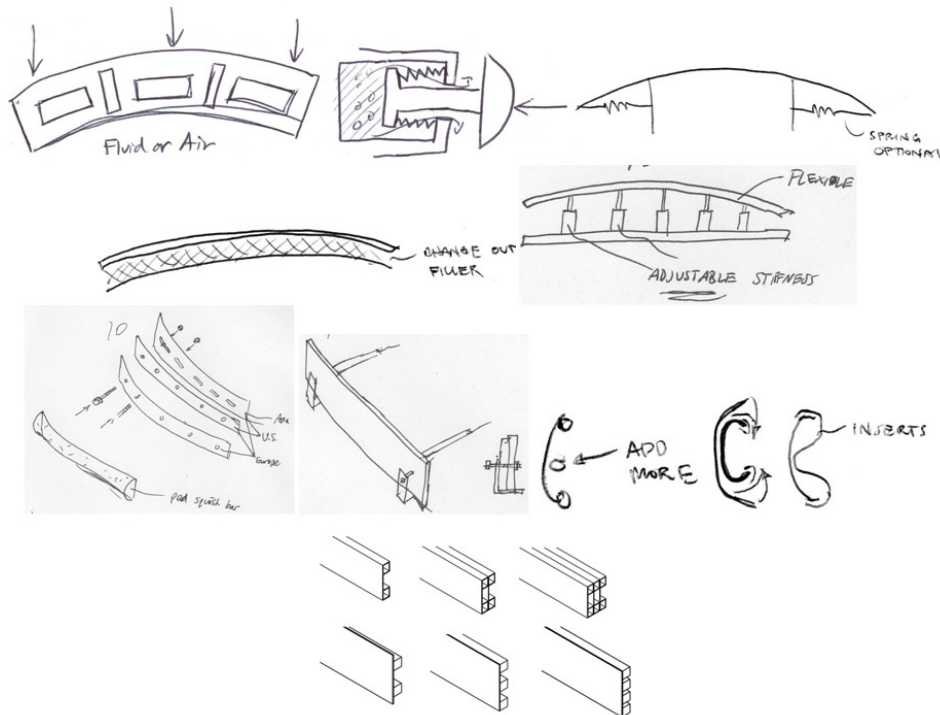


Figure 7. Plug-n-Play concepts

Analysis Tools

The following analysis tools were developed and applied in various steps of the design process. These tools include:

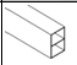

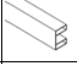
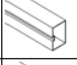
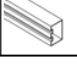
- Preliminary Analysis used to quickly and efficiently select the most promising designs from a broad base of ideas.
- B-MAC 3000 used to quickly generate rough estimates for how various designs will perform.
- 2-D Static FEA used to compare the performance of general cross section shapes.
- 3-D Dynamic FEA used to approximate the actual performance of beams.

Preliminary Analysis

Decision matrices and spreadsheets were used at the beginning of many steps in the design process. These preliminary analyses helped to identify the best performing concepts from a large pool of brainstormed concepts. Examples of these preliminary analysis tools are found in the Appendix C.

The following is an example of a preliminary analysis tool used to determine beam cross section shapes. The spreadsheet in Table 2 compares the stiffness and weight of various beam cross sections. Area is directly correlated with the weight of the beam and the quantity of material required in manufacturing it. The moment of inertia is directly correlated with the beam's stiffness and maximum bending stress. The Bumper Universal Parameter (BUP) is the ratio of a beams moment of inertia, I , over the cross-sectional area, A , and the distance from the neutral axis to the outer surface, c . BUP was helpful in evaluating how efficiently material was used in a given cross-section. Spreadsheets such as this were useful in developing a basic understanding of how various shapes affected cross sectional properties.

Table 2. Cross section comparison spreadsheet

| Shape | Picture | Ix (mm ⁴) | Iy (mm ⁴) | Iz (mm ⁴) | c (mm) | Area (mm ²) | BUP - Ix/(Ac) (mm) | Ix/A (mm ²) | Iy/A (mm ²) | Iz/A (mm ²) | Incr. Ix (%) | Incr. Iy (%) | Incr. Iz (%) | Incr. A (%) | Ix/A ² (-) | Iy/A ² (-) | Iz/A ² (-) |
|-------|---|-----------------------|-----------------------|-----------------------|--------|-------------------------|--------------------|-------------------------|-------------------------|-------------------------|--------------|--------------|--------------|-------------|-----------------------|-----------------------|-----------------------|
| 5 |  | 7.04E+05 | 1.17E+06 | 1.87E+06 | 36.50 | 842 | 22.91 | 836 | 1390 | 2221 | 8.47 | 0.00 | 2.75 | 19.60 | 0.99 | 1.65 | 2.64 |
| 6 |  | 7.59E+05 | 1.35E+06 | 2.11E+06 | 36.50 | 980 | 21.22 | 774 | 1378 | 2153 | 16.95 | 15.38 | 15.93 | 39.20 | 0.79 | 1.41 | 2.20 |
| 7 |  | 6.21E+05 | 1.33E+06 | 1.95E+06 | 40.44 | 882 | 17.41 | 704 | 1508 | 2211 | -4.31 | 13.68 | 7.14 | 25.28 | 0.80 | 1.71 | 2.51 |
| 8 |  | 6.64E+05 | 1.17E+06 | 1.84E+06 | 37.66 | 744 | 23.70 | 892 | 1573 | 2473 | 2.31 | 0.00 | 1.10 | 5.68 | 1.20 | 2.11 | 3.32 |
| 9 |  | 6.77E+05 | 1.21E+06 | 1.89E+06 | 38.69 | 784 | 22.32 | 864 | 1543 | 2411 | 4.31 | 3.42 | 3.85 | 11.36 | 1.10 | 1.97 | 3.07 |

B-MAC 3000 - Excel spreadsheet to analyze simplified beams

The Bumper Multifaceted Analysis Calculator 3000 (B-MAC 3000) shown in Appendix D has been developed to analyze cross section and material properties using energy methods and simple beam theory. These methods simplify real world situations to depict trends between cross section and material combinations. This spreadsheet offers a more efficient approach than finite element analysis because it can quickly and easily analyze many different combinations. After using this tool to narrow down design options, FEA models can be developed for more detailed analysis.

To evaluate whether the bumper passes or fails requirements for a region, the total energy is calculated from the moving system. 80% of the total energy in an impact travels through the bumper system. The total energy transferred to the bumper system is then translated into a deflection. For the current combinations of cross-section and material choice, a maximum deflection is calculated. To remain elastic, the deflection due to energy must be less than the maximum deflection calculated from simple beam analysis. If the deflection exceeds this value, the beam has plastically deformed.

Much of the theory in the spreadsheet is useful only for elastic deformation. Plastic deformation was approximated using energy and a material's stress-strain curve. This is especially useful for the IHS test and the RCAR test in which plastic deformation typically occurs. The energy analysis for plastic deformation does assume that the geometry of the beam will not change, which is known to be false. However, the analysis offers a good comparison between different materials and a sense of how well a certain material and cross-section absorb energy through both the elastic and plastic regions.

Three point bending is used to find the maximum deflection of the bumper beam. The max deflection is the greatest distance the center line of the beam can intrude without failing the Distortion-Energy criterion.

Buckling is the last analysis tool used in the spread sheet. Because the overall beam is too complex for simple theory, the horizontal sections of the beam are assumed to carry most of the load during an impact and would be the first place buckling would occur. Each section acts like a column with a height equal to the depth of the section and a cross-section equal to the thickness of metal used and the length of the beam. Using Euler's equation for column buckling, and factoring in how many horizontal surfaces there are in the beam, an approximate value for the critical stress can be found. If the critical stress exceeds the yield strength of the material, the Tangent modulus is substituted instead of the elastic modulus.

Top cross section and Plug-n-Play designs will be analyzed with the BMAC-3000 to determine which material gives the best performance for each design. Using this method to rank the materials will result in a top choice to examine with complex finite element analysis.

2-D Static FEA

In addition to comparing the elastic behaviors of cross section shapes on the basis of their area moment of inertia, the inelastic behaviors of cross section shapes were compared using a static finite element analysis (FEA). This allowed for the consideration of local plastic yielding of the beam that is commonly seen near the crush cans.

In this analysis, a 2-D FE model (shown in Figure 8) was created of the beam's cross section. Boundary conditions applied to the back side of the beam constrain the beam from translating. A rigid barrier located at the front of the beam crushes the cross section.

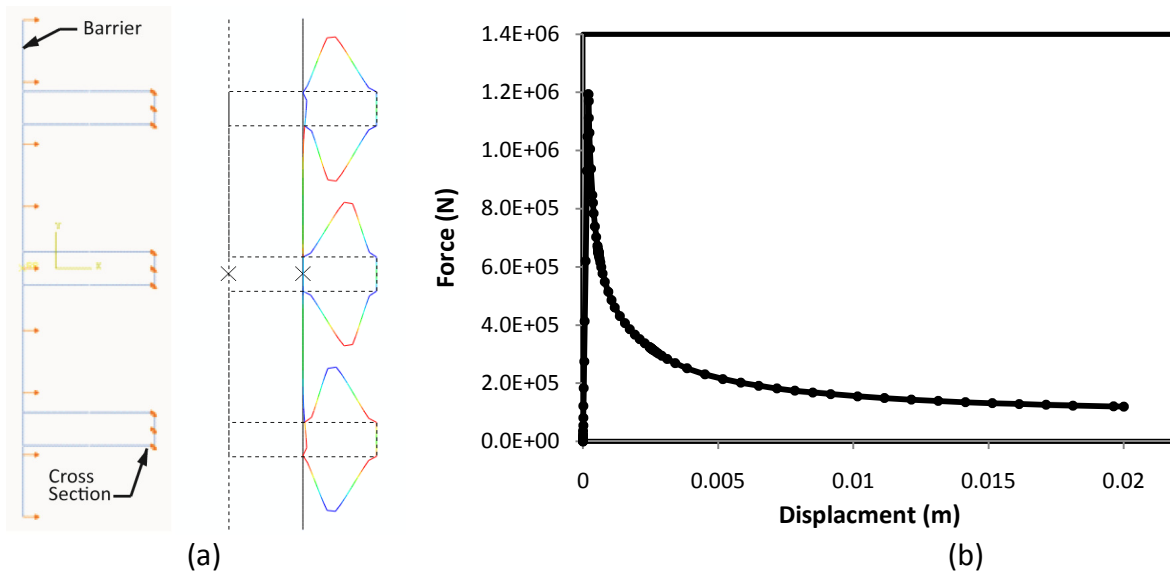


Figure 8. (a) Cross section models are crushed by a rigid barrier and (b) force-displacement data are collected and plotted.

As the barrier crushes the cross section, force and displacement data was collected and plotted as in Figure 8. The area under the force-displacement curve represents the amount of energy absorbed by the cross section as it is crushed. This area is approximated using trapezoidal numerical integration.

By using 2-D static FEA to calculate the energy absorbed by various cross sections, the best shape can be determined by maximizing the energy absorption. A cross section that absorbs more energy requires more force to crush and will be more likely to maintain its designed shape during an impact.

3-D Dynamic FEA

In order to approximate the actual, real-life performance of the bumper beam, 3-D dynamic FEA was performed. This FE model considers the coupled effects of cross section geometry, beam shape, material type, crush cans, and inertial effects.

As shown in Figure 9, the FE models contain three major parts: the beam, crush cans, and an impact barrier. The beam includes the reinforcement beam and energy absorber. The crush cans are modeled as non-linear springs using static force-displacement data obtained through testing. Different barriers can be used to model the GB17354-1998 pendulum, IIHS and RCAR full frontal and offset, and EuroNCAP pedestrian tests.

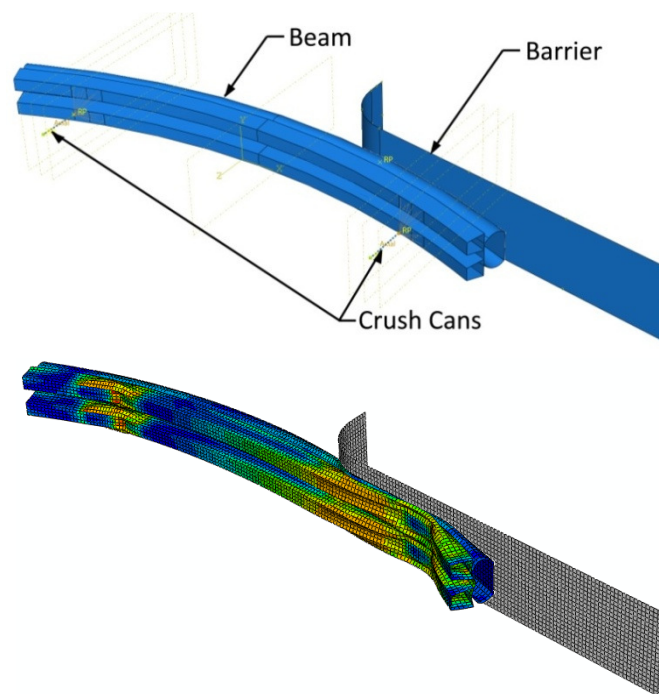


Figure 9. 3-D dynamic FEA model to simulate a RCAR 40% offset test.

From the FEA, much useful information about the performance of the beam can be obtained. These include:

- Displacements at any location in the beam as a function of time. (The centerline and crush can displacements were especially useful.)
- Forces on the barrier and at the frame rails as a function of time.
- Stresses within the beam as a function of time.
- Accelerations and velocity of the barrier as a function of time.

See Appendix E for more detail on the FEA model.

Design Plan

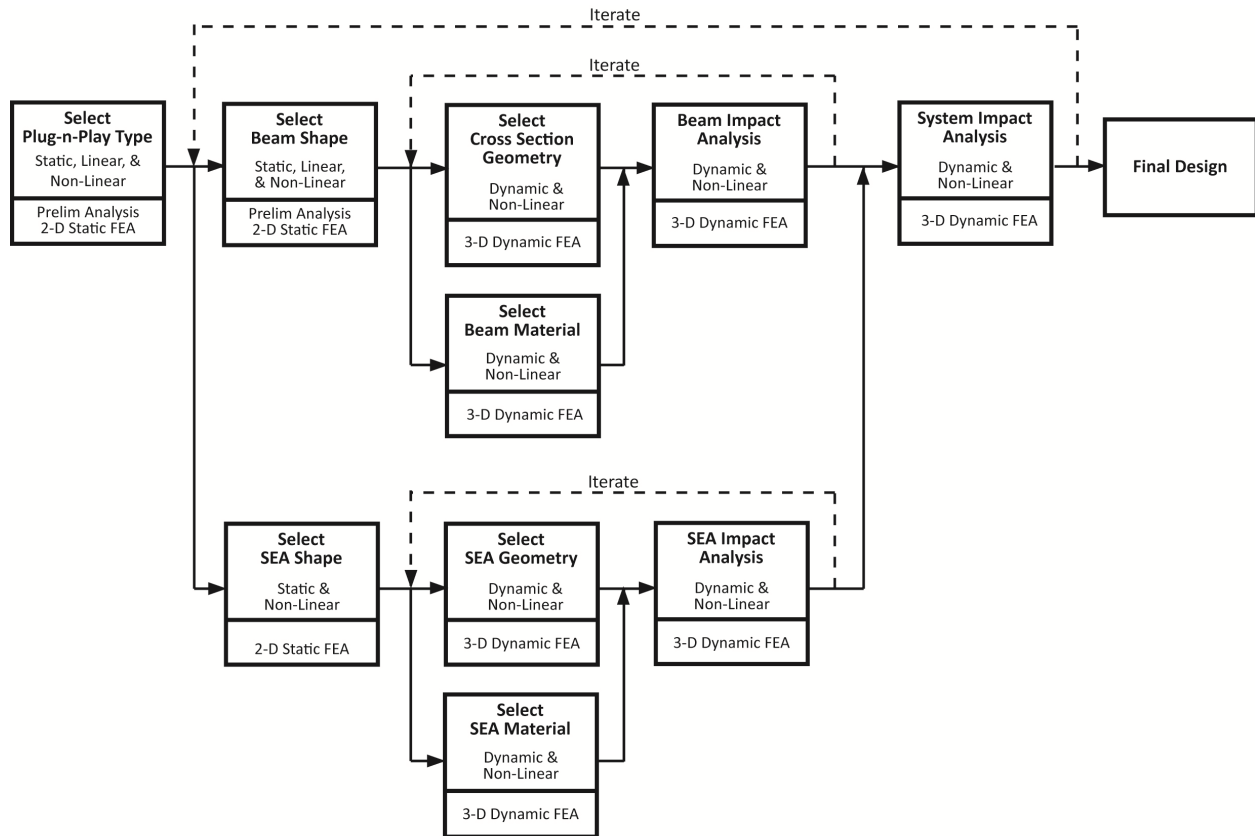


Figure 10. Design plan layout.

The team's design plan is displayed graphically in Figure 10. The map shows each component of the bumper system to be selected, the type of analysis that was used, and the specific method used in the analysis. The plan contains three major milestones: selecting a Plug-n-Play type, selecting a beam, and selecting an energy absorber.

Selection of a Plug-n-Play type consists of a simple preliminary analysis and a 2-D static FEA. Because there were many Plug-n-Play ideas, a more complex analysis would have taken a long time. To make this step in the design plan more efficient, applying simple and quick analysis techniques was crucial.

Selection of a beam and an energy absorber was performed simultaneously. Similar to the Plug-n-Play type analysis, selection of the beam and energy absorber began with a simplified analysis in order to identify the best shape from a large pool of possibilities. Once a specific shape was chosen, a more complex 3-D dynamic FEA was used to determine the best performing cross section geometry and beam material.

To finish the design plan, a 3-D dynamic FEA was performed on the entire bumper system to determine if the overall design met impact test requirements.

Selecting a Plug-n-Play Type

The first step in the design process was to select a Plug-n-Play type. The best type of Plug-n-Play system is one that maximizes the performance of the beam while keeping the beam's weight at a minimum. The final design includes a base bumper beam marketed toward China, a Plug-n-Play attachment that is added to base beam to accommodate North American markets, and another Plug-n-Play attachment for European markets. The addition of Plug-n-Play options gives each market's design a different cross section and a different mass. The mass of the Chinese beam was limited to 4 kg, the North American beam to 5 kg, and the European beam to 6 kg. Plug-n-Play types considered include:

- Stacking identical cross sections horizontally
- Adding reinforcement bars to a plate
- Changing the manufacturing process to add reinforcements to individual cross sections
- Adding reinforcements to the front or inside of a cross section

An analysis of moments of inertia, areas, and c values was performed on several different designs for each Plug-n-Play type. C is the greatest distance from the cross section's neutral axis to the outside edge. The goal was to maximize moment of inertia while minimizing cross sectional area and c value, resulting in high strength with low weight.

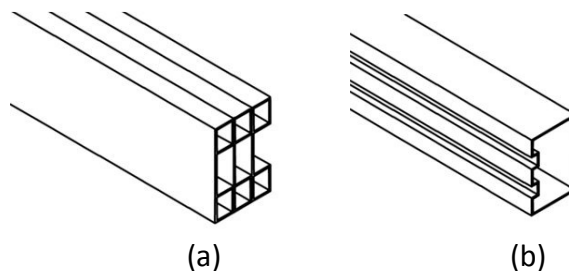


Figure 11. (a) Horizontal stacking a common B-section and (b) manufacturer reinforcements.

Due to large weight increases, the horizontal stacking method seen in Figure 11(a) was eliminated. Manufacturer reinforcements such as those in Figure 11(b) resulted in only very small improvements compared to the other Plug-n-Play types. A modification like this may be useful in the final design, but it is not sufficient as the primary method of reinforcement. This initial analysis narrowed down the Plug-n-Play types to three final options:

- Flat plate with reinforcement bars
- Simple cross section with internal reinforcements
- Simple cross section with external reinforcements

Preliminary analysis of these Plug-n-Play types is presented in Table 6 of Appendix C. Data from this spreadsheet was plotted on bar charts in order to visually examine the change in performance resulting from each Plug-n-Play addition.

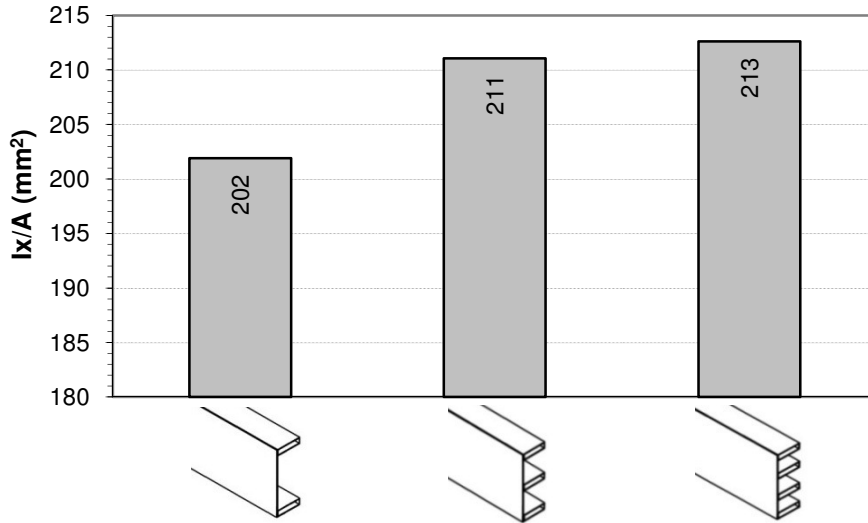


Figure 12. Comparison of normalized moment of inertia for the base bumper, first Plug-n-Play addition, and second Plug-n-Play addition of the reinforced flat plate design.

Figure 12 shows the change in the normalized moment of inertia for one Plug-n-Play design. By factoring in the area, the weight of the beam and the moment of inertia are considered. As this design shows, the second shape provided a 4.5% increase over the base beam, while the third provided a 0.9% increase over the second.

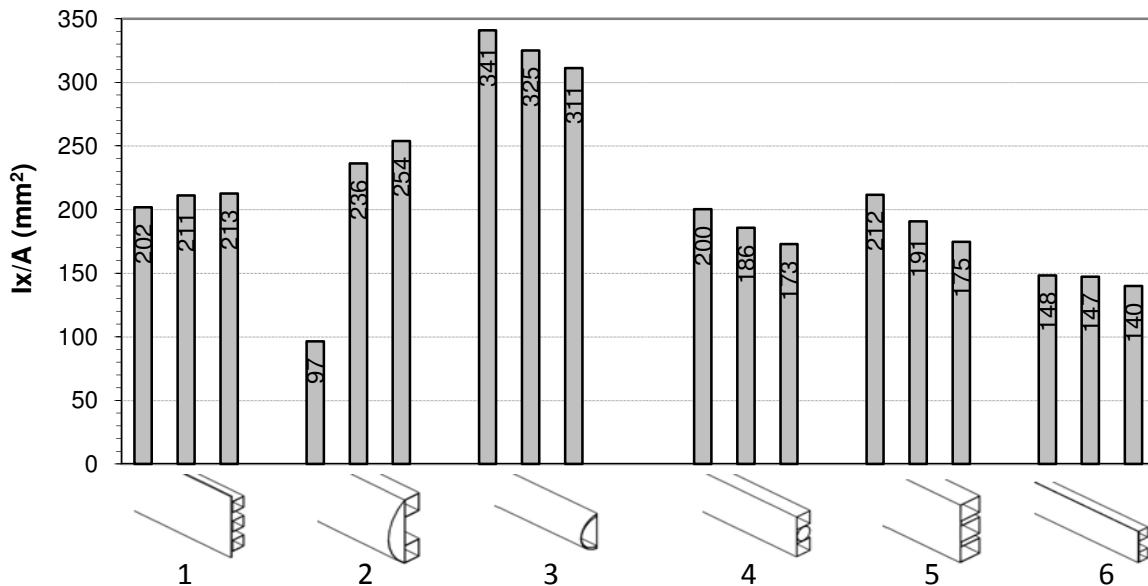


Figure 13. Normalized moments of inertia for several Plug-n-Play designs.

As in Figure 12, data for normalized moment of inertia is presented in Figure 13, however this time six different Plug-n-Play designs are included. The first column of each design represents the base beam, the second is includes the first Plug-n-Play addition, and the third includes the second Plug-n-Play addition. Design 1 is a flat plate with reinforcement bars. Designs 2 and 6 added external reinforcements, while designs 3 and 4 added internal reinforcements to the cross section. Manufacturing modifications are compared in Design 5.

Simple cross section analysis showed that Design 3 had the best moment of inertia to weight ratio, but this is a simplified analysis which only compares the elastic behavior of each Plug-n-Play type. In order to further analyze and compare each type, 2-D Static FEA was used to compare the energy absorption capabilities of each design.

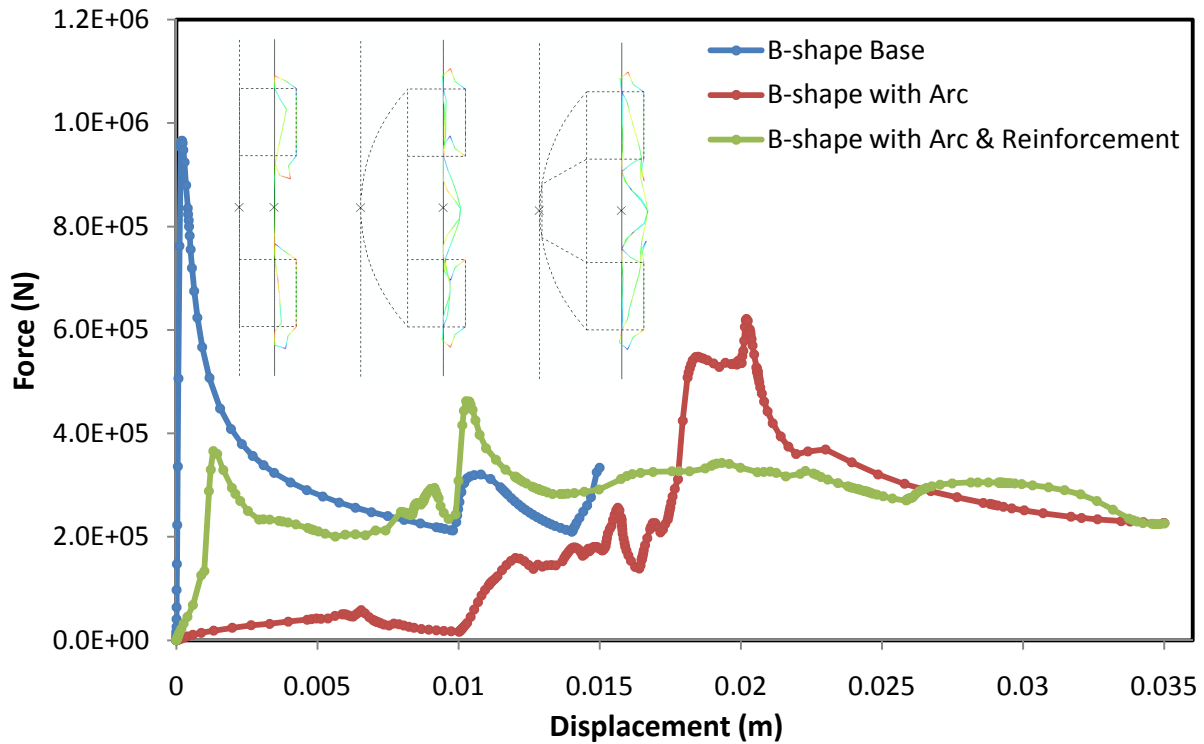


Figure 14. Plug-n-Play force-deflection curves for an external reinforcement design.

Using 2-D Static FEA, force-displacement graphs such as the one in Figure 14 were generated to compare the plastic behavior of each cross section for each Plug-n-Play type. Pictures of all three Plug-n-Play cross sections are displayed in their undeformed and deformed states. Because the areas under the curves represent the amount of energy absorbed while crushing, the effect of adding each Plug-n-Play attachment can be compared. While this is not the primary energy absorbing mechanism during a bumper impact, it is important to maximize the absorbing capability for each Plug-n-Play addition to create an ideal cross section. Similar plots were generated for the other five designs considered in the analysis and are included in

Appendix F. The results of the Plug-n-Play analyses were compared using the decision matrix in Figure 15.

| | | ALTERNATIVES | | | | | | |
|----------|--|--------------------------------|--------------------------------------|--------------------------------------|--------------|-----------------------------|--|--------------|
| | | | | | | | | |
| CRITERIA | Weighting Factor | Reinforce Flat Plate with Bars | B-shape with External Reinforcements | B-shape with Internal Reinforcements | E-section | Ellipse with Reinforcements | B-shape with Flat Plate Reinforcements | |
| | Lightweight Base | 10.5 | 75% 7.875 | 100% 10.5 | 50% 5.25 | 25% 2.625 | 100% 10.5 | 10% 1.05 |
| | Lightweight Base with 1st Attachment | 10.5 | 100% 10.5 | 100% 10.5 | 50% 5.25 | 50% 5.25 | 75% 7.875 | 10% 1.05 |
| | Lightweight Base with 1st & 2nd Attachment | 10.5 | 75% 7.875 | 90% 9.45 | 25% 2.625 | 50% 5.25 | 100% 10.5 | 10% 1.05 |
| | Large Energy Absorption Base | 5.2 | 90% 4.68 | 100% 5.2 | 90% 4.68 | 25% 1.3 | 10% 0.52 | 50% 2.6 |
| | Large Energy Absorption Base with 1st Attachment | 5.2 | 100% 5.2 | 75% 3.9 | 100% 5.2 | 50% 2.6 | 10% 0.52 | 25% 1.3 |
| | Large Energy Absorption Base with 1st & 2nd Attachment | 5.2 | 75% 3.9 | 50% 2.6 | 90% 4.68 | 100% 5.2 | 10% 0.52 | 25% 1.3 |
| | Large Increase Energy Absorption Due to 1st Attachment | 5.2 | 90% 4.68 | 90% 4.68 | 100% 5.2 | 90% 4.68 | 25% 1.3 | 0% 0 |
| | Large Increase Energy Absorption Due to 1st & 2nd Attachment | 5.2 | 75% 3.9 | 50% 2.6 | 90% 4.68 | 100% 5.2 | 25% 1.3 | 0% 0 |
| | Large Moment of Inertia Base | 10.5 | 90% 9.45 | 10% 1.05 | 50% 5.25 | 90% 9.45 | 100% 10.5 | 25% 2.625 |
| | Large Moment of Inertia Base with 1st Attachment | 10.5 | 75% 7.875 | 90% 9.45 | 50% 5.25 | 50% 5.25 | 100% 10.5 | 10% 1.05 |
| | Large Moment of Inertia Base with 1st & 2nd Attachment | 10.5 | 90% 9.45 | 90% 9.45 | 50% 5.25 | 25% 2.625 | 100% 10.5 | 25% 2.625 |
| | Manufacturability | 10.5 | 100% 10.5 | 90% 9.45 | 75% 7.875 | 25% 2.625 | 75% 7.875 | 100% 10.5 |
| | Overall Satisfaction | 100 | 85.885 | 78.83 | 61.19 | 52.055 | 72.41 | 25.15 |

Figure 15. Decision matrix for Plug-n-Play types.

The criteria for the decision matrix were broken down into five main sections:

- Weight
- Energy absorption
- Plug-n-Play effectiveness (increase in energy absorption due to each attachment)
- Moment of inertia
- Manufacturability

These categories are described by criteria listed in the left-hand column. The top of the matrix contains the six different designs under consideration. The weighting factor for each criterion is a measure of its importance. Energy absorption was given a lower weight factor because cross section buckling is not the primary energy absorbing mechanism. Rather, the majority of the energy absorption occurs during deflection of the overall beam.

Using the criteria in the left column, each design was ranked on a 0-100% scale, which is presented in the upper left of each square. Multiplying this score by the weight factor gives the numerical score seen in the bottom right of each square. The sum of the individual scores yields the overall score at the bottom of the table. The design with the highest overall score best meets the criteria.

A reinforced plate of Figure 16 is the best performing Plug-n-Play design based on the analysis. It was ranked in the top three for every criterion and was the top performer in several categories. This is a flexible design which allows for many different reinforcement shapes and cross sections.

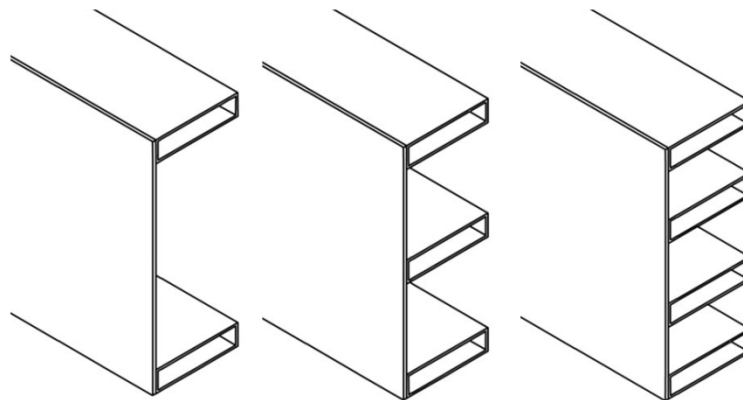


Figure 16. Best Plug-n-Play design: Flat plate with reinforcements

Selecting a Cross Section

During low-speed tests, a bumper beam’s cross section plays an important role in absorbing impact energy. While a majority of the energy is absorbed elastically as the beam bends, there are local plastic deformations and buckling of the cross section. An efficient cross section geometry absorbs a large amount of energy and resists matchbooking.

Many different cross section geometries can be derived from the reinforced plate design as shown in Figure 17. The Plug-n-Play attachments can be made wider and taller and the horizontal walls can be angled. The left side walls can be omitted. The shapes are not limited to rectangles. The attachments can be circular or elliptical.

The best cross section for the bumper beam was determined based on the beam’s performance in four sequential analyses. First, general Plug-n-Play shapes were compared using a preliminary analysis and 2-D Static FEA in order to identify the best performing shape that should be analyzed further. Second, a cross section geometry was chosen. This was done by changing various dimensional parameters of the cross section and identifying the dimensions that gave the beam the best performance. Third, a material was selected by comparing the effects of various grades of steel on performance. Finally, a 3-D beam impact FEA was conducted to verify if the chosen beam dimensions and material resulted in the best performance. If the performance was found to be unsatisfactory, this section of the design process was iterated.

The following sections discuss in detail each of the four steps summarized above.

Selecting a Cross Section Shape

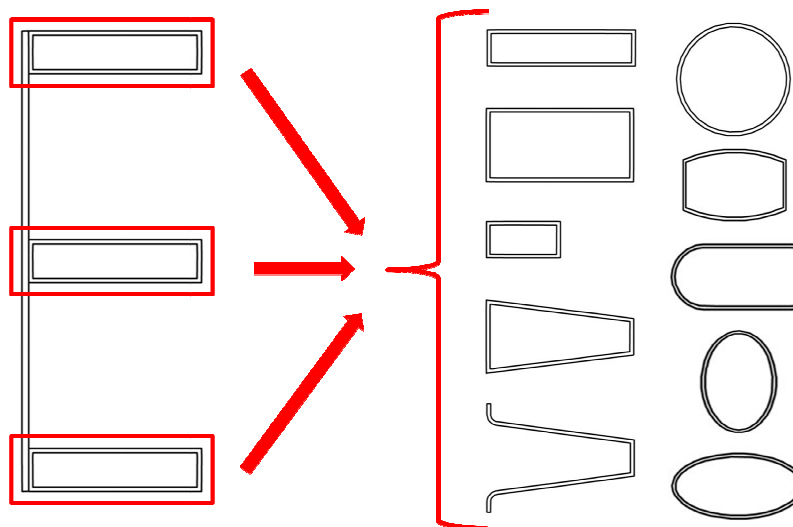


Figure 17. Various geometries for the bar attachments of the Reinforced Plate design

A simplified approach was used to identify which of the Plug-n-Play shapes in Figure 17 perform well and should be analyzed further. This analysis was similar to that of the Plug-n-Play. The cross sections were compared by their normalized moments of inertia and the amount of energy they absorbed when crushed in a 2-D FEA model.

SolidWorks models of the Reinforced Plate and various shapes of Plug-n-Play attachments were built to determine their moments of inertia and cross section area. Figure 18 compares the attachment shapes by their moments of inertia which have been normalized with their cross section area. Through this analysis, the rectangular shaped Plug-n-Play attachments were found to be more rigid in elastic bending than the elliptical and circular attachments.

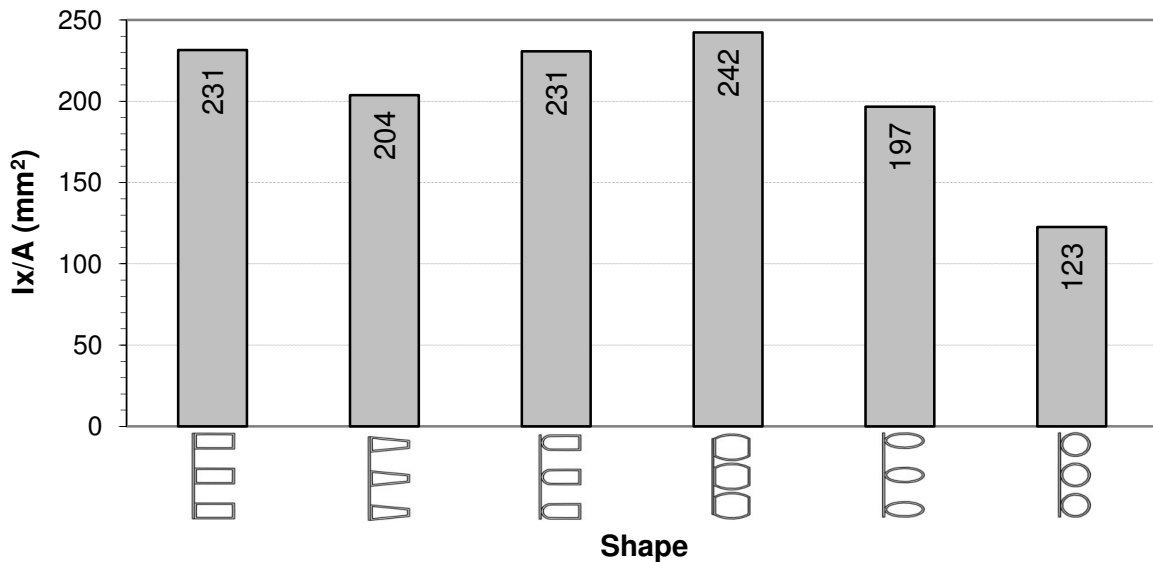


Figure 18. Plug-n-Play attachment shapes are compared by their normalized moments of inertia.

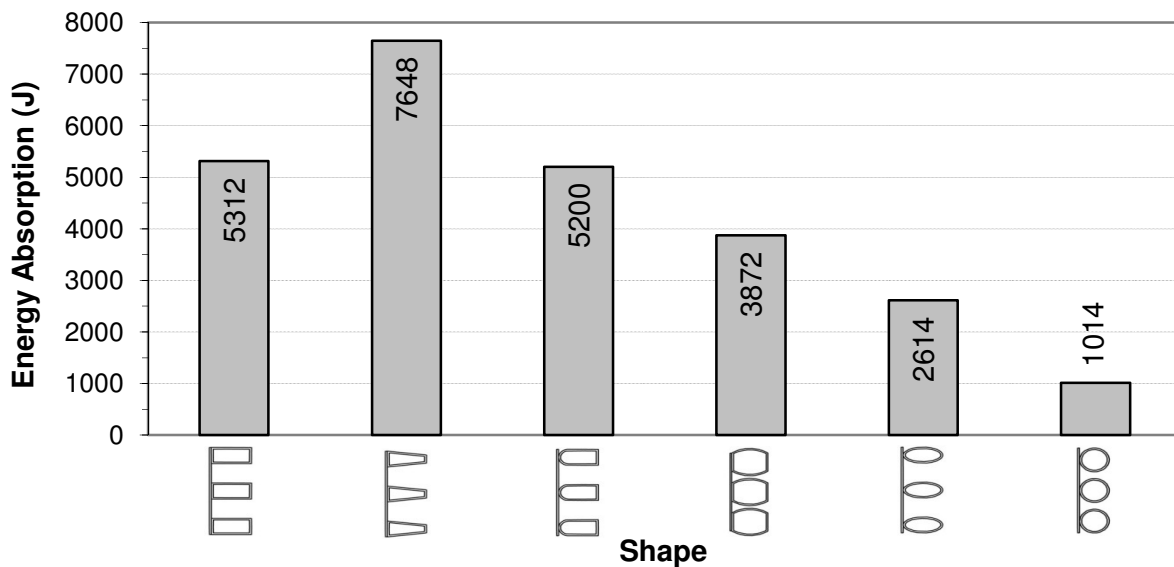


Figure 19. Plug-n-Play attachment shapes are compared by their energy absorption.

To analyze the plastic behavior of each shape, a 2-D Static FEA was conducted to determine their energy absorption capabilities. Figure 19 compares the Plug-n-Play attachment shapes by the amount of energy they absorbed.

Having determined each Plug-n-Play attachment’s normalized moment of inertia and energy absorption, the decision matrix in Figure 20 was used to identify the best cross section shape. The decision matrix considers the area of the cross section (weight of the beam), the energy absorption where localized yielding occurs, the area moment of inertia, and ease of manufacturability. Most of the weight was placed on moment of inertia because it is the dominant factor in deciding the beam’s performance since most of the deformation occurs in the material’s elastic region. The decision matrix shows that the best performing cross section is one which contains tapered Plug-n-Play attachments.

| Rating (%) | Description |
|------------|---|
| 100 | Complete satisfaction; objective satisfied in every respect |
| 90 | Extensive satisfaction; objective satisfied in all important aspects |
| 75 | Considerable satisfaction; objective satisfied in the majority of aspects |
| 50 | Moderate satisfaction; a middle point between complet and no satisfaction |
| 25 | Minor satisfaction; objective satisfied in some but less than half of the aspects |
| 10 | Minimal satisfaction; obective satisfied to a very small extent |
| 0 | No satisfaction; object not satisfied in any respect |

| | | ALTERNATIVES | | | | | | |
|----------|-------------------------|------------------|-------------|-----------|------------------------------|---------------------------------|-------------|------------|
| | | | | | | | | |
| | | Weighting Factor | Tapered | Rectangle | Rectangle with Circular Side | Rectangle with Two Curved Sides | Ellipse | Circle |
| CRITERIA | Lightweight | 20 | 75% 15 | 25% 5 | 75% 15 | 10% 2 | 100% 20 | 100% 20 |
| | Large Energy Absorption | 20 | 100% 20 | 90% 18 | 90% 18 | 50% 10 | 25% 5 | 10% 2 |
| | Large Moment of Inertia | 50 | 75% 37.5 | 90% 45 | 75% 37.5 | 100% 50 | 25% 12.5 | 10% 5 |
| | Manufacturability | 10 | 90% 9 | 90% 9 | 10% 1 | 25% 2.5 | 50% 5 | 100% 10 |
| | Overall Satisfaction | 100 | 81.5 | 77 | 71.5 | 64.5 | 42.5 | 37 |

Figure 20. Decision matrix to determine the optimal Plug-n-Play shape

Matchbooking Study

Before selecting cross section dimensions, a matchbooking study was conducted in order to help determine how various dimensional parameters affect the stability of the beam's cross section. Matchbooking occurs when the horizontal walls of the cross section buckle during impact. After buckling, the beam's cross section flattens. Since the cross section has changed significantly, it can no longer resist the bending loads that it was designed for. Because the plastic deformation involved in matchbooking is very complex, 2-D FEA was performed to compare the stability of different section geometries. Stability was quantified by the amount of energy a cross section can absorb as it collapses.

The buckling of cross section shapes was analyzed via a modified version of the 2-D Static FEA model presented in the Analysis Tools section. The modification was made to the rigid barrier. Instead of being vertical, the rigid barrier was angled by 5 degrees forcing the cross section of the beam to crush at an angle. An example of the FE model is shown in Figure 21 along with a deformed cross section after matchbooking. As with previous 2-D Static FEA model, this analysis allows for the cross section's energy absorption to be determined. A cross section's resistance to matchbooking is quantified by the amount of energy it absorbs.

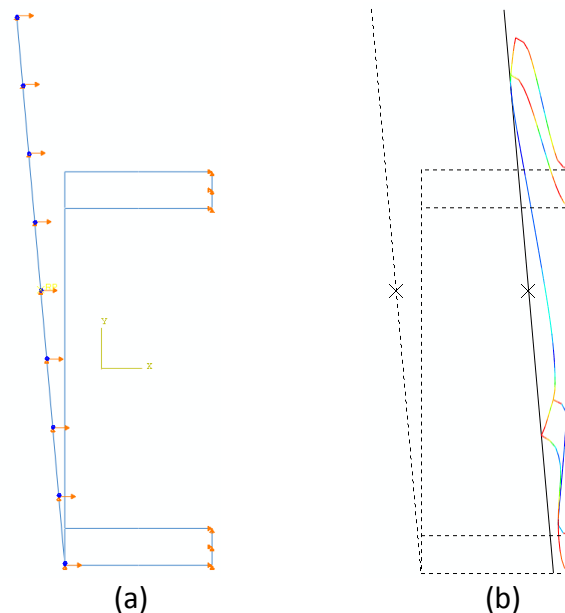


Figure 21. (a) Example FEA model for the base of the Reinforced Plate design and (b) the deformed cross section after matchbooking.

This analysis was determined how changing geometric parameters of the cross section affected the buckling energy absorption. These parameters are shown in Figure 22. Multiple FEA studies were performed on cross sections while modifying only a single parameter at a time. This method allowed for the isolation of the effects on buckling of each parameter. The force-displacement plot in Figure 23 compares the effects of varying the angle α of the walls of the cross section. The plots show that a larger angle α absorbs more energy and therefore is less

prone to matchbooking. Similar plots were made for other parameters and are included in Appendix G.

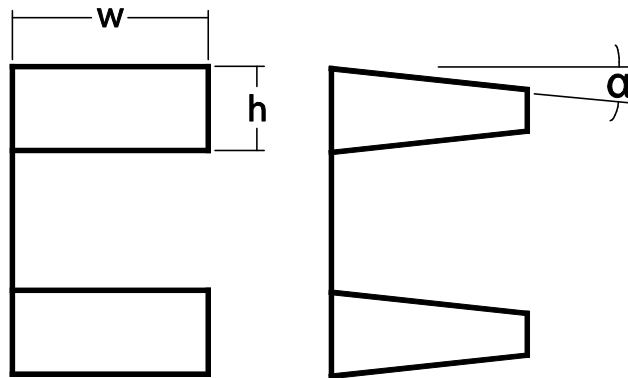


Figure 22. Geometric parameters considered in the matchbooking study.

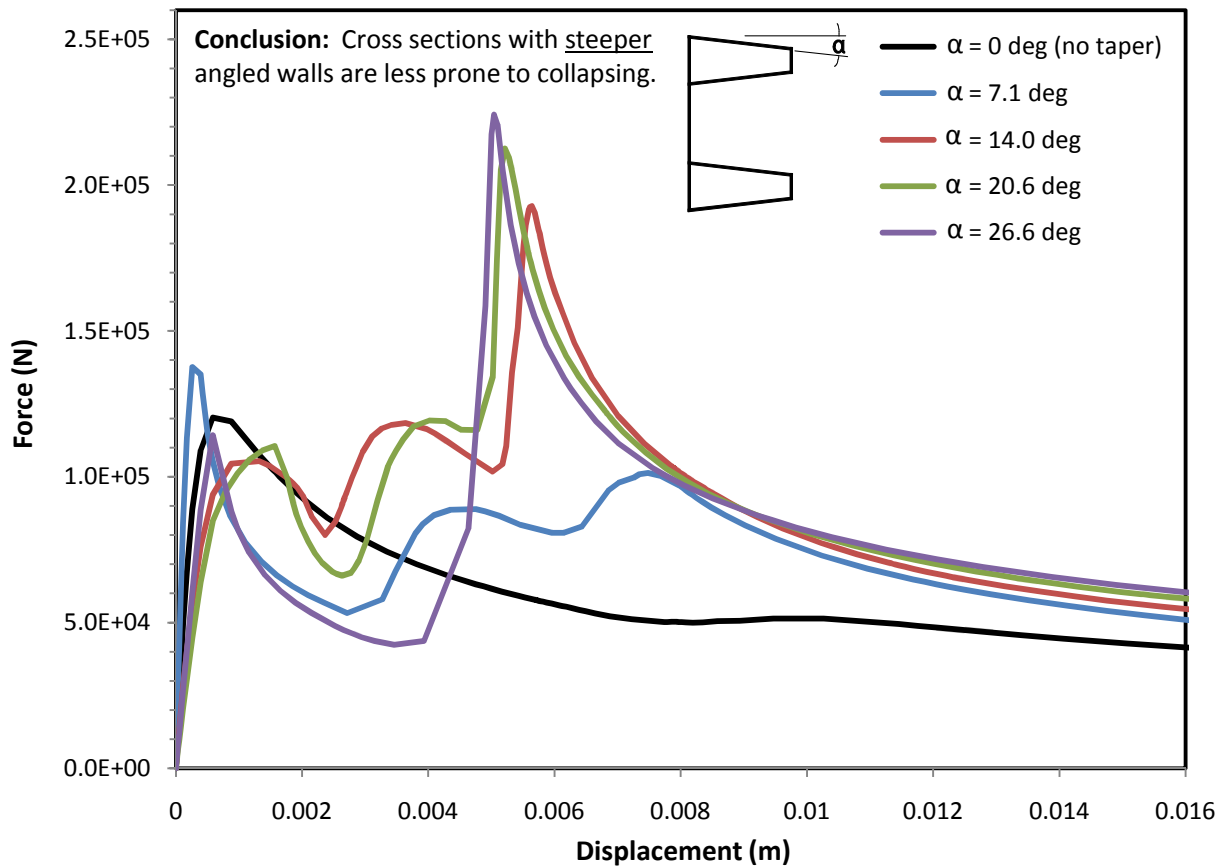


Figure 23. Force-displacement plots at various α values

Table 3 lists conclusions based on the matchbooking parameter study about cross section stability. Using this table as a guide, dimensions for the cross section were selected and tested with 3-D Dynamic FEA.

Table 3. Conclusions drawn from the match booking parameter study.

| Conclusion | Description |
|------------------------------------|--|
| Width w should be minimized | Cross sections with shorter horizontal walls are less prone to collapsing. |
| Height h has no affect | The height of vertical walls on the right side of the cross section do not influence buckling. |
| Tapering increases performance | Cross sections with angled instead of horizontal walls are more stable. |
| Angle α should be maximized | Walls at steeper angles require more energy to matchbook. |

Selecting a Beam Material

As cross section geometries were tested, the effects of various materials on beam performance were also studied through 3-D Dynamic FEA. As described in Figure 24 materials fall into three major categories: strong, tough, and ductile.

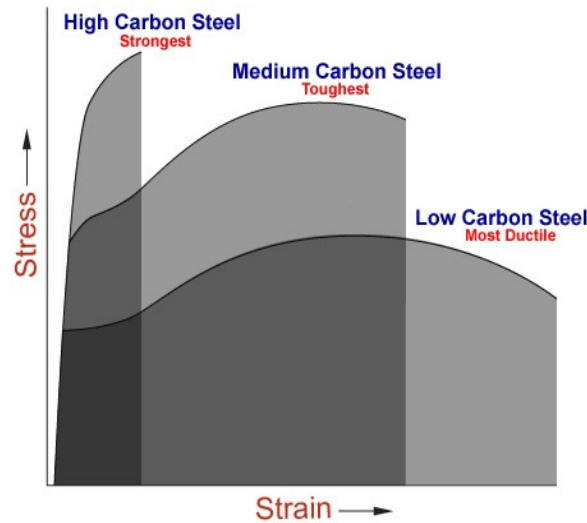


Figure 24. Material Trends relating to stress-strain curves

The higher the yield strength, the more energy the material can absorb elastically but the less energy the material can dissipate overall. Through 3-D FEA, it was found that the beam remained elastic through much of the impact. Because of this, ultra high strength steels were found to be most effective at limiting intrusion. Lower strength steels, such as tough and ductile steels, prove more useful in the case of the pedestrian impacts where a large amount of energy must be dissipated. Since the bumper beam needed to meet challenging intrusion targets, it was decided that the beam should provide the necessary stiffness required to minimized deflection and the energy absorber should provide the necessary softness to meet pedestrian requirements.

Appendix H compares all the materials listed in the AISI passenger car and pickup truck design manual by their strain energy. Strain energy is not true energy and therefore cannot be used to evaluate which material will work under a given impact, but between materials, the strain energy differences clearly show which materials emphasize strength and which emphasize ductility.

Beam Impact Analysis

After choosing the geometry and material of the cross section, a beam impact analysis was done using 3-D Dynamic FEA. This analysis determined whether or not the beam with the selected parameters would meet intrusion and frame rail force requirements specified in Table 1 on page 9. Through many iterations of the beam design phase, a two tapered beam was found to offer the best performance. Designs with three tapers were excessively heavy and stiff.

The RCAR 40% Offset test proved to be the most challenging to meet. Because of this, the dimensions of the beam were greatly influenced by this test. After many iterations with 3-D RCAR FEA model, three characteristics were discovered that allowed beams to pass the test:

- 1) Beams must be rigid in bending. They must have a large moment of inertia in order to minimize intrusion.
- 2) Beams must be crushable. Their cross sections must be able to crush and absorb energy in order to reduce frame rail forces.
- 3) Beams should have thin widths. A thinner width greatly reduces the weight of the beam and also takes up less of the car's package space. When the beam fills up less of the package space, there is extra room for more intrusion of the beam.

These three characteristics are interrelated and work against each other. For example, in order to have a large moment of inertia, a cross section must be wide or have thick walls. Since the width should be minimized, a large moment of inertia can be attained with thicker walls. However, a cross section with thicker walls is not as easy to crush as one with thin walls. Because the three characteristics cannot all be fulfilled, the final designs are the result of the best balance.

From 3-D Dynamic FEA, the Flat Plate Reinforcement Plug-n-Play type from Figure 16 was found to be ineffective. Adding additional reinforcements did not absorb enough of the impact energy required of the IIHS and RCAR tests. More energy could be absorbed by adding attachments to the front of the beam instead. Since steel energy absorbers (discussed in the following section) proved useful in absorbing energy, and two tapers satisfied test requirements, a simple B-shape cross section was chosen as the base beam. The Plug-n-Play attachments took the form of various steel energy absorbers. This new Plug-n-Play design resembles the B-shape with

External Reinforcement that was found to be the second best Plug-n-Play type as shown in the decision matrix in Figure 15.

Because the steel energy absorber plays a critical role in the performance of the overall bumper system, it is difficult to design the beam's cross section without considering it. Instead of determining the dimensions of the cross section through a subsystem analysis, they must be determined through a system-wide analysis. This was done in the System Impact Analysis step of the design process.

Energy Absorber

Introduction

The European New Car Assessment Program (EuroNCAP) requires that a test leg must experience accelerations of less than 150 g's upon impact at 25 mph. In a normal collision with no energy absorption mechanism, the leg experiences much greater acceleration than above, due to a high stiffness of the beam. The solution to this problem is to attach an energy absorber to the front of the bumper beam which is specifically designed to reduce the acceleration of a pedestrian leg during impact.

Two candidates were initially investigated for use as an energy absorber: Expanded Polypropylene (EPP) foam and steel.

EPP foam typically has a low yield strength and can deform over a long distance (Figure 25). These properties are excellent at reducing the force an object feels on impact and effectively reduces the stiffness of the overall bumper system. As foam density increases, the yield strength becomes larger. Foam deflects at approximately a constant force until 80% of its original length, and then it exponentially approaches infinity. In addition to having easily modifiable mechanical properties, EPP foam has a much lower density than steel which makes for a light weight addition to a bumper.

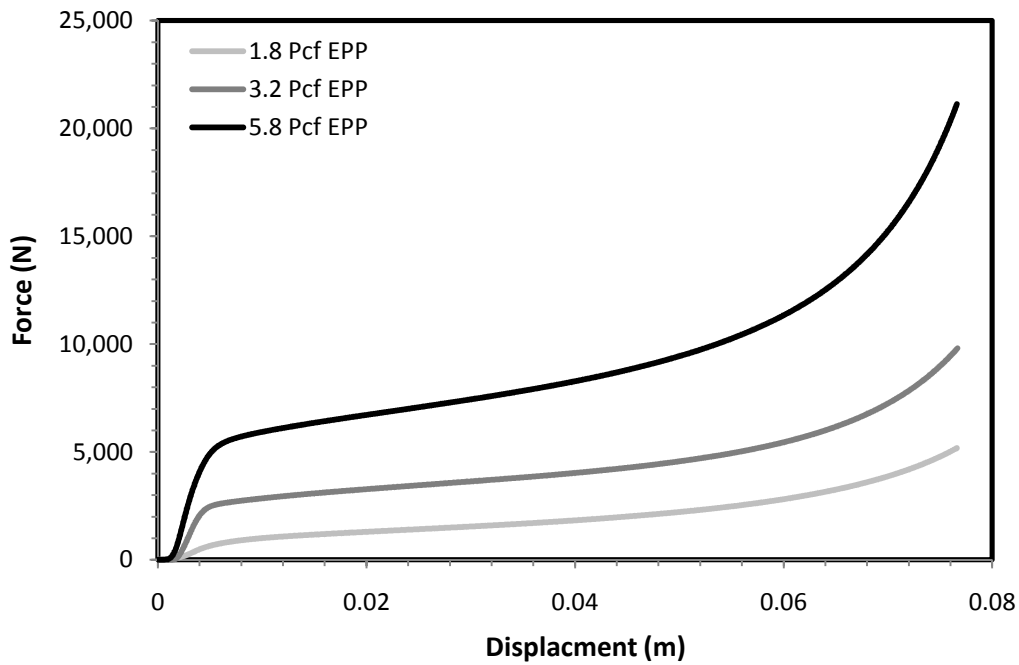


Figure 25. Uniaxial compression tests for different densities of EPP.

Steel energy absorbers (SEA) are another method used to reduce the impact acceleration. The goal of SEAs is the same as EPP, but is accomplished through design of the cross section instead of density. Unlike foam, a steel energy absorber is also useful during an impact to reinforce the bumper beam by adding to its bending stiffness. This allows for a lighter base beam than would be required with a foam EA.

Preliminary Analysis

Preliminary analysis using the 2-D Static FEA model showed that an SEA made out of 140T Steel with the shape seen in Figure 26 could be competitive with EPP foam. A small yield stress and a large deflection at a constant force are characteristic traits of foam that need to be matched or exceeded. SEA Susie (Figure 26) closely matched the force-displacement curve of EPP foam.

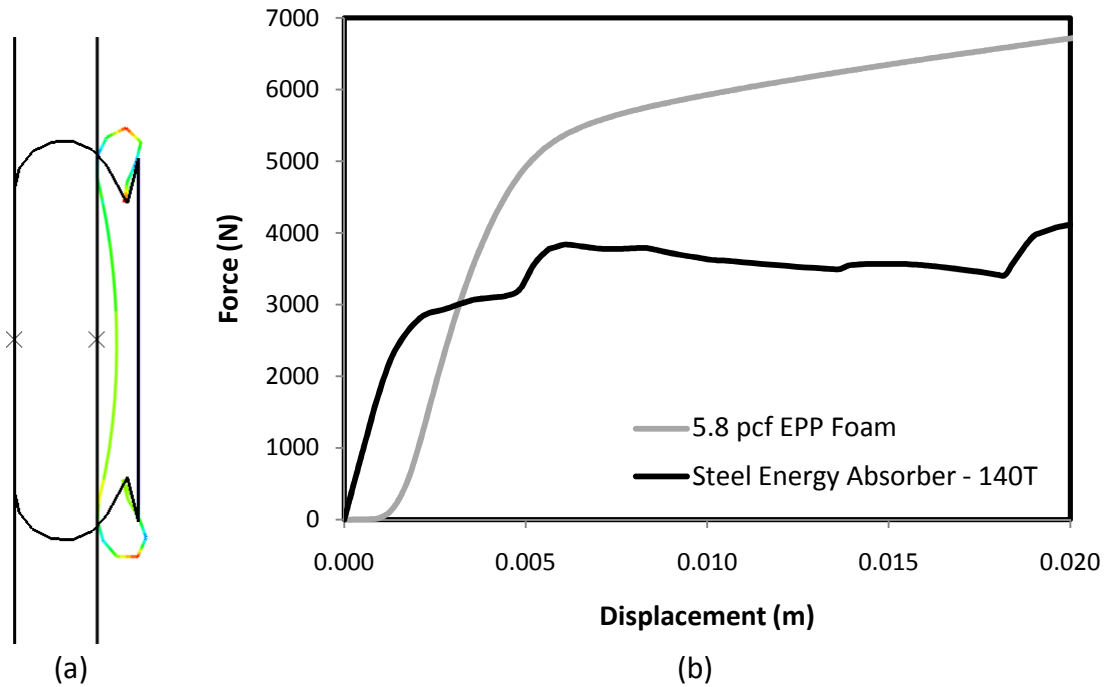


Figure 26. Preliminary Steel Energy Absorber design “Susie” plastically deforms similarly to how EPP foam deflects under a given load.

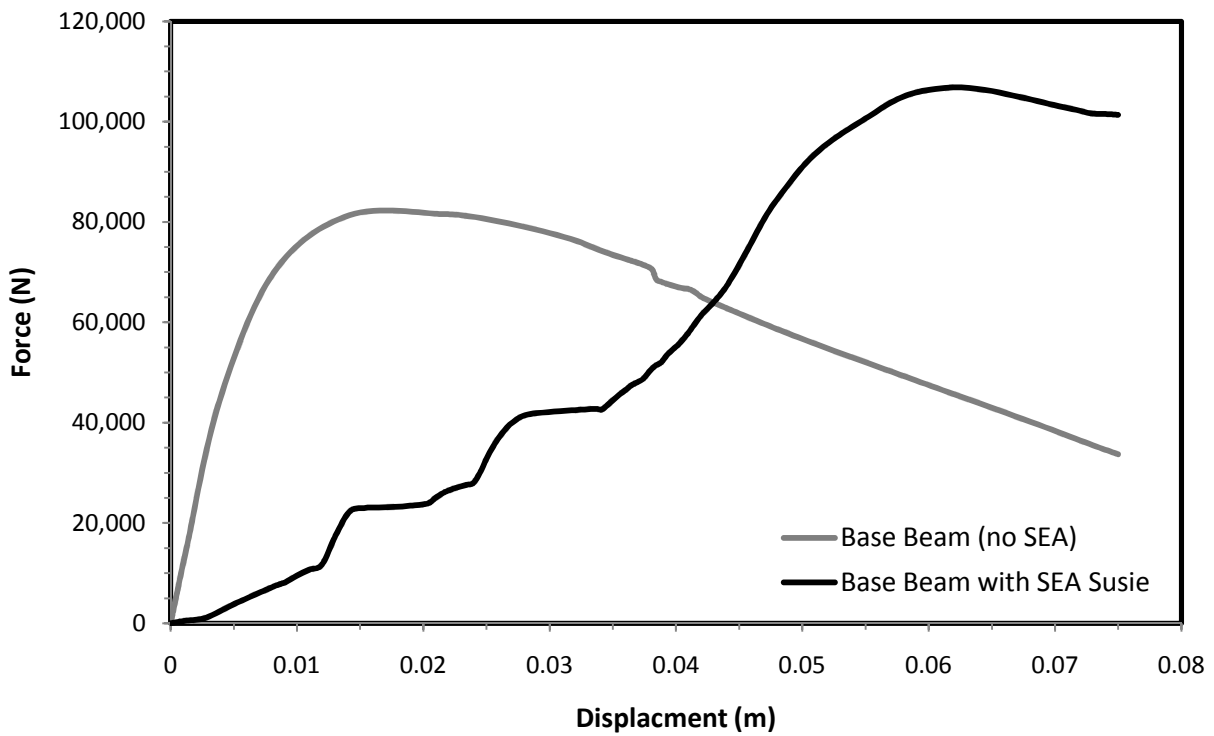


Figure 27. Static 3-D FEA test comparison which demonstrates the influence a SEA has on a bumper beam.

Figure 27 depicts the force deflection curves resulting from a static 3-D FEA three point bending test. The graph demonstrates the influence a steel energy absorber has on a bumper beam. The force on a simple bumper beam rises quickly at the start then tapers off as deflection increases. In contrast, a bumper beam that has an SEA gradually rises to its peak force. The initial spring stiffness of the base beam is 8.56 kN/mm, while the bumper beam with the SEA has a value of 1.38 kN/mm.

For the pedestrian impact test, a lower stiffness results in energy dissipation over a longer time span. This decreases the acceleration the pedestrian test leg experiences during an impact. Another benefit of a SEA is that after the SEA has been crushed, the remaining material reinforces the bumper beam, which provides more elastic energy absorption before any plastic yielding of the bumper beam takes place.

SEA Impact Analysis

Because initial tests showed promise for the use of steel as the energy absorbing material, detailed analysis was performed to determine the best material and geometry for a steel energy absorber.

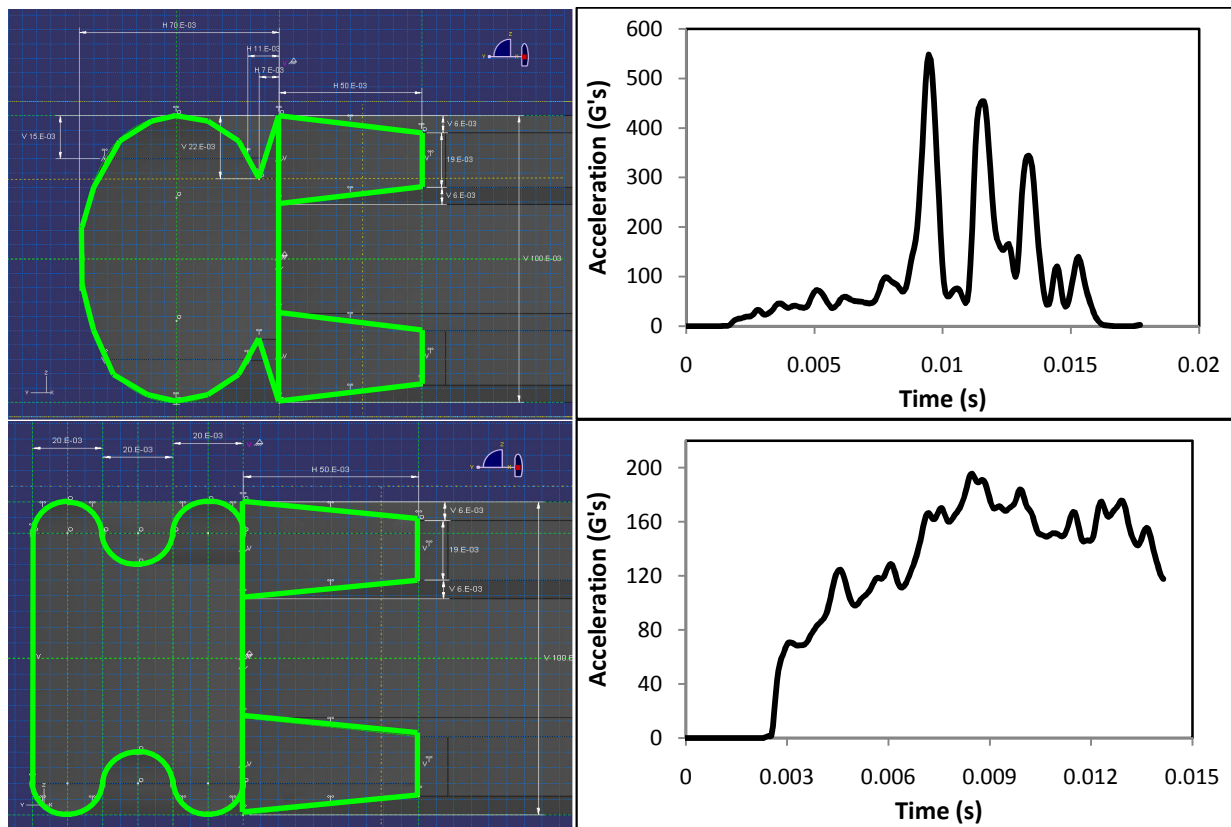


Figure 28. 3D dynamic impact of various SEAs prototype provided acceleration data of the leg.

Complex geometry coupled with the effect of material properties required many iterations of the SEA to arrive at a final design. Experimentation depicted in Figure 28 determined the intricacies of the SEA geometry: curvature of the SEA, where or where not to include sharp corners, overall height, overall width, wall thickness, etc.

Material selection had a significant impact on the performance of the SEA. Higher strength steels resulted in a stiffer EA and higher accelerations on the leg. Conversely, low strength steels were too soft and allowed the leg to deflect so far that it impacted the bumper beam.

Through iteration, a design was selected which maintains leg acceleration under 150 g's. This design and its corresponding acceleration curve is displayed in Figure 29.

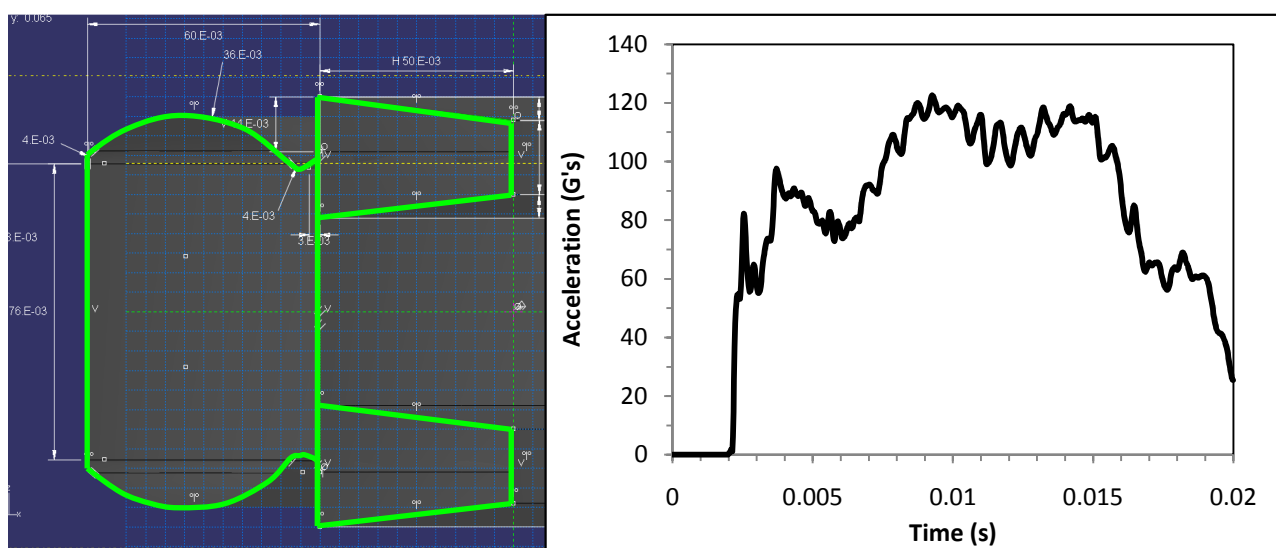


Figure 29. FEA acceleration results of a successful SEA design.

Advanced Impact Analysis

After designing a SEA that met pedestrian requirements and deciding on a general B-shape beam cross section, a system-wide 3-D Dynamic FEA model was used to determine the specific dimensions of the beam's cross section. Much iteration with various geometric parameters were run in the 3-D Dynamic FEA. Tables of results are provided in Appendix I. The tables list the beam's dimensions (overall beam height and width, the taper height and angle, and the material thickness) along with intrusion and frame rail force results for each iteration. After over one hundred iterations, the best performing beams for the Chinese, North American, and European markets were selected based on whether or not they satisfied their corresponding region's performance requirements and on their masses. These designs are presented in Chapter 4.

CHAPTER 4: FINAL DESIGN

The final designs for the Chinese, North American, and European bumper reinforcement beams are shown in Figure 30. They are assembled using at most two of the following three parts: a B-shape base beam and two D-shaped steel energy absorbers, each of a different thickness.

Bumpers marketed toward China only consist of the B-shape base beam. These bumpers are not fitted with any type of energy absorber. For the North American markets, a 0.7 mm thick steel energy absorber is attached to the front of the base beam to provide extra stiffness and energy absorption capabilities. Bumpers marketed toward Europe consist of the base beam fitted with a 1.1 mm thick steel energy absorber. The thicker energy absorber adds even more stiffness to the beam and also absorbs enough energy to meet Euro NCAP pedestrian requirements.

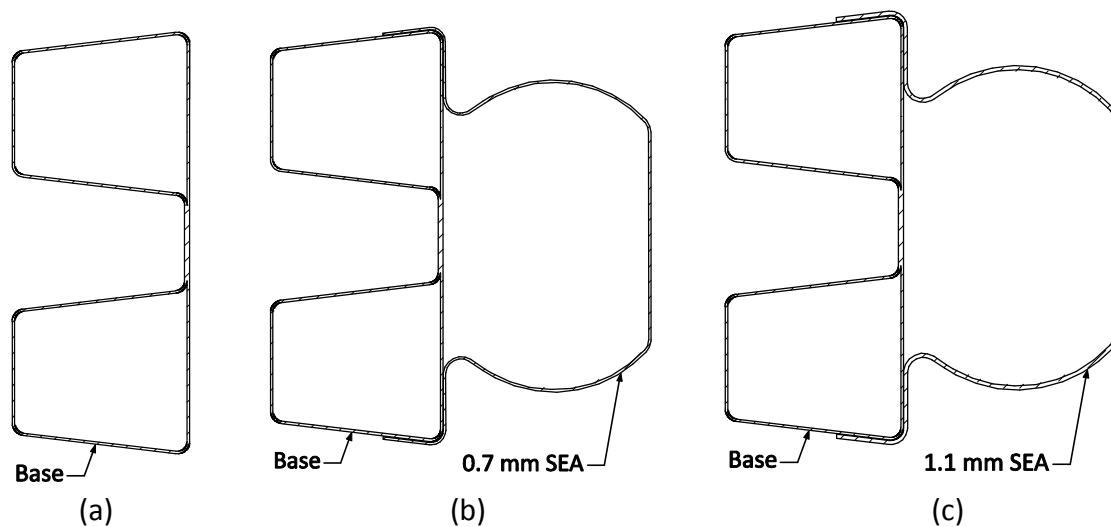


Figure 30. Final beam reinforcement designs for (a) Chinese, (b) North American, and (c) European markets.

Packaging space

The average D-segment packaging space contains an available region that a bumper beam can be placed in. Figure 31 shows the available space with applicable dimensions.

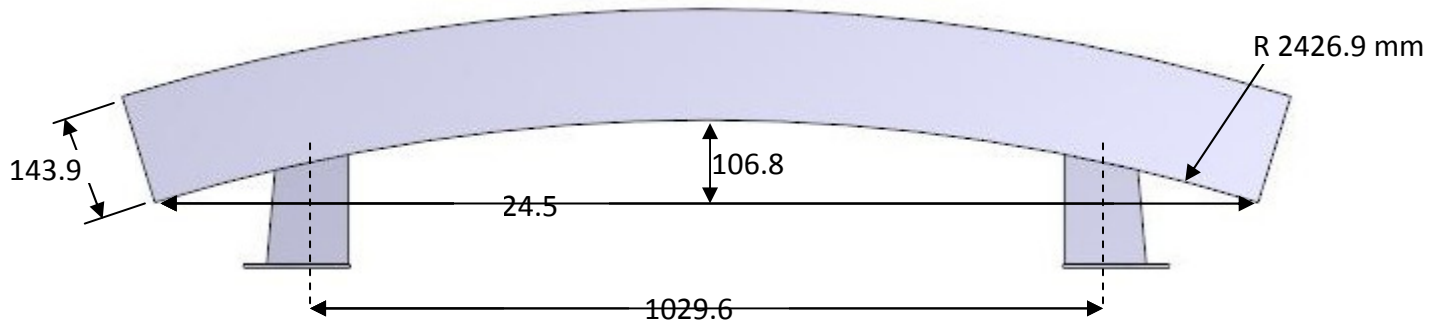


Figure 31. Average D-segment packaging space with dimensions

The designed B-section bumper beam has a higher sweep than the packaging space, yet is still able to fit within it. In fact, the higher sweep leaves portions at the front of the package space unfilled allowing for greater creativity and possibility when styling the fascia of the car. Figure 32 depicts how the beam fits within the space.



Figure 32. Cal Poly bumper beam fit to packaging space

Base Beam – B-shape



Figure 33. Base Beam for bumper system

The base beam is roll formed from M220. Details on the mechanical properties of M220 are attached in Appendix H. All inside radii are four times the thickness to prevent failure of material during the roll forming process. For example, the RCAR SEA is 1.1mm thick so the radii are 4.4mm. Complete part drawings depicting size, sweep, and holes for attaching crush cans are attached in Appendix J.

Steel Energy Absorber (SEA)



Figure 34. Steel energy absorber for bumper system

The Steel Energy Absorber is stamped from EG-HF 60. Details on the mechanical properties of EG-HF 60 are attached in Appendix H. Sheets of steel are cut prior to stamping in order to make the details shown in Figure 35. Six equally spaced tabs line the top and bottom measuring 30mm x 20mm. Slots in the tabs, as shown in Figure 35, measure 20mm x 5mm as recommended by Shape Corp. Also cuts on the SEA are made to provide room to bolt the bumper and SEA to the crush cans. The extended tabs of the SEA are welded to the base beam with slot welds. Detail drawings are attached in Appendix J.

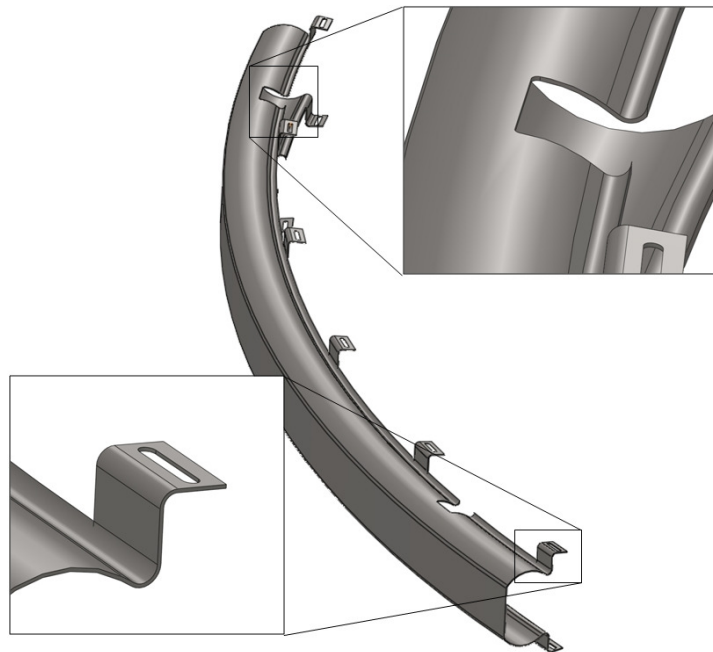


Figure 35. Enlarged view of the SEA tabs and cuts

M8 Plain steel nuts are used to fasten the beam to the crush cans. For the prototype, an extra nut is used between the beam and the crush cans to accommodate gap introduced when using a beam with larger sweep than the crush cans are designed for. M8 Stainless steel washers are placed between the nut and the back side of the base beam. An assembly view in Figure 36. A dimensioned drawing with a Bill of Materials is attached in Appendix J.

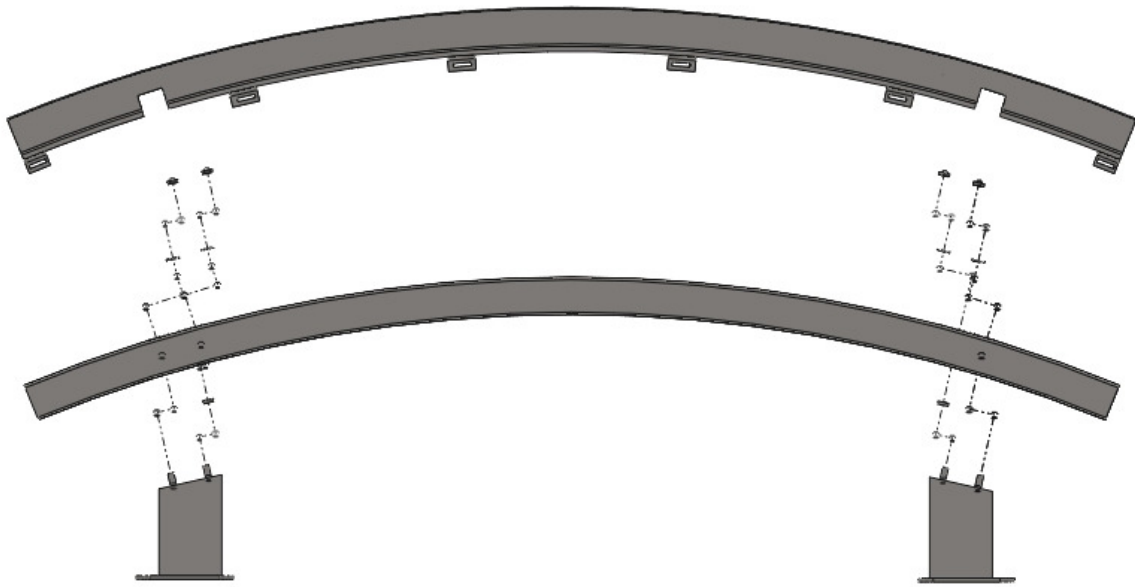


Figure 36. Assembly layout for Bumper Beam system

For the prototype design, the crush can shown in Figure 37 is used. These crush cans should be redesigned specifically for this beam by increasing the angle of the face so that they are flush.



Figure 37. Crush Can provide by SHAPE CORP.

Analysis Results

Table 4. Test summary for final bumper designs.

| Test | Test Results | | | | | | | | | |
|-------------------|------------------|--------------------|----------------|--------------------------|---------------------------|----------------------|-----------------------|---------------------|-----------------|--------------------|
| | Test Speed (m/s) | Max Intrusion (mm) | Intrusion (mm) | Left Crush Can Disp (mm) | Right Crush Can Disp (mm) | Left Rail Force (kN) | Right Rail Force (kN) | Intrusion Pass/Fail | Crush Can Force | EA |
| GB17354-1998 | 0.745 | 88.9 | 31.6 | 0.5 | 1.2 | 11.7 | 11.0 | Passed by 57.3mm | Pass | Base beam only |
| IIHS Full Frontal | 2.485 | 88.9 | 88.1 | 1.4 | 3.8 | 31.3 | 30.6 | Passed by 0.8mm | Pass | With D6080-0.7 SEA |
| IIHS 15% Offset | 1.242 | 10.0 | 46.1 | 0.2 | 1.7 | 4.2 | 31.6 | Failed by 36.1mm | Pass | With D6080-0.7 SEA |
| RCAR Full Frontal | 2.485 | 88.9 | 77.4 | 1.5 | 4.1 | 33.1 | 29.6 | Passed by 11.5mm | Pass | With D6080-1.1 SEA |
| RCAR 40% Offset | 3.727 | 88.9 | 87.7 | 0.8 | 85.1 | 17.9 | 65.0 | Passed by 1.2mm | Pass | With D6080-1.1 SEA |

FEA results of the final designs are summarized in Table 4. Crash test goals were:

- Rear bumper intrusion could not exceed 55 mm beyond the back of the package space
- Rail force could not exceed 80 kN in either rail

The China beam passed the GB17354-1998 test by the largest margin of 57.3 mm. The US bumper passed IIHS full frontal test, but failed the IIHS offset test. The European beam passed the RCAR full frontal test. For the RCAR 40% offset test, the beam passed with the second narrowest margin 1.2 mm.

In the offset test, the barrier impacts the right 15% of the car. Given the current configuration, the barrier has no direct contact with the crush can. To improve performance on this test, the bumper system configuration must be changed.

Maintaining the rail force below 80kN dictated beam design for the RCAR 40% offset test. In this test, some energy was absorbed by the SEA and the collapse of the beam's cross section, but the primary energy absorber was the crush can. As seen in Table 4, the crush can deflected 85.1 mm in this test, which is very near the limit of the crush can's ability to collapse. Force increases dramatically beyond this point as seen in Figure 51 of the Appendix E.

For the EuroNCAP pedestrian test, the test leg had a maximum acceleration of 122.6 g's which is 18.3 % below the required acceleration. The rotation of the knee and shear force were not considered.

For FEA validation, see Appendix E.

CHAPTER 5: PRODUCT REALIZATION

The base beam and the SEA attachments were designed to be mass produced. The base beam is to be rolled formed and the SEA is to be stamped. While these manufacturing methods offer low unit cost of production, they require a large investment in capital. Because the actual bumper design cannot be easily fabricated, only simplified versions of the bumper will be prototyped for testing.

The base beam has a shape similar to existing beams for the Nissan Altima and was not prototyped because test data for similar beams are available. However, the SEA has a unique shape and a simplified version of it was prototyped for testing.

The SEA was simplified by eliminating the sweep (making it flat) and only fabricating 609mm long section for testing. It was made of AISI 1008 sheet steel measuring 0.84 mm thick instead of the final design's 1.1mm HF-60. A sheet metal break was used to create the cross section, with several short, straight sections approximating the curved edge. Using this fabrication method, the complete prototype could not be made from a single sheet of steel. Instead, as shown in Figure 38, the SEA was first bent on the sheet metal break, then cut in half to create two identical pieces, and finally TIG welded together. The location of the weld down the center of the front face of the beam was selected because the pedestrian FEA model showed little deformation of the front face.

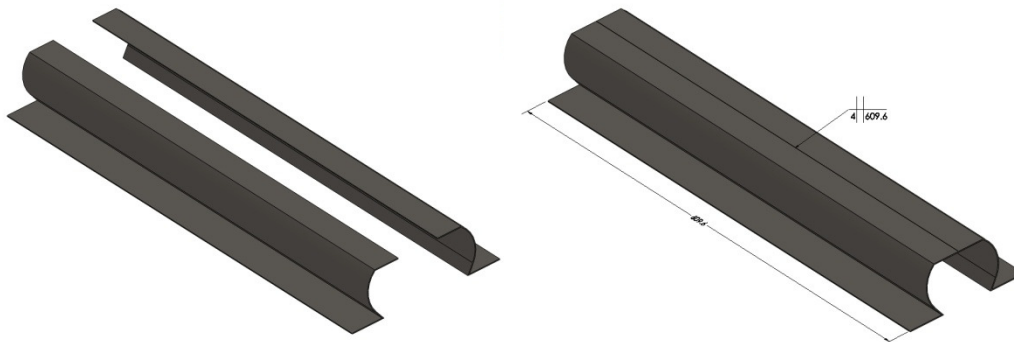


Figure 38. The SEA for testing was fabricated from two pieces of sheet metal. Two side were bent on a sheet metal brake and TIG welded together.

When the bumper is actually mass produced, the cold working of the steel as it is formed should be taken into consideration. The bumper may need to be annealed after fabrication. Also, the steel may require heated during fabrication so that it does not crack. This could be done by hot roll forming the base beam and hot stamping the SEA.

CHAPTER 6: DESIGN VERIFICATION

The complexity of the bumper design limits the degree to which it can be replicated as a prototype. Therefore, verification of the final design was performed through a series of FEA

model validations. Real world tests were modeled and simulated using the FEA model. The results of the simulation were compared data collected during testing. A pendulum impact tester replicated the IIHS full frontal test, and drop tests with a legform represented a scaled down version of the pedestrian impact test.

Pendulum Impact Test

A Cal Poly senior project and a master thesis have developed a pendulum impact test apparatus designed to simulate a car crashing into a bumper system. The testing apparatus can apply a maximum force of 3000 lb at a speed of 5 mph. A diagram of the test rig is shown in Figure 39. The existing bumper fixture can be used to mount the bumper beam prototype and is designed to replicate the IIHS and RCAR Full Frontal impacts. Load cells and position transducers provide accurate force and deflection data of the bumper system. An emitting diode IR receiver measures the impact speed of the pendulum carriage.

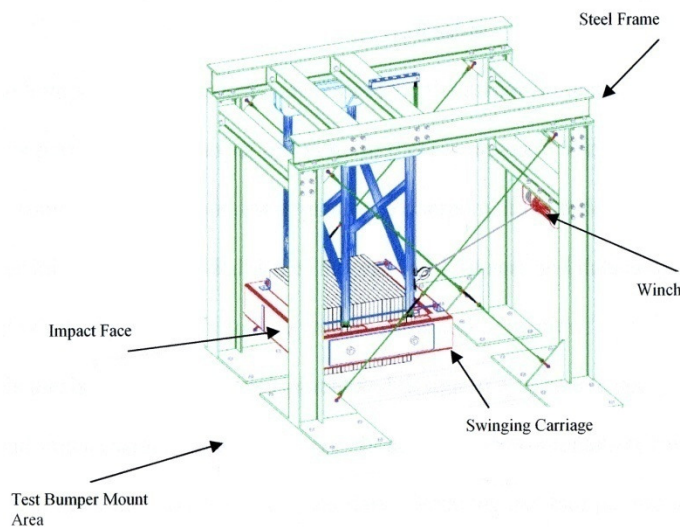


Figure 39. Pendulum Impact Test Setup

Team Mjollnir, the group in charge of refurbishing the pendulum tester, provided data from several different tests performed on the same bumper design. For comparison, our ABAQUS FEA model was used to simulate the same impact.

Average data from 10 bumper impact tests were compared to FEA results below. In order to closely match test conditions, the average speed of the test was used as the speed input for the FEA model. Results show that the FEA model over predicts both the intrusion and crush can force. An average intrusion of 39.0 mm was measured, while simulations predicted 60.3 mm (54.6% above test measurements). The average measured force was 75.9 kN, with a prediction of 78.8 kN (3.8% above test measurements).

Table 5. Summary of comparison between testing and FEA data

| | Intrusion (mm) | Force (kN) | Speed (km/h) |
|-------------|----------------|------------|--------------|
| Test Data | 39.0 | 75.9 | 8.0 |
| FEA Results | 60.3 | 78.8 | 8.0 |

This comparison indicates that FEA predictions are on the conservative side, with the real world bumper performing better than expected. Therefore, the final design for this project should also show performance improvements over FEA predictions.

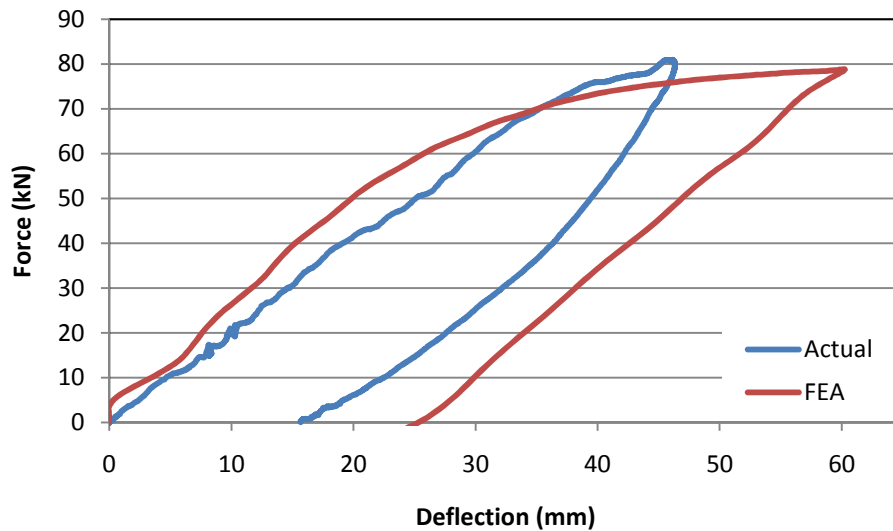


Figure 40. FEA was conservative in deflection predictions

Impacts were also compared graphically for one of the tests. The force-deflection curves in Figure 40 show a similar elastic modulus for both tests. The spring back rate was also almost identical. The FEA model appears to have predicted more plastic deformation, resulting in an increased deflection, and an increased permanent deflection by about 10 mm.

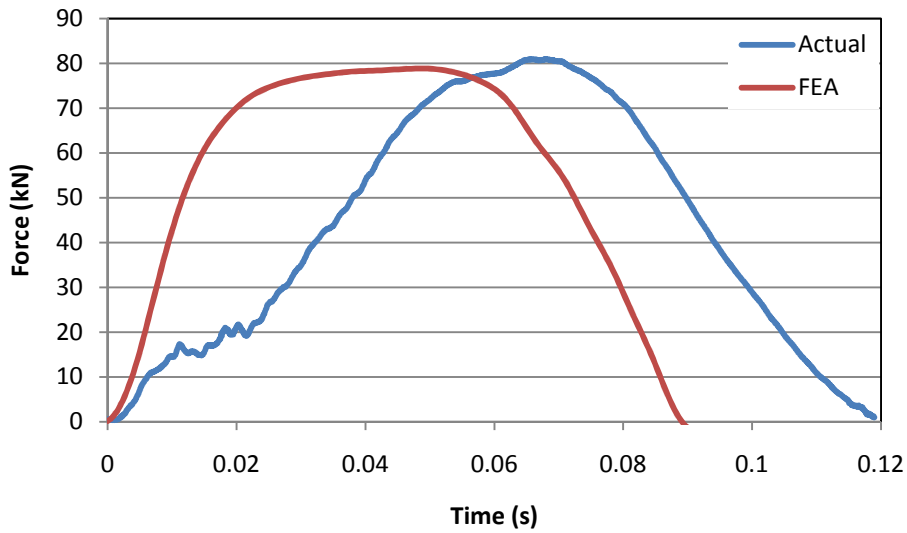


Figure 41. Compared to testing, simulated results depicted a nearly identical peak force

Rail force increased much quicker in the FEA prediction than the actual test, which fits with the general assumption that an FEA model will be stiffer than the real part.

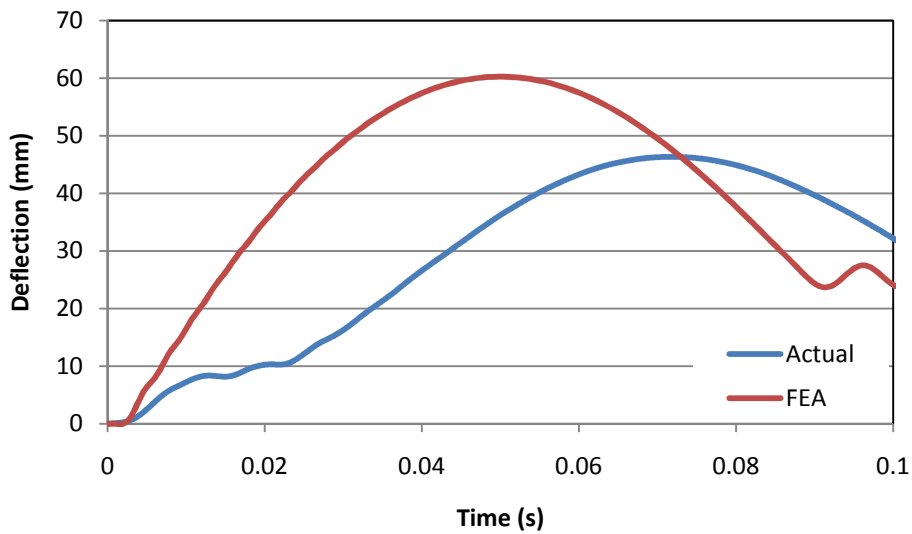


Figure 42. Deflection-Time comparison

A deflection comparison shows the FEA model to be rather conservative. As seen in Figure 42, the model predicted about 60 mm, while the test measured about 45 mm. This result indicates that the final design may deflect less than predicted, resulting in increased performance.

Pedestrian Impact Test

The Steel Energy Absorber was designed to be stamped but the cost of prototype manufacturing would have been excessive. Therefore, only small simplified sections of the SEA were fabricated and tested. The test consisted of dropping a model legform from a 20 feet tall balcony onto a section of the SEA on the ground. The leg was made of a 3 inch diameter steel pipe wrapped in foam pipe insulation. An accelerometer mounted vertically on the legform captured acceleration data. These data were then compared to FEA acceleration data from a simulated drop test. An overview of the testing set-up is shown in Figure 43.



Figure 43. A legform was dropped from a 20 ft tall balcony onto a test section of SEA on the ground below.

Test Set-Up

The SEA prototype was bolted to a 4' x 4' wooden test platform shown in Figure 44 and placed at the base of the balcony. A high speed camera was placed approximately 10 feet from the test platform and at a level height with the SEA to record footage of the deformation and the axial angle at which the legform impacted the SEA. The high speed camera recorded the impact at 20,000 frames per second at a screen resolution of 250x250 pixels. Another camera captured any rotation from the horizontal plane which could also affect acceleration data. Both angles were used in transforming raw acceleration data to report true vertical acceleration.



Figure 44. A test section of SEA was bolted onto a plywood test platform and placed beneath a balcony for the legform to be dropped on it.

The test legform shown in Figure 45 wrapped with 0.5 inch thick foam pipe insulation to simulate human tissue and protect the accelerometers. The total test leg weighed 12 pounds. Figure 45's exploded view shows the accelerometer mount, which consisted of a square bracket welded to the surface of the steel pipe and threaded for secure mounting.

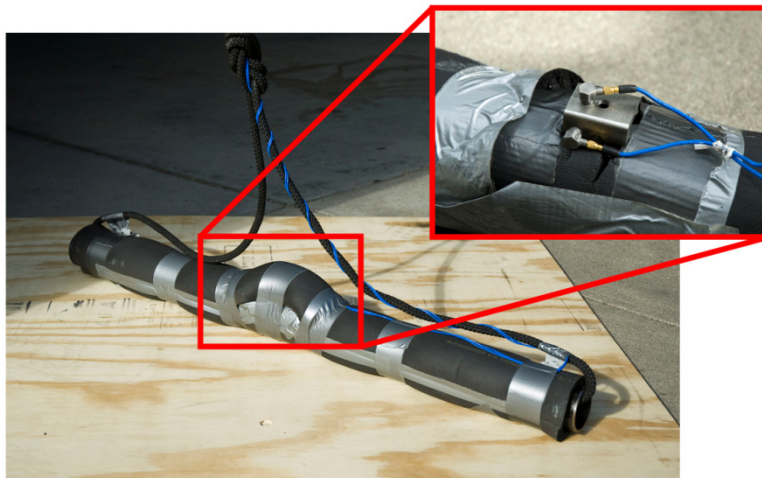


Figure 45. Legform used for drop testing

A data acquisition system was placed on the balcony and connected to the accelerometers via BNC cables to measure the legform's acceleration upon impact. To protect the BNC cables and accelerometers from damage, rope was tied between the pipe and balcony railing to prevent erratic rebounding after impact. Accelerometers on the top of the legform were covered with an extra layer of protective foam. The BNC wires were wrapped around a rope to prevent them from falling freely.

The leg was held parallel to the ground and released after a countdown. Upon countdown, the DAQ began recording data points at 2560Hz. Upon impact, the high speed camera was triggered and captured a total of 4 seconds of footage.

Results

The acceleration data obtained during testing is plotted against the data from the FEA model in Figure 46.

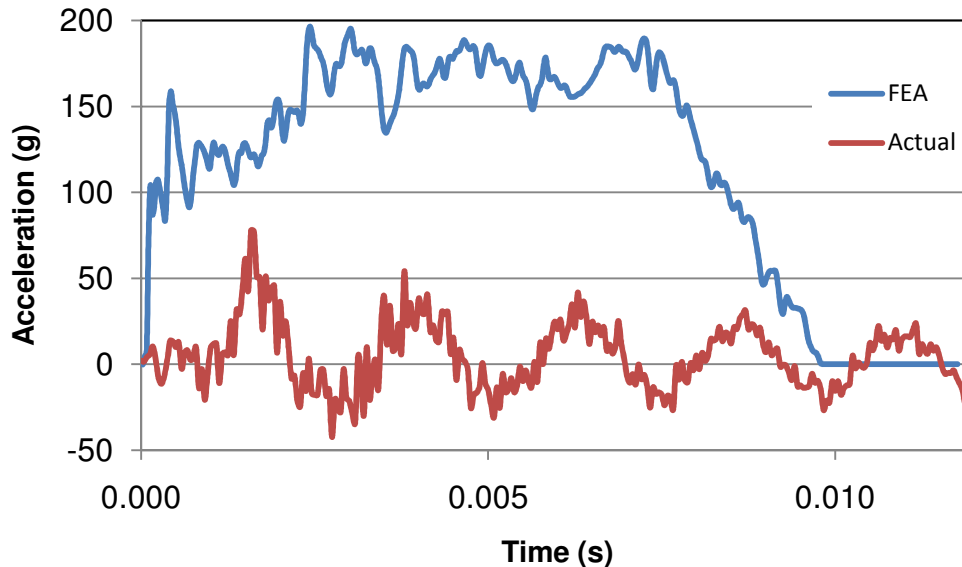


Figure 46. Pedestrian Leg Drop Test Comparison

The acceleration measured in the actual test was significantly lower than the acceleration predicted by the FEA model. This could be due to a few factors. The pedestrian leg was modeled as a rigid body, thus it could not absorb any of the impact energy through its own deflection. The legform used in testing was covered in foam to imitate human tissue, which could have absorbed some of the impact energy. Also, the plywood absorbs some of the energy and much of the energy is stored elastically in the leg and did not dissipate into the beam. In addition, high speed footage shows the legform deflecting on impact, and vibrating immediately after (Figure 46 clearly shows this vibration). These energy absorbing characteristics of the legform may account for the discrepancy between measured and predicted acceleration. Regardless, because the model proved to be conservative, the final design is expected to exhibit a lower max acceleration than predicted by FEA.

Figure 47 shows a deformation comparison between the prototype SEA and FEA model. It is clear from this visual comparison that the prototype bumper deformed as expected, and the deflection distances were very similar for both.

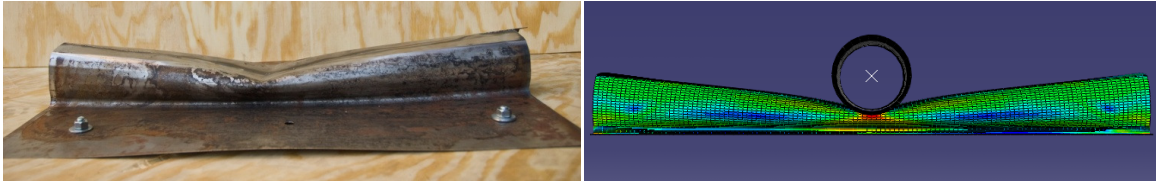


Figure 47. Comparison of deformation of the SEA from the actual leg drop test and the FEA model.

Recommendations

During testing, the leg after impact rebounded and rotated aggressively in the air. The micro dot cables connected to the accelerometers broke at the connection points by the twisting and turning of the leg after impact. In addition, a halogen light broke upon contact with the nylon support rope immediately following a drop test.

For future tests, rope should be used to anchor both ends of the legform to resist rotation. The method used in testing only utilized one support line, and proved insufficient at controlling the rebound of the legform. Also, the steel energy absorber should be bolted to an elevated platform as opposed to resting on the ground. During impact, the legform would rotate and hit the ground, reducing the amount of energy transferred to the SEA. Elevating the SEA would reduce unintended collisions with the ground.

To prevent damage to the halogen lights, they should only be turned on right before the drop test, and turned off immediately after. Leaving the lights on between drops increased the temperature and made them more susceptible to vibration damage. If more powerful lights were used, they could be placed further from the impact zone. This way, if the bumper were to rebound out of control, it would be less likely to hit the light fixtures.

CHAPTER 7: CONCLUSIONS

It is feasible for a steel bumper system consisting of Plug-n-Play attachments with a Steel Energy Absorber to perform competitively across markets on a global scale. The current bumper design passes China, IIHS Full Frontal, RCAR Damageability, RCAR low speed impact, and EuroNCAP pedestrian tests. It is recommended that the packaging space be lengthened in order to meet IIHS Offset Testing. As vehicle and pedestrian crash test standards become more stringent, new and innovative ways of absorbing impact energy must be incorporated in future bumper designs. One method that should be further explored is the incorporation of a steel energy absorber (SEA) in place of the traditional foam energy absorber. The SEA not only adds structural rigidity to the bumper beam, but also absorbs impact energy by plastically deforming which allows the system to meet pedestrian crash test requirements. Pedestrian testing demonstrated that the acceleration requirement for the EuroNCAP test is safely met by the current SEA design.

Verification of the FEA model also proved successful. This validation was accomplished by comparing results of real world tests and simulation results. Comparisons show that the FEA model predictions were either very close or conservative when compared to actual results. The FEA over predicts deflection by 54% and crush can force by 3.8%. This final comparison demonstrates with a high level of confidence that the steel bumper system created with the FEA model will perform better than predicted.

REFERENCES

1. China National Standard. "Testing Specification Summary: GB17354-1998." Shape Corp.
2. "Cold Forming Principles." National Machinery. February 2009.
http://nationalmachinery.com/coldforming_principles/coldformingprinciples.php
3. "Design for Manufacture in Cost-Effective and Recyclable brass." Copper Development Association. February 2009. <<http://www.brass.org/Training/Lecture/sld038.htm>>
4. "Roll Forming Basics." SAMCO. Thefabricator.com. February 2009.
http://www.thefabricator.com/RollForming/RollForming_Article.cfm?ID=1032
5. Sindrey, D.A. "Steel Bumper Systems for Passenger Cars and Light Trucks." SAE Technical Paper Series. 1999.
6. "Steel Bumper System for Passenger Cars and Light Trucks." *American Iron and Steel Institute*. June 30, 2006: 123-129.
7. "Toughness". NDT Resource Center. March 2009. <http://www.ndt-ed.org/EducationResources/CommunityCollege/Materials/Mechanical/Toughness.htm>
8. Uikay, D.U. et al. "Bumper System Development to Improve Compatibility per Proposed IIHS Bumper Barrier Criteria." SAE Technical Paper Series. 2006.
9. US Department of Transportation. "Testing Specification Summary: CFR49 Part 581." Shape Corp.

APPENDICES

| | |
|---|----|
| Appendix A: QFD Table | 53 |
| Appendix B: Gantt Chart | 54 |
| Appendix C: Preliminary Analysis | 57 |
| Appendix D: BMAC 3000..... | 61 |
| Appendix E: FEA Model Description | 62 |
| Appendix F: Plug-n-Play 2-D FEA Results | 70 |
| Appendix G: Matchbooking Study | 74 |
| Appendix H: Material Comparison..... | 77 |
| Appendix I: FEA Data Sheets | 81 |
| Appendix J: Detailed Drawings | 85 |
| Appendix K: Pedestrian Test Plan | 92 |

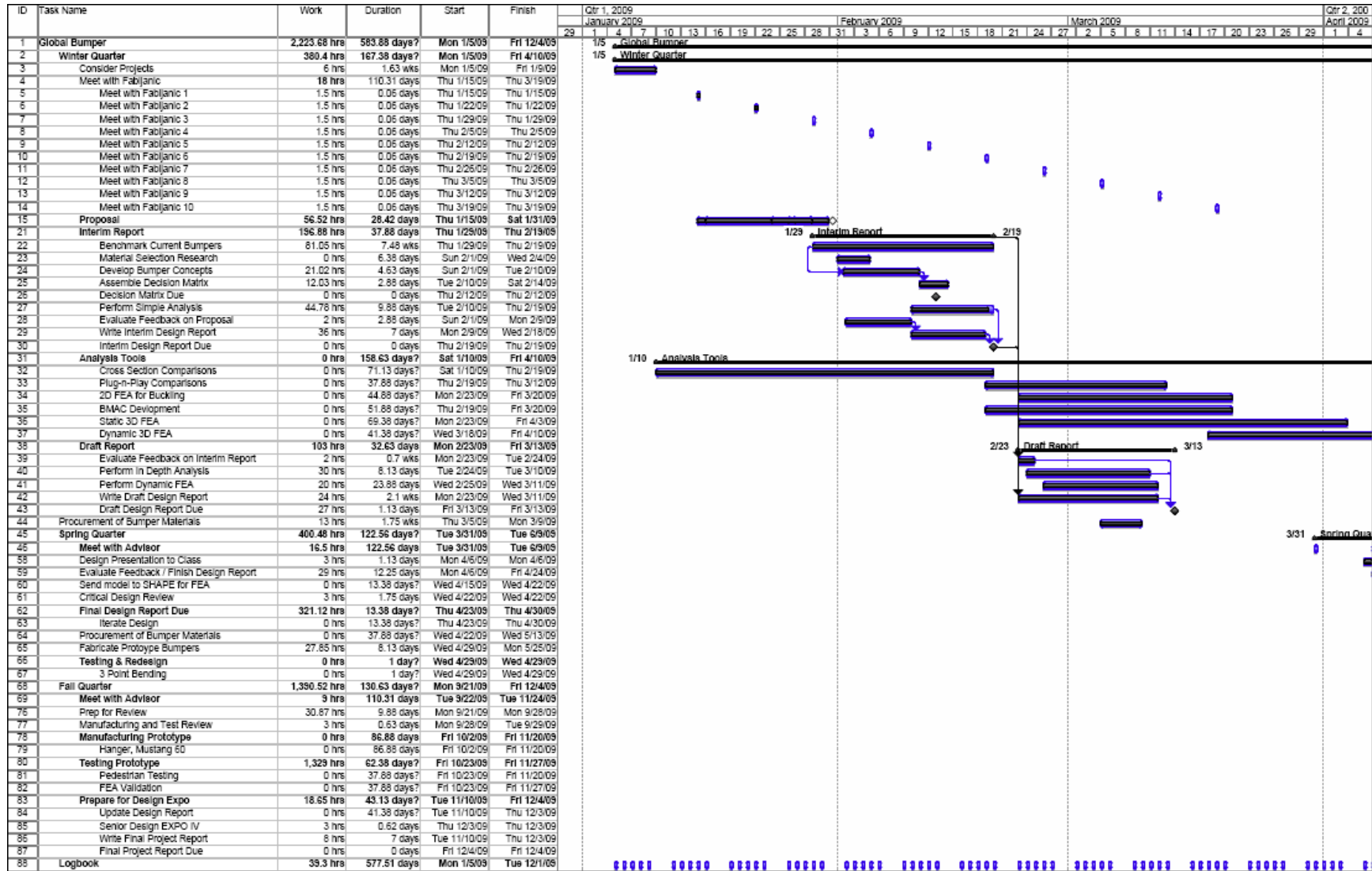
APPENDIX A: QFD TABLE

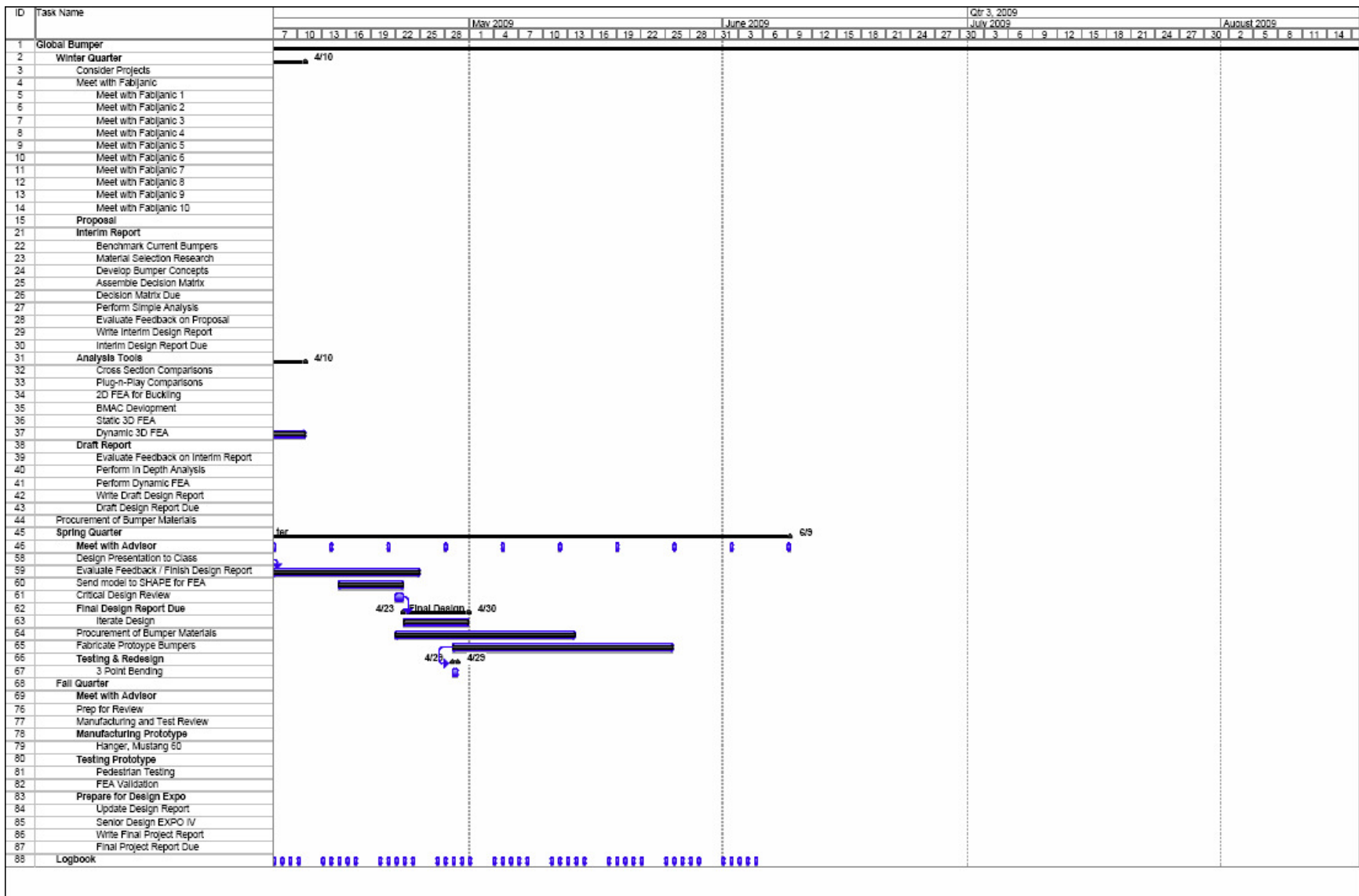
Best-in-class Bumper

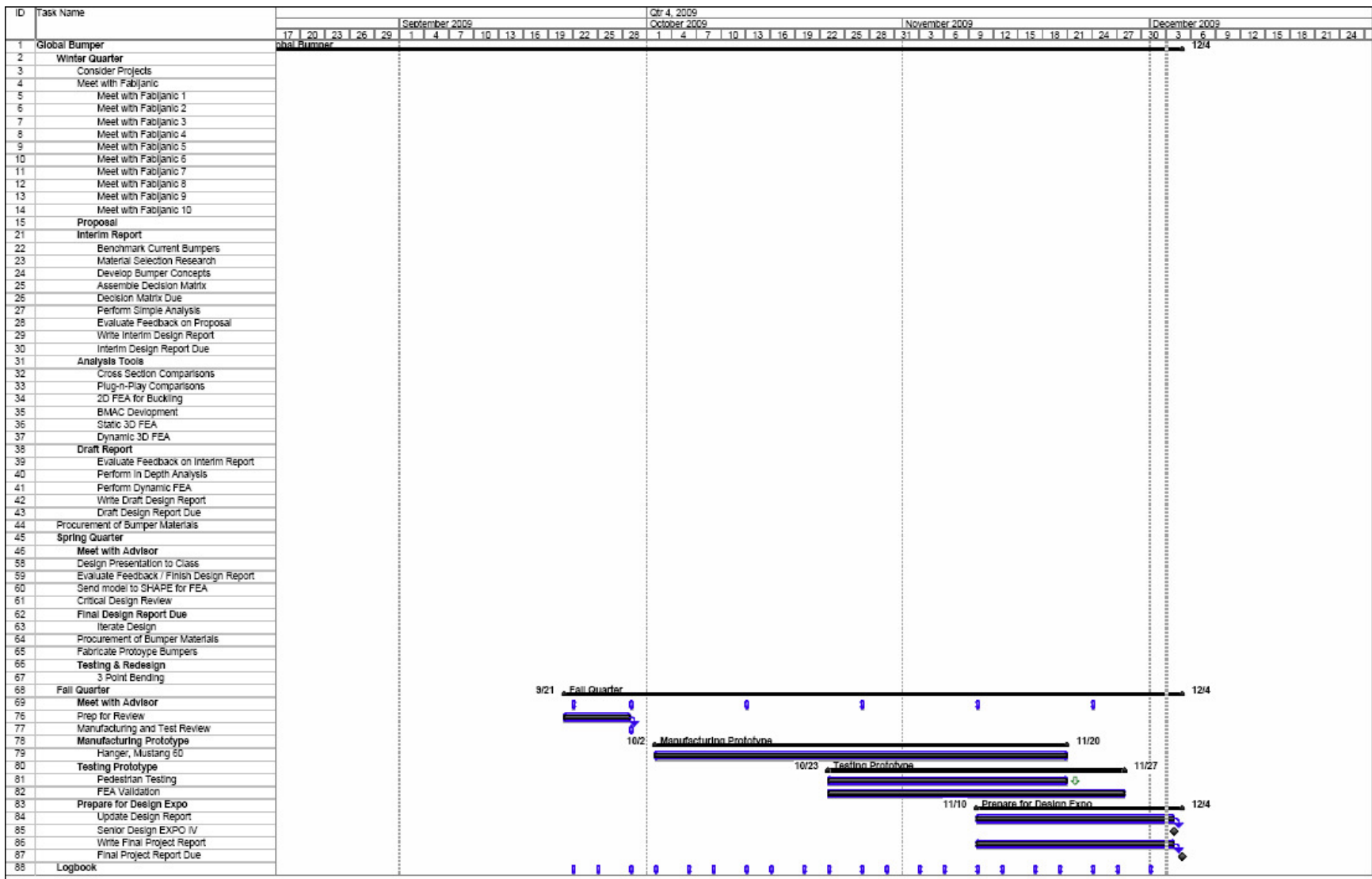
| | | Engineering Requirements | | | | | | | | | | | | | | | |
|-----------------------|--|--------------------------|---------------------------|------------------------|--------------------------|----------------------------------|---------------------------------------|--------------------------------------|-------------------------------------|----------------------------|--------------------------------|--------------------------------|--|---------------------------------------|---------------------------------------|--------------------------------------|---|
| | | AISI | Asian cross beam 4 kg max | US cross beam 5 kg max | Euro cross beam 6 kg max | Crush can mass less than 0.45 kg | Beam and energy absorber 1450 mm wide | Beam and energy absorber 107 mm high | Beam and energy absorber 73 mm deep | Beam sweep depth of 139 mm | Beam set-up from ground 420 mm | Must have towing/recovery hook | Full frontal intrusion limit less than 55mm @ centerline | Front corner intrusion less than 10mm | Uses existing manufacturing processes | Max acceleration for ped leg is 150g | Full frontal / front corner peak force per rail less than 80 kN |
| Customer Requirements | Low cross beam mass | 9 | 9 | 9 | 9 | | | | | | | | | | | | |
| | Crush can mass less than 0.45 kg | 8 | | | | 9 | | | | | | | | | | | |
| | Meets China, USA, Euro damage requirements | 9 | | | | | | | | | | 9 | 9 | | | 9 | 9 |
| | Fits packaging space | 7 | | | | | 9 | 9 | 9 | 9 | 9 | | | | | | |
| | Competitive performance in each market | 9 | 3 | 3 | 3 | 3 | 1 | 1 | 1 | 1 | 1 | | 9 | 9 | 3 | 9 | 3 |
| | Uses current manufacturing technologies | 6 | | | | | | | | 3 | | 3 | | | 9 | | |
| | Plug-and-Play attachments | 7 | 1 | 3 | 3 | | 3 | 3 | 3 | 3 | 1 | 1 | | | 3 | | |
| | Full frontal intrusion limit less than 55mm @ centerline | 9 | | | | | | | | | | | 9 | | | | |
| | Front corner intrusion less than 10mm | 9 | | | | | 1 | | | | | | | 9 | | 3 | 3 |
| | Meets Euro ped safety requirements | 7 | | | | | | 1 | 1 | | 1 | | | | | 9 | 1 |
| | Minimize bumper overhang | 5 | | | | | 3 | | 3 | | | | | | | | |
| | Max force to each rail 80 kN | 9 | | | | | | | | | | | | | | | 9 |
| | Importance Scoring | | 115 | 129 | 129 | 99 | 126 | 109 | 124 | 111 | 86 | 25 | 243 | 243 | 102 | 252 | 223 |
| Importance (%) | | 5.4 | 6.1 | 6.1 | 4.7 | 6.0 | 5.2 | 5.9 | 5.2 | 4.1 | 1.2 | 11.5 | 11.5 | 4.8 | 11.9 | 10.5 | |

- = 9 Strong Correlation
- = 3 Medium Correlation
- △ = 1 Small Correlation
- Blank No Correlation

APPENDIX B: GANTT CHART







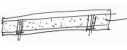


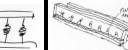

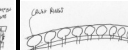




APPENDIX C: PRELIMINARY ANALYSIS

BEST-IN-CLASS GLOBAL BUMPER PROJECT

Concept Decision Matrix

| Rating (%) | Description |
|------------|---|
| 100 | Complete satisfaction; objective satisfied in every respect |
| 90 | Extensive satisfaction; objective satisfied in all important aspects |
| 75 | Considerable satisfaction; objective satisfied in the majority of aspects |
| 50 | Moderate satisfaction; a middle point between complet and no satisfaction |
| 25 | Minor satisfaction; objective satisfied in some but less than half of the aspects |
| 10 | Minimal satisfaction; objective satisfied to a very small extent |
| 0 | No satisfaction; object not satisfied in any respect |

| | | ALTERNATIVES | | | | | | | | | | |
|----------|----------------------|------------------|---|---|---|--|---|---|---|---|---|---|
| | | Weighting Factor |  |  |  |  |  |  |  |  |  |  |
| CRITERIA | Easy to Assemble | 10 | 75% 7.5 | 75% 7.5 | 75% 7.5 | 90% 9 | 50% 5 | 75% 7.5 | 25% 2.5 | 75% 7.5 | 90% 9 | 90% 9 |
| | Size | 15 | 75% 11.25 | 75% 11.25 | 75% 11.25 | 75% 11.25 | 75% 11.25 | 75% 11.25 | 50% 7.5 | 50% 7.5 | 100% 15 | 100% 15 |
| | Low Cost | 20 | 90% 18 | 75% 15 | 90% 18 | 90% 18 | 50% 10 | 75% 15 | 25% 5 | 50% 10 | 90% 18 | 90% 18 |
| | Plug & Play | 25 | 25% 6.25 | 25% 6.25 | 50% 12.5 | 50% 12.5 | 50% 12.5 | 75% 18.75 | 10% 2.5 | 50% 12.5 | 100% 25 | 100% 25 |
| | Easy to Manufacture | 10 | 75% 7.5 | 50% 5 | 75% 7.5 | 50% 5 | 25% 8 | 75% 7.5 | 10% 1 | 25% 2.5 | 90% 9 | 90% 9 |
| | Light Weight | 10 | 50% 5 | 75% 7.5 | 50% 5 | 50% 5 | 75% 8 | 25% 2.5 | 10% 1 | 50% 5 | 75% 7.5 | 75% 7.5 |
| | Simplicity | 10 | 50% 5 | 50% 5 | 25% 2.5 | 75% 7.5 | 50% 8 | 50% 5 | 10% 1 | 25% 2.5 | 50% 5 | 75% 7.5 |
| | Overall Satisfaction | 100 | 60.5 | 57.5 | 64.25 | 68.25 | 62.75 | 67.5 | 20.5 | 47.5 | 88.5 | 91 |

BEST-IN-CLASS GLOBAL BUMPER PROJECT

Material Decision Matrix

| Rating (%) | Description |
|------------|---|
| 100 | Complete satisfaction; objective satisfied in every respect |
| 90 | Extensive satisfaction; objective satisfied in all important aspects |
| 75 | Considerable satisfaction; objective satisfied in the majority of aspects |
| 50 | Moderate satisfaction; a middle point between complet and no satisfaction |
| 25 | Minor satisfaction; objective satisfied in some but less than half of the aspects |
| 10 | Minimal satisfaction; obective satisfied to a very small extent |
| 0 | No satisfaction; object not satisfied in any respect |

| | | ALTERNATIVES | | | | | | | |
|-----------------|-------------------------------------|------------------|---|--------------------------|---------------|-------------------------------|------------------|--|---|
| | | Weighting Factor | Lescalloy® D6AC VAC-ARC HSS Alloy | MS 1300 Mpa TS Steels | DI-FORM™ 140T | AISI 1018 Steel cold drawn | Aluminum 6061-T9 | Torlon® 5030 Polyamide-Imide 30% Glass Fiber Filled | Hexcel® UHM Carbon Fiber (12,000 Filaments) |
| CRITERIA | Stiffness | 20 | 90% 18 | 90% 18 | 90% 18 | 90% 18 | 75% 15 | 0% 0 | 100% 20 |
| | Lightweight | 15 | 90% 13.5 | 90% 13.5 | 90% 13.5 | 25% 3.75 | 75% 11.25 | 75% 11.25 | 100% 15 |
| | Low Cost | 25 | 90% 22.5 | 90% 22.5 | 90% 22.5 | 100% 25 | 75% 18.75 | 100% 25 | 25% 6.25 |
| | Fits Intermdediate Passenger Car | 30 | 100% 30 | 90% 27 | 90% 27 | 0% 0 | 75% 22.5 | 0% 0 | 100% 30 |
| | Easy to Manufacture | 10 | 90% 9 | 90% 9 | 90% 9 | 90% 9 | 90% 8 | 90% 9 | 90% 9 |
| | Overall Satisfaction | 100 | 93 | 90 | 90 | 55.75 | 75.5 | 45.25 | 80.25 |

Table 6. Comparison between different Plug-n-Play methods. Each method was evaluated by its cross-sectional properties.




















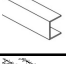

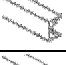
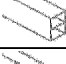
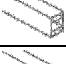

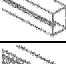



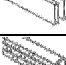
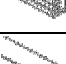
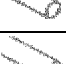
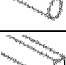


| Shape | Picture | Ix (mm4) | Iy (mm4) | Iz (mm4) | c (mm) | Area (mm2) | Weight (kg) | BUP - Ix/(Ac) (mm) | Ix/A (mm2) | Iy/A (mm2) | Iz/A (mm2) | Incr. Ix (%) | Incr. A (%) | Incr. BUP (%) |
|-------|---|----------|----------|----------|--------|------------|-------------|--------------------|------------|------------|------------|--------------|-------------|---------------|
| 1 |  | 7.12E+04 | 6.08E+05 | 6.79E+05 | 29.45 | 353 | 4.01 | 6.86 | 202 | 1725 | 1927 | 0.00 | 0.00 | 0.00 |
| 2 |  | 9.47E+04 | 6.10E+05 | 7.05E+05 | 27.43 | 449 | 5.11 | 7.69 | 211 | 1360 | 1571 | 33.00 | 27.23 | 12.23 |
| 3 |  | 1.16E+05 | 6.73E+05 | 7.88E+05 | 26.12 | 545 | 6.20 | 8.14 | 213 | 1235 | 1448 | 62.66 | 54.47 | 18.73 |
| 4 |  | 3.07E+04 | 4.29E+05 | 4.60E+05 | 14.30 | 318 | 3.62 | 6.75 | 97 | 1349 | 1447 | 0.00 | 0.00 | 0.00 |
| 5 |  | 1.04E+05 | 5.58E+05 | 6.62E+05 | 21.90 | 440 | 5.01 | 10.79 | 236 | 1268 | 1505 | 238.76 | 38.36 | 59.87 |
| 6 |  | 1.30E+05 | 5.69E+05 | 6.98E+05 | 24.47 | 512 | 5.83 | 10.38 | 254 | 1111 | 1363 | 323.45 | 61.01 | 53.70 |
| 7 |  | 1.29E+05 | 4.22E+05 | 5.50E+05 | 29.56 | 378 | 4.30 | 11.53 | 341 | 1116 | 1457 | 0.00 | 0.00 | 0.00 |
| 8 |  | 1.68E+05 | 5.60E+05 | 7.28E+05 | 26.30 | 518 | 5.89 | 12.36 | 325 | 1082 | 1407 | 30.66 | 37.01 | 7.18 |
| 9 |  | 1.81E+05 | 4.70E+05 | 6.52E+05 | 27.60 | 583 | 6.63 | 11.28 | 311 | 807 | 1118 | 40.91 | 54.27 | -2.18 |
| 13 |  | 6.19E+04 | 4.09E+05 | 4.71E+05 | 19.54 | 309 | 3.52 | 10.25 | 200 | 1324 | 1524 | 0.00 | 0.00 | 0.00 |
| 14 |  | 7.75E+04 | 4.26E+05 | 5.04E+05 | 18.88 | 417 | 4.75 | 9.83 | 186 | 1022 | 1207 | 25.22 | 35.07 | -4.06 |
| 15 |  | 8.81E+04 | 6.96E+05 | 7.84E+05 | 18.73 | 510 | 5.81 | 9.23 | 173 | 1364 | 1536 | 42.46 | 65.07 | -9.97 |
| 16 |  | 7.32E+04 | 3.91E+05 | 4.64E+05 | 18.24 | 346 | 3.94 | 11.60 | 212 | 1130 | 1341 | 0.00 | 0.00 | 0.00 |
| 17 |  | 7.84E+04 | 4.42E+05 | 5.21E+05 | 18.74 | 411 | 4.68 | 10.18 | 191 | 1075 | 1268 | 7.10 | 18.79 | -12.24 |
| 18 |  | 8.33E+04 | 5.08E+05 | 5.91E+05 | 19.11 | 477 | 5.43 | 9.14 | 175 | 1065 | 1239 | 13.80 | 37.86 | -21.21 |
| 19 |  | 5.32E+04 | 4.67E+05 | 5.20E+05 | 16.85 | 359 | 4.08 | 8.80 | 148 | 1303 | 1451 | 0.00 | 0.00 | 0.00 |
| 20 |  | 6.85E+04 | 5.69E+05 | 6.38E+05 | 19.99 | 466 | 5.30 | 7.36 | 147 | 1223 | 1370 | 28.88 | 29.83 | -16.32 |
| 21 |  | 8.01E+04 | 6.71E+05 | 7.52E+05 | 22.14 | 573 | 6.52 | 6.32 | 140 | 1172 | 1312 | 50.58 | 59.65 | -28.22 |

Table 7. Conceptual Spreadsheet comparing cross section properties.

| Shape | Picture | Ix (mm4) | Iy (mm4) | Iz (mm4) | c (mm) | Area (mm2) | BUP - Ix/(Ac) (mm) | Ix/A (mm2) | Iy/A (mm2) | Iz/A (mm2) | Incr. Ix (%) | Incr. Iy (%) | Incr. Iz (%) | Incr. A (%) | Ix/A^2 (-) | Iy/A^2 (-) |
|-------|---|----------|----------|----------|--------|------------|--------------------|------------|------------|------------|--------------|--------------|--------------|-------------|------------|------------|
| 1 |  | 6.49E+05 | 1.17E+06 | 1.82E+06 | 36.50 | 704 | 25.26 | 922 | 1662 | 2585 | 0.00 | 0.00 | 0.00 | 0.00 | 1.31 | 2.36 |
| 2 |  | 2.82E+05 | 9.87E+05 | 1.27E+06 | 51.18 | 498 | 11.06 | 566 | 1982 | 2550 | -56.55 | -15.64 | -30.22 | -29.26 | 1.14 | 3.98 |
| 3 |  | 4.10E+05 | 6.49E+05 | 1.06E+06 | 36.50 | 704 | 15.96 | 582 | 922 | 1506 | -36.83 | -44.53 | -41.76 | 0.00 | 0.83 | 1.31 |
| 4 |  | 4.32E+05 | 1.28E+06 | 1.71E+06 | 46.04 | 827 | 11.35 | 522 | 1548 | 2068 | -33.44 | 9.40 | -6.04 | 17.47 | 0.63 | 1.87 |
| 5 |  | 7.04E+05 | 1.17E+06 | 1.87E+06 | 36.50 | 842 | 22.91 | 836 | 1390 | 2221 | 8.47 | 0.00 | 2.75 | 19.60 | 0.99 | 1.65 |
| 6 |  | 7.59E+05 | 1.35E+06 | 2.11E+06 | 36.50 | 980 | 21.22 | 774 | 1378 | 2153 | 16.95 | 15.38 | 15.93 | 39.20 | 0.79 | 1.41 |
| 7 |  | 6.21E+05 | 1.33E+06 | 1.95E+06 | 40.44 | 882 | 17.41 | 704 | 1508 | 2211 | -4.31 | 13.68 | 7.14 | 25.28 | 0.80 | 1.71 |
| 8 |  | 6.64E+05 | 1.17E+06 | 1.84E+06 | 37.66 | 744 | 23.70 | 892 | 1573 | 2473 | 2.31 | 0.00 | 1.10 | 5.68 | 1.20 | 2.11 |
| 9 |  | 6.77E+05 | 1.21E+06 | 1.89E+06 | 38.69 | 784 | 22.32 | 864 | 1543 | 2411 | 4.31 | 3.42 | 3.85 | 11.36 | 1.10 | 1.97 |
| 10 |  | 4.21E+05 | 1.40E+06 | 1.82E+06 | 36.50 | 712 | 16.20 | 591 | 1966 | 2556 | -35.13 | 19.66 | 0.00 | 1.14 | 0.83 | 2.76 |
| 11 |  | 4.36E+05 | 1.12E+06 | 1.56E+06 | 36.50 | 576 | 20.74 | 757 | 1944 | 2708 | -32.82 | -4.27 | -14.29 | -18.18 | 1.31 | 3.38 |
| 12 |  | 7.63E+05 | 1.17E+06 | 1.93E+06 | 36.50 | 984 | 21.24 | 775 | 1189 | 1961 | 17.57 | 0.00 | 6.04 | 39.77 | 0.79 | 1.21 |
| 13 |  | 7.07E+05 | 1.30E+06 | 2.00E+06 | 39.67 | 1026 | 17.36 | 688 | 1264 | 1953 | 8.88 | 10.91 | 10.12 | 45.80 | 0.67 | 1.23 |
| 14 |  | 2.81E+05 | 2.81E+05 | 5.63E+05 | 36.50 | 446 | 17.28 | 631 | 631 | 1261 | -56.65 | -75.96 | -69.09 | -36.63 | 1.41 | 1.41 |
| 15 |  | 3.82E+05 | 6.90E+05 | 1.07E+06 | 36.50 | 447 | 23.41 | 855 | 1543 | 2397 | -41.13 | -41.05 | -41.11 | -36.49 | 1.91 | 3.45 |
| 16 |  | 5.16E+05 | 9.67E+05 | 1.48E+06 | 41.15 | 636 | 19.73 | 812 | 1522 | 2334 | -20.47 | -17.31 | -18.48 | -9.70 | 1.28 | 2.39 |
| 17 |  | 4.67E+05 | 8.52E+05 | 1.32E+06 | 42.98 | 614 | 17.71 | 761 | 1388 | 2149 | -27.99 | -27.19 | -27.51 | -12.80 | 1.24 | 2.26 |

APPENDIX D: B-MAC 3000

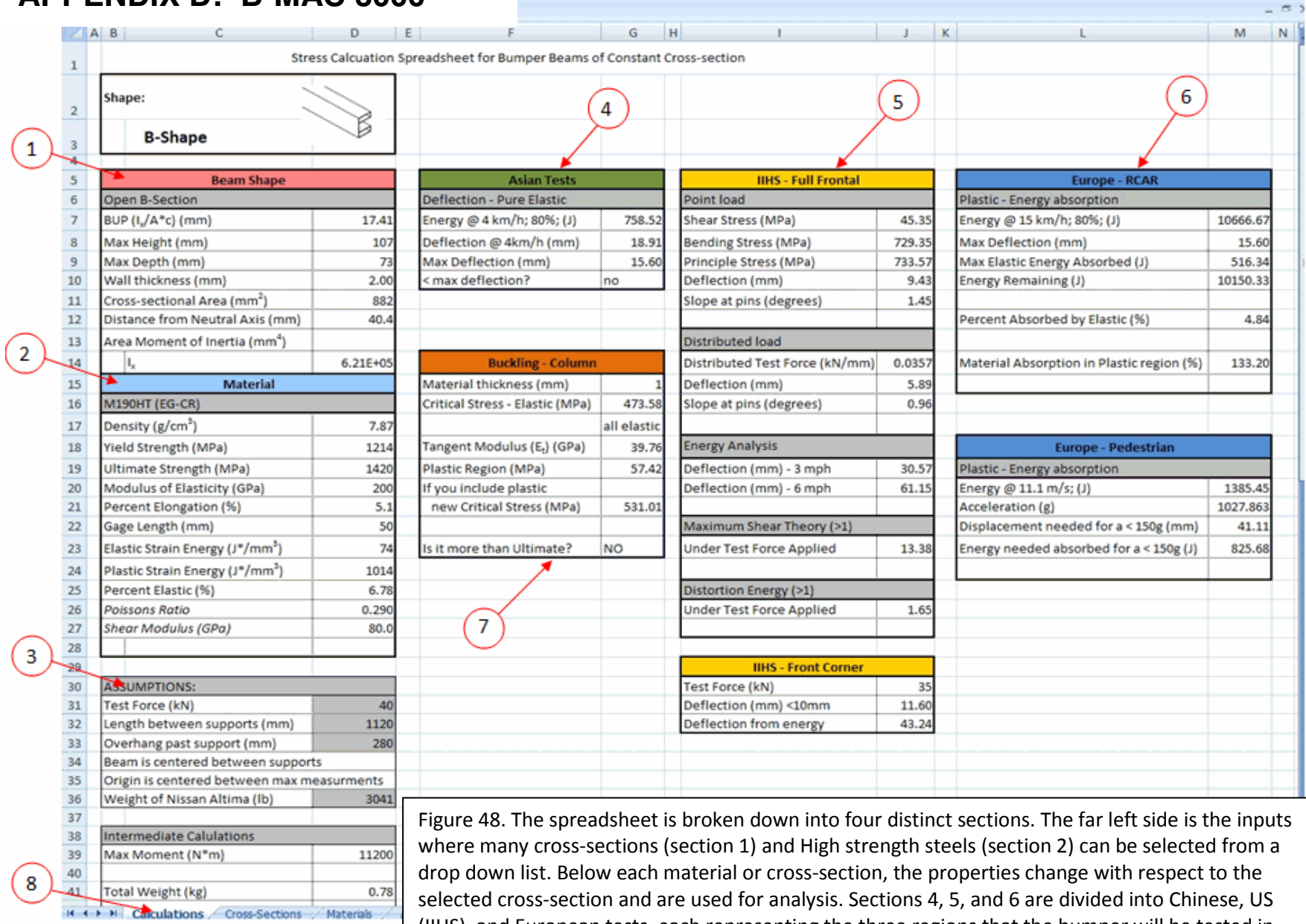


Figure 48. The spreadsheet is broken down into four distinct sections. The far left side is the inputs where many cross-sections (section 1) and High strength steels (section 2) can be selected from a drop down list. Below each material or cross-section, the properties change with respect to the selected cross-section and are used for analysis. Sections 4, 5, and 6 are divided into Chinese, US (IIHS), and European tests, each representing the three regions that the bumper will be tested in.

APPENDIX E: FEA MODEL DESCRIPTION

All FEA was done using Abaqus/CAE Version 6.7-1 software.

Static FEA models were developed to analyze cross sections buckling and failure modes. While this information was helpful in the analysis, there was still a strong desire to have the capability to analyze the coupled effects of cross section geometry, beam shape, material type, crush cans, and inertial effects. While static analysis was being performed, a dynamic model was simultaneously being developed to accomplish this goal. The final model allows the user to output data at any of the nodes, and can analyze all reaction forces, displacements, and accelerations of interest.

The Barriers

Four rigid barriers were created to mimic each of the required crash tests. All were limited to motion along 1 axis and were not allowed rotation about any axis.

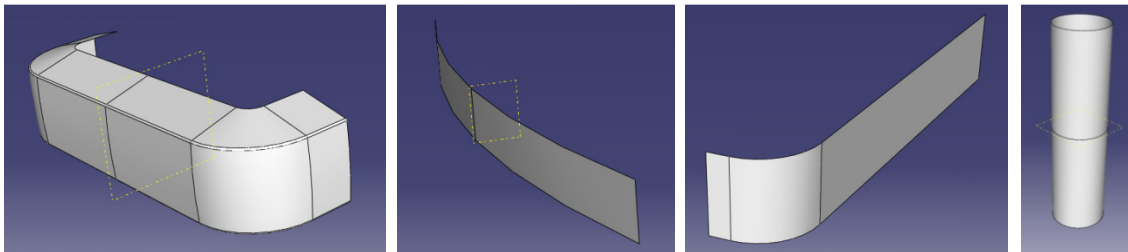


Figure 48. From left to right: GB17354-1998 Pendulum Barrier, IIHS and RCAR Full Frontal Barrier, RCAR Offset Barrier, Pedestrian Legform.

The Beam

To create the beam, a cross section was sketched and swept along an arc to the desired size. The EA was sketched and extruded along with the beam, but assigned different section properties.

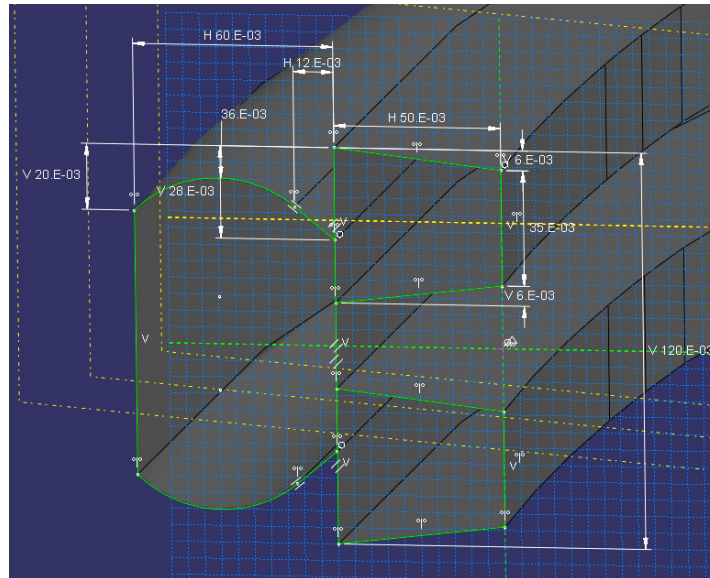


Figure 49. Extruded cross section sketch.

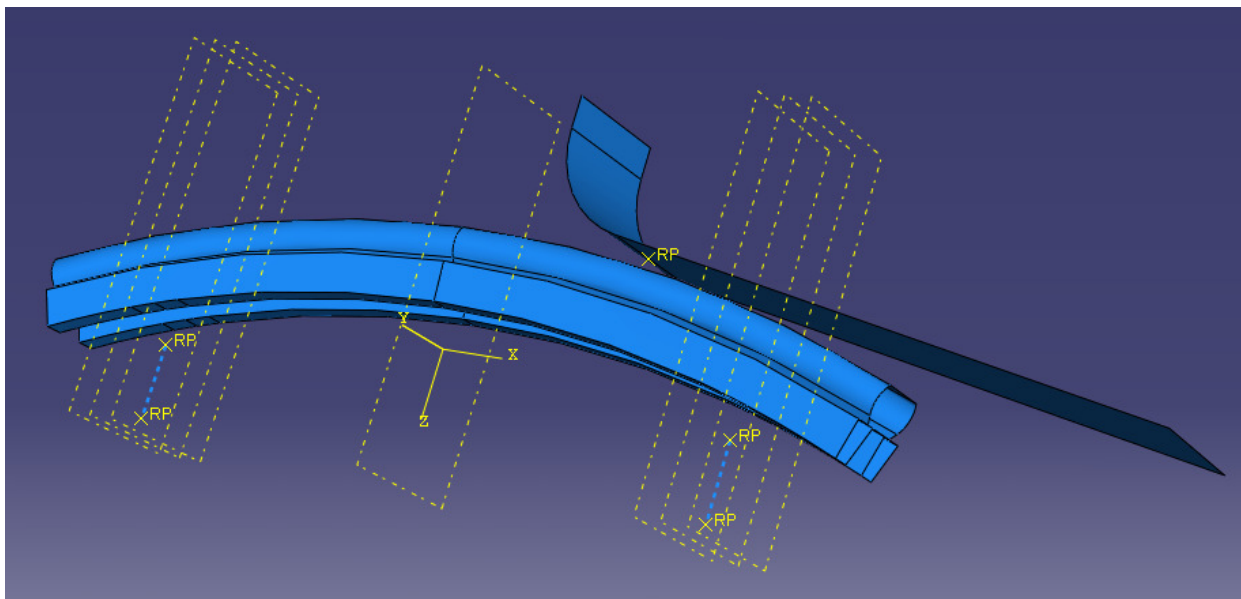


Figure 50. Assembly of the base beam with D6080-1.1 SEA and RCAR 40% Offset barrier.

Crush cans

Nonlinear springs were added to the model to represent the crush cans that will be attached to the bumper during an impact. These are displayed as dashed blue lines in Figure 50. The rear node of the crush can was fixed, and the front was free to move with the beam. Force-deflection data for these crush cans was provided by Shape for a static test and used to approximate the crush can response during an impact. This data can be seen in Figure 51.

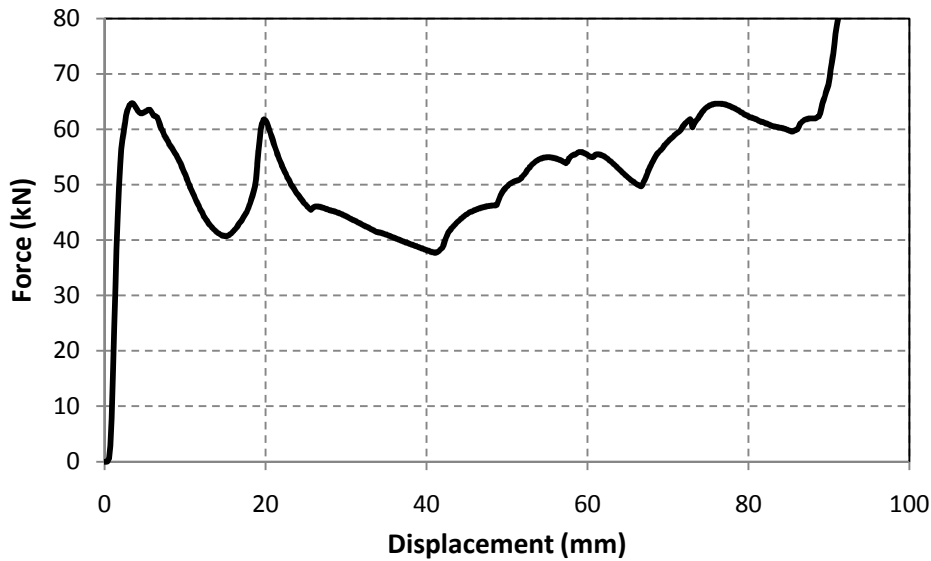


Figure 51. Crush can static force-deflection data.

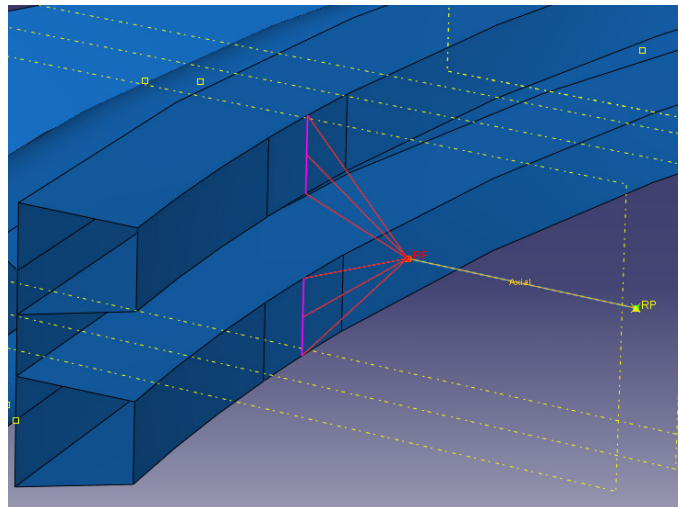


Figure 52. Left crush can constrained to move with the back of the bumper beam.

For the frontal impact tests, crush cans were constrained to a node region down the center of the crush can area. This essentially created a pin along the purple line seen in Figure 52, and the beam was free to rotate about this axis. By fixing the crush cans to the beam in this way, results were conservative because there was no moment resisting rotation. For the offset tests, much of the force is absorbed by the crush cans, and the beam tends to rotate about the crush cans more than the frontal tests. Using pin allowed the beam to freely rotate, which was very unrealistic for this scenario. Therefore, instead of using pin constraints, the crush cans were tied to the area to which the crush can attach.

Mesh

Analysis was generally performed with 1 cm linear shell elements. Some models were developed which included construction fillets, and required much finer meshes to imitate the sharp radius of the fillet. Runs with elements as small as 2 mm were attempted, but the computers were unable to perform an analysis which lasted longer than 24 hours.

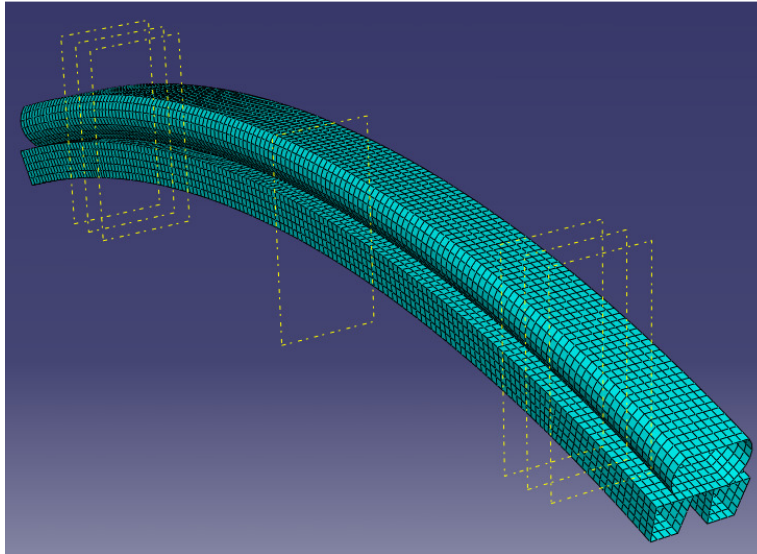


Figure 53. Typical meshed beam.

Figure 53 shows a typical mesh for one of the bumper beams with EA attached. Due to concerns about the effect fillets might have on the performance of the SEA, an analysis was performed with a fine localized mesh around the SEA's fillets. This analysis proved that the fillets did not significantly affect EA performance. A similar technique was attempted on a filleted model of the entire beam, but proved unsuccessful.

Results

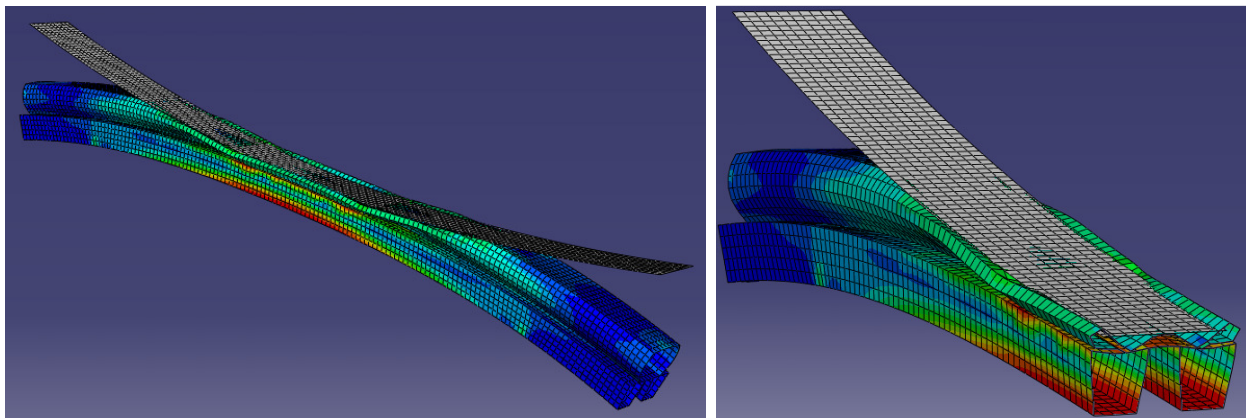


Figure 54. Full bumper (left) and section view (right) of stress contours during impact.

Contour plots were generated to view stress concentrations, deflections, or any other parameter of interest. Tabular data was also outputted and analyzed to quantify the performance of the beam. An example of one of the spreadsheets for IHS Full Frontal test has been broken up to fit on one page and is displayed in Figure 55, Figure 56, and Figure 57.

Figure 55 shows the primary dimensions of the bumper being tested, the depth of sweep, weight, and total weight if an EA is included. Weights were calculated without filleted edges or welds, so actual weight will be slightly different from the displayed values.

Figure 56 contains test data from the finite element simulation. The max intrusion is calculated by adding the 55 mm limit to the width of the package space, and then subtracting the width of the EA/beam combination. Crush can displacement is the measured displacement of the front node of the crush can. Crush can force is measured at the back node of the spring and represents the force transmitted into the frame rails of the vehicle. Finally, pass/fail columns quickly display the outcome of the test.

Information about the FEA model and test are recorded in Figure 57 as a reference, but also to ensure repeatability of test conditions. Before discovering how to create a non-linear, plastically deforming spring, several different crush can models were tested. This column now varies between Pin and Area to describe whether the beam and crush can were free to rotate or fixed across the crush can area. Barrier model also indicates the test performed. The base beam material is followed by notes to conclude the data recorded for each run. Notes contains the type of EA, if any, and any other information about the run, such as errors or anomalies in the test.

| Model # | Beam Geometry | | | | | | | | | | |
|---------|---------------------|------------------|-------------------|---------------------|-------------------|----------------|--------|------------|-------------------------|-------------|--------------|
| | Overall Height (mm) | Taper Width (mm) | Taper Height (mm) | Taper Distance (mm) | Taper Angle (deg) | Thickness (mm) | | Sweep (mm) | Area (mm ²) | Weight (kg) | Total Weight |
| | | | | | | Plate | Tapers | | | | |
| 9 | 120 | 50 | 40 | 6 | 6.843 | 0.7 | 1.3 | 140.7 | 449.87 | 5.22 | 8.02 |
| 10 | 120 | 50 | 35 | 6 | 6.843 | 0.7 | 0.7 | 140.7 | 274 | 3.18 | 5.98 |
| 11 | 120 | 50 | 35 | 6 | 6.843 | 0.7 | 0.7 | 140.7 | 274 | 3.18 | 5.98 |
| 12 | 120 | 50 | 35 | 6 | 6.843 | 1.4 | 0.7 | 140.7 | 358 | 4.15 | 6.95 |
| 13 | 120 | 50 | 35 | 6 | 6.843 | 0.7 | 0.7 | 140.7 | 274 | 3.18 | 5.98 |
| 14 | 120 | 50 | 35 | 6 | 6.843 | 0.7 | 0.7 | 140.7 | 274 | 3.18 | 5.98 |

Figure 55. Beam geometry.

| Model # | Test Requirements and Results | | | | | | | |
|---------|-------------------------------|----------------|--------------------------|---------------------------|---------------------------|----------------------------|---------------------|---------------------------|
| | Max Intrusion (mm) | Intrusion (mm) | Left Crush Can Disp (mm) | Right Crush Can Disp (mm) | Left Crush Can Force (kN) | Right Crush Can Force (kN) | Intrusion Pass/Fail | Crush Can Force Pass/Fail |
| 9 | 88.9 | 87.3 | 1.5 | 3.5 | 31.6 | 30 | Passed by 1.6mm | Pass |
| 10 | 88.9 | 231.0 | 1.9 | 5.2 | 41.2 | 40.7 | Failed by 142.1mm | Pass |
| 11 | 88.9 | 152.6 | 4.0 | 4.3 | 65 | 64.9 | Failed by 63.7mm | Pass |
| 12 | 88.9 | 134.5 | 1.8 | 1.7 | 38.8 | 37.4 | Failed by 45.6mm | Pass |
| 13 | 88.9 | 170.3 | 2.5 | 2.6 | 55.2 | 55.7 | Failed by 81.4mm | Pass |
| 14 | 88.9 | 95.8 | 1.5 | 5.5 | 30.8 | 35.7 | Failed by 6.9mm | Pass |

Figure 56. Test requirements and results.

| Model # | Model Description | | | |
|---------|-------------------|---------------|----------|--------------------------|
| | Crush Can Model | Barrier Model | Material | Notes |
| 9 | Spring/Pin | Curved | M220 | D6080-0.7 |
| 10 | Spring/Pin | Curved | M220 | No EA |
| 11 | Spring/Pin | Curved | M220 | 10840226 Reinforcement |
| 12 | Spring/Pin | Curved | M220 | No EA; Plate across back |
| 13 | Spring/Pin | Curved | M220 | 110404010 0.7 |
| 14 | Spring/Pin | Curved | M220 | 40 reinforcing beam |

Figure 57. FEA model description.

Assumptions List

The dynamic FEA model opened up an unexpected analysis capability. While this tool proved invaluable in the design of the bumper beam and EA, there are many simplifications which need to be addressed.

- Pin vs area crush can models
 - Pins allow the beam to freely rotate, so the model overpredicts the deflection. On the other hand, the area model completely restricts rotational motion of the crush can area, resulting in an underprediction of the deflection. In order to accurately replicate the response of the crush cans, a full 3D model of the crush cans is needed.
- Crush cans are axial springs only
 - Does not take into account translational force imposed on the beam or moments provided at the connection between the can and bumper beam
- The non-linear spring used to approximate the crush cans is built from static test data. No verification has been performed to prove that this is representative of the actual performance.
- One side of the beam is free to translate outward

- This is to imitate the tendency of the frame to bow outwards because the crush can force is not a one-dimensional load. A real beam's outward translation is somewhat restricted by the frame
- A completely filleted model was not able to run using the available computers
 - Verification that a filleted model will perform as well as an unfilleted model has not been performed
- The change in performance due to welded edges is unknown
- Due to the difficulty in modeling complex geometry, non-essential material has not been removed. Removing material could create a lighter beam.
- Elements are larger than the industry standard of about 4 mm. Analysis was performed with 1 cm elements
- 80% of the kinetic energy of the collision is assumed to enter the beam. While this has been proven a good approximation, the actual energy into the beam may be higher.
- The "car" is constrained from rotation. Some of the energy of the collision may go into rotational energy of the vehicle.
- The barriers are all rigid bodies and are not outfitted with energy absorbers. This results in higher forces into the bumper.
- Pedestrian test
 - Only analyzes acceleration
 - Shear forces and rotation of the leg are not accounted for
 - The legform is a rigid cylinder
 - The diameter of the leg is assumed

FEA Model Validation

To verify the accuracy of the FEA model, results were compared to Shape Corp.'s advanced dynamic 3-D FEA. Identical bumper beams were used in both models.

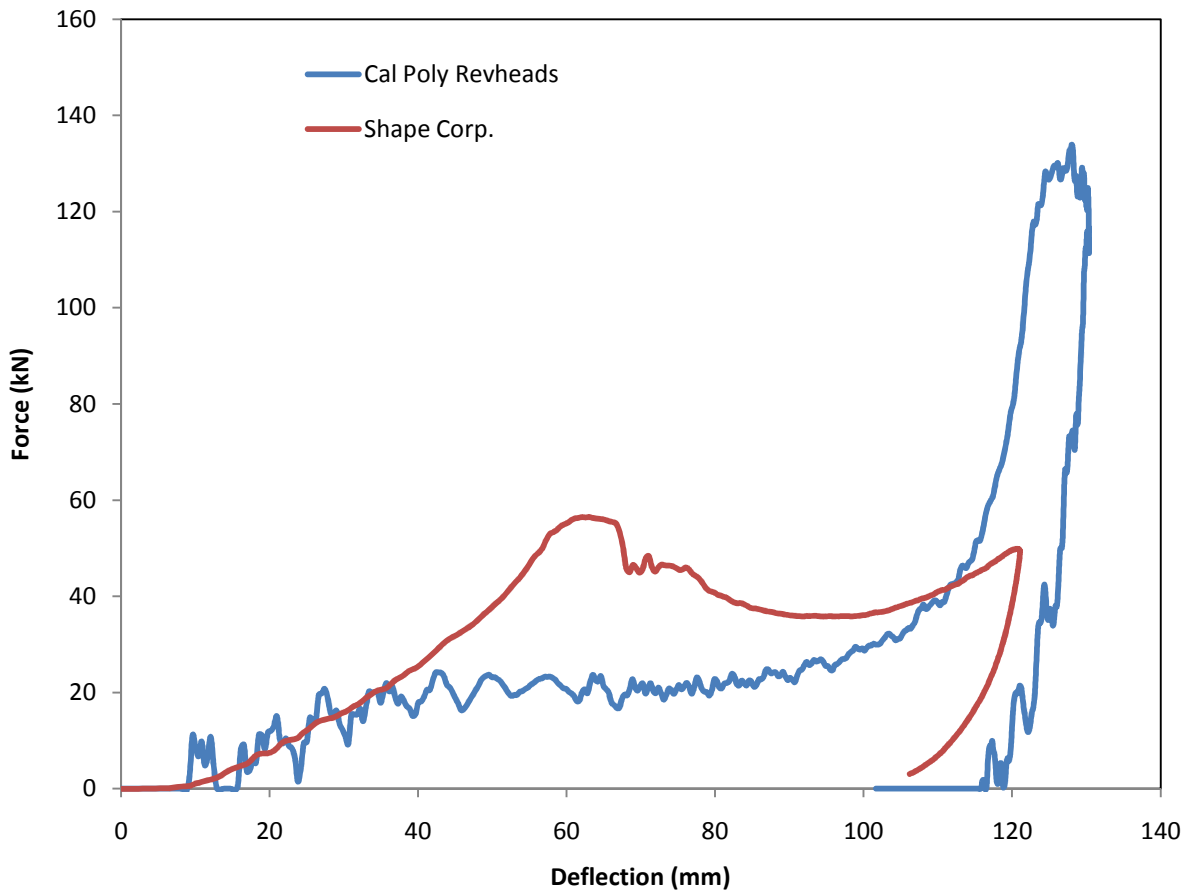


Figure 58. FEA comparison and validation

As seen in Figure 58, the force-deflection curve has a similar shape but the Cal Poly model over predicts force and deflection. Therefore, all results from Cal Poly FEA are conservative.

APPENDIX F: PLUG-N-PLAY 2-D FEA RESULTS

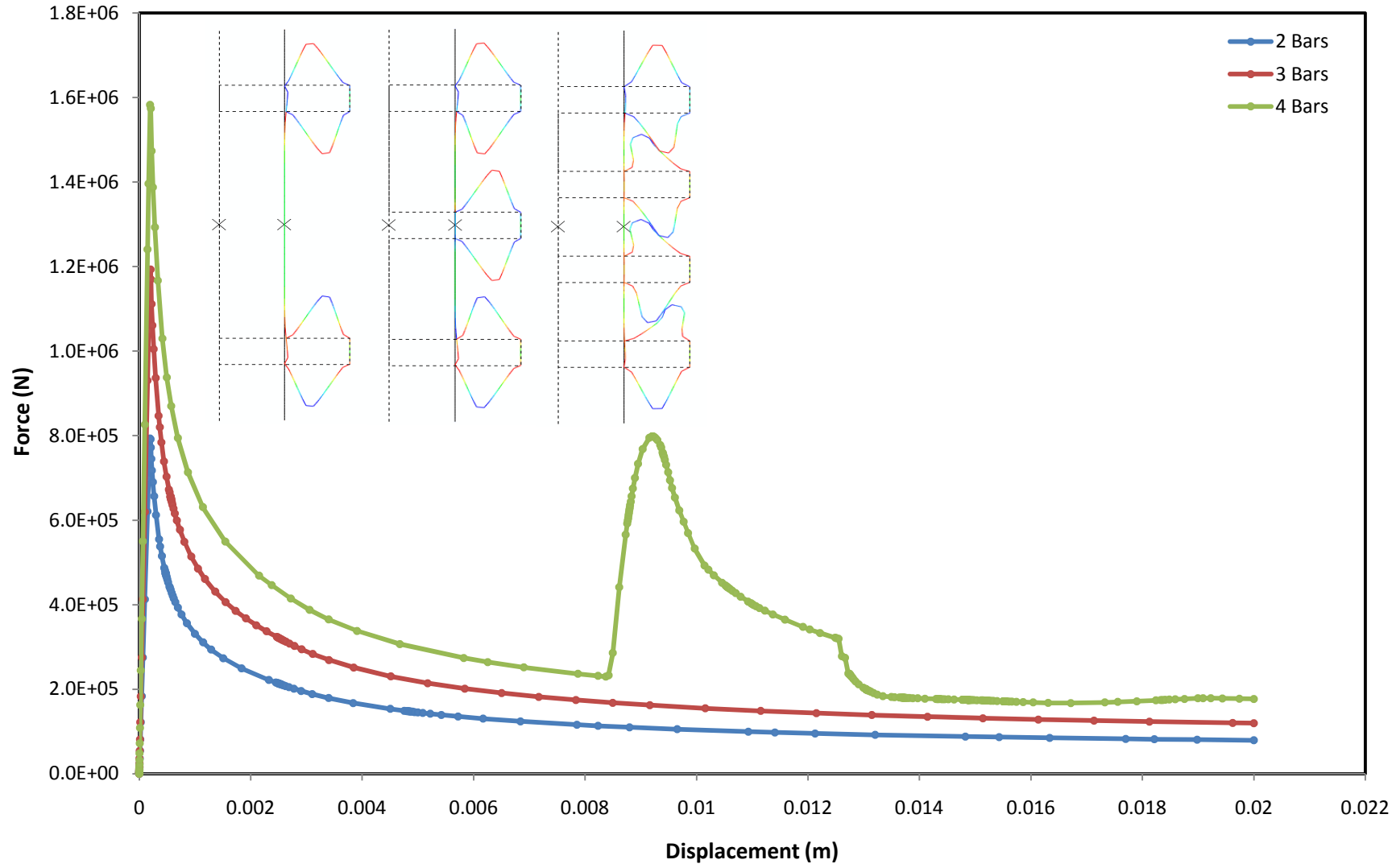


Figure 59. Plug-n-Play force-deflection curves for a flat plate with reinforcement bars design.

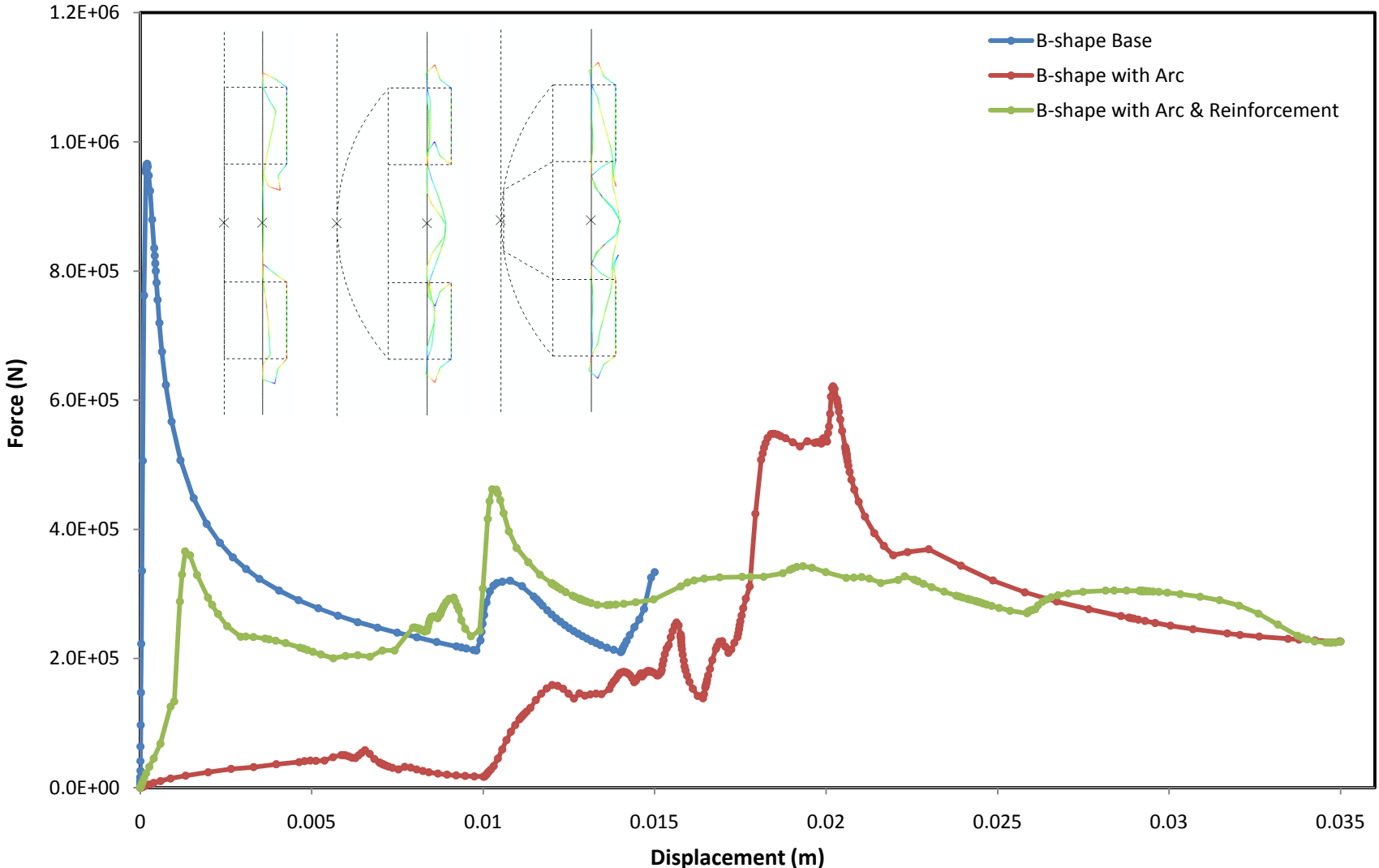


Figure 60. Plug-n-Play force-deflection curves for an external reinforcement design.

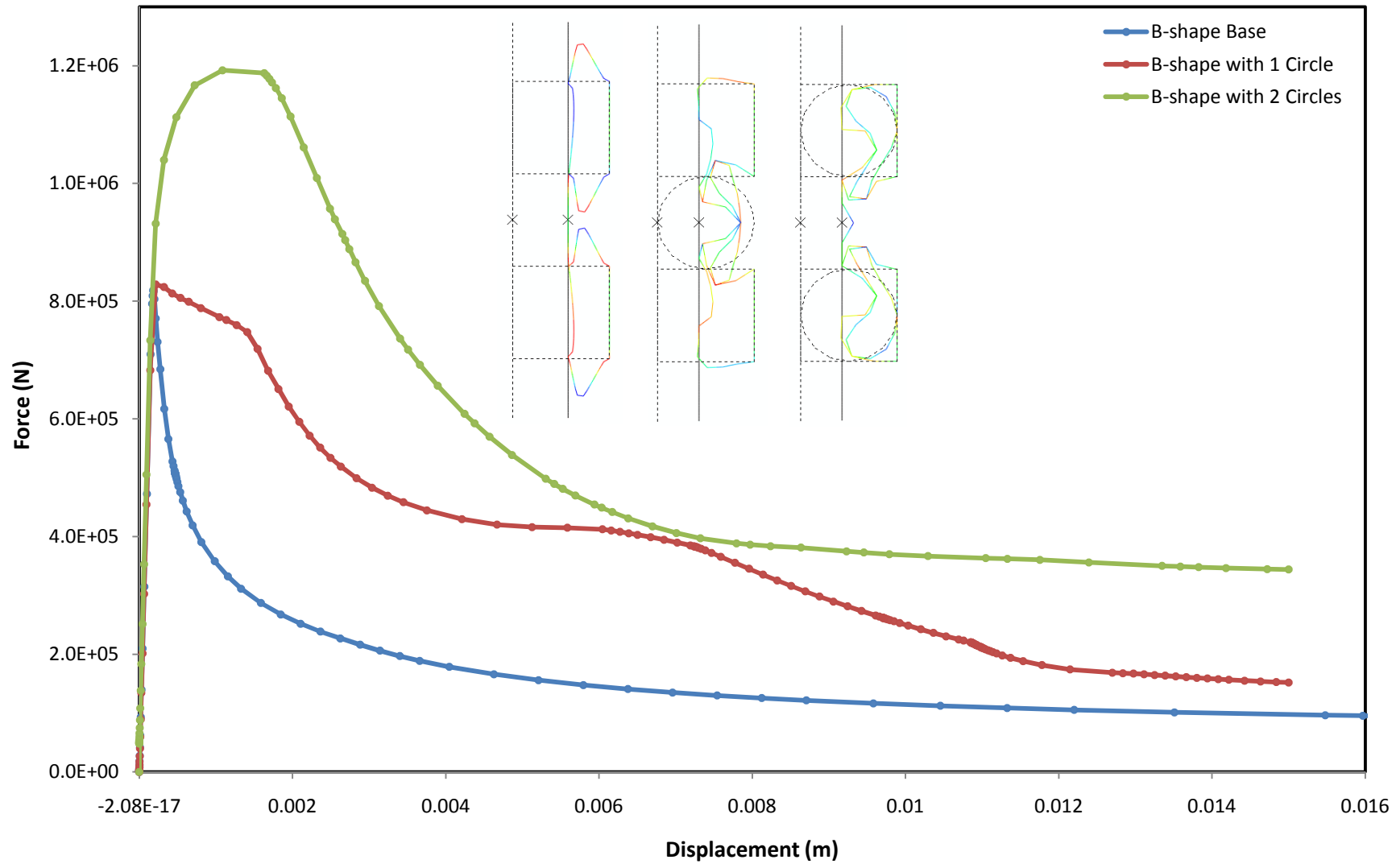


Figure 61. Plug-n-Play force-deflection curves for an internal reinforcement design.

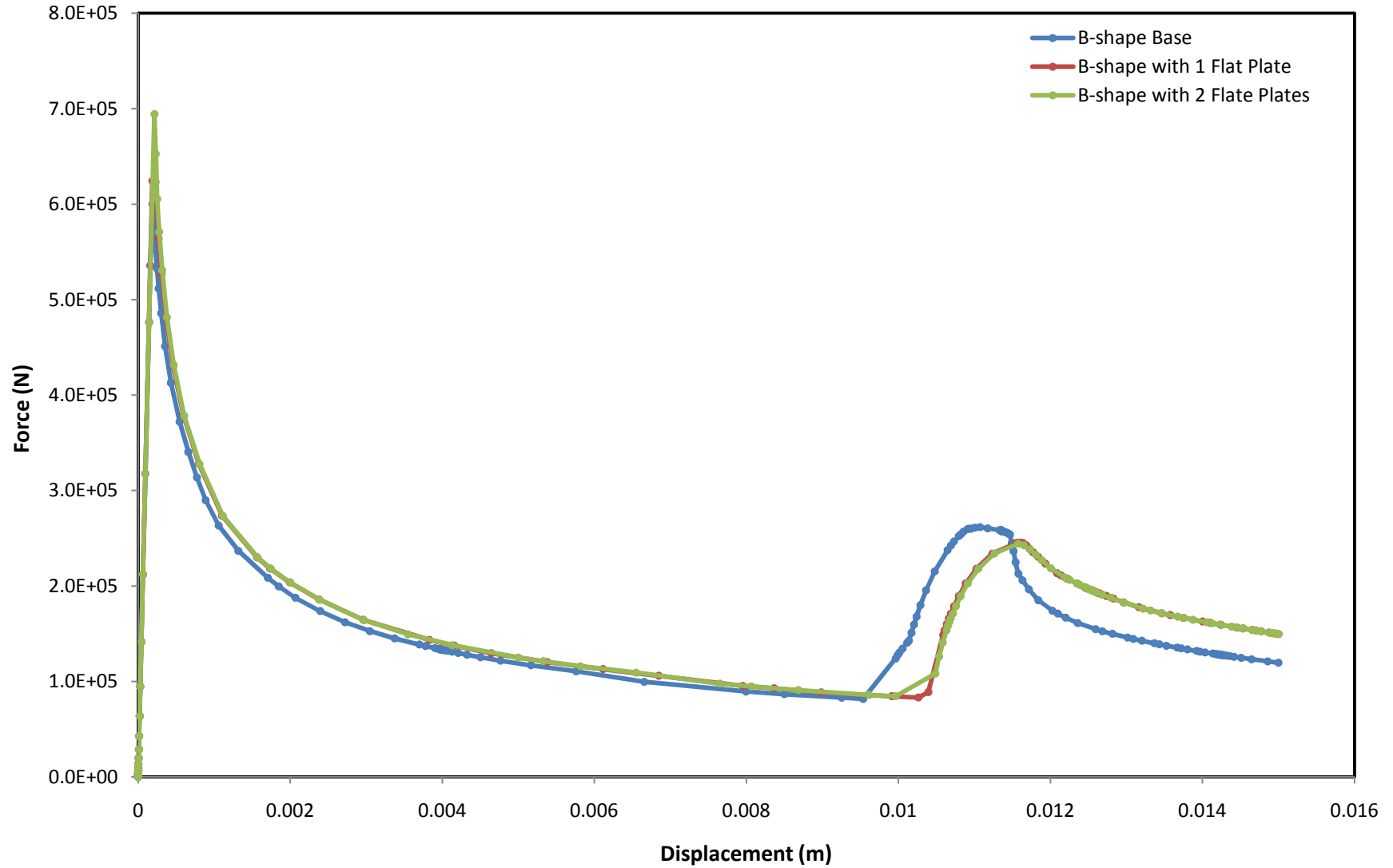


Figure 62. Plug-n-Play force-deflection curves for a B-shape with reinforcing flat plates design.

APPENDIX G: MATCHBOOKING STUDY

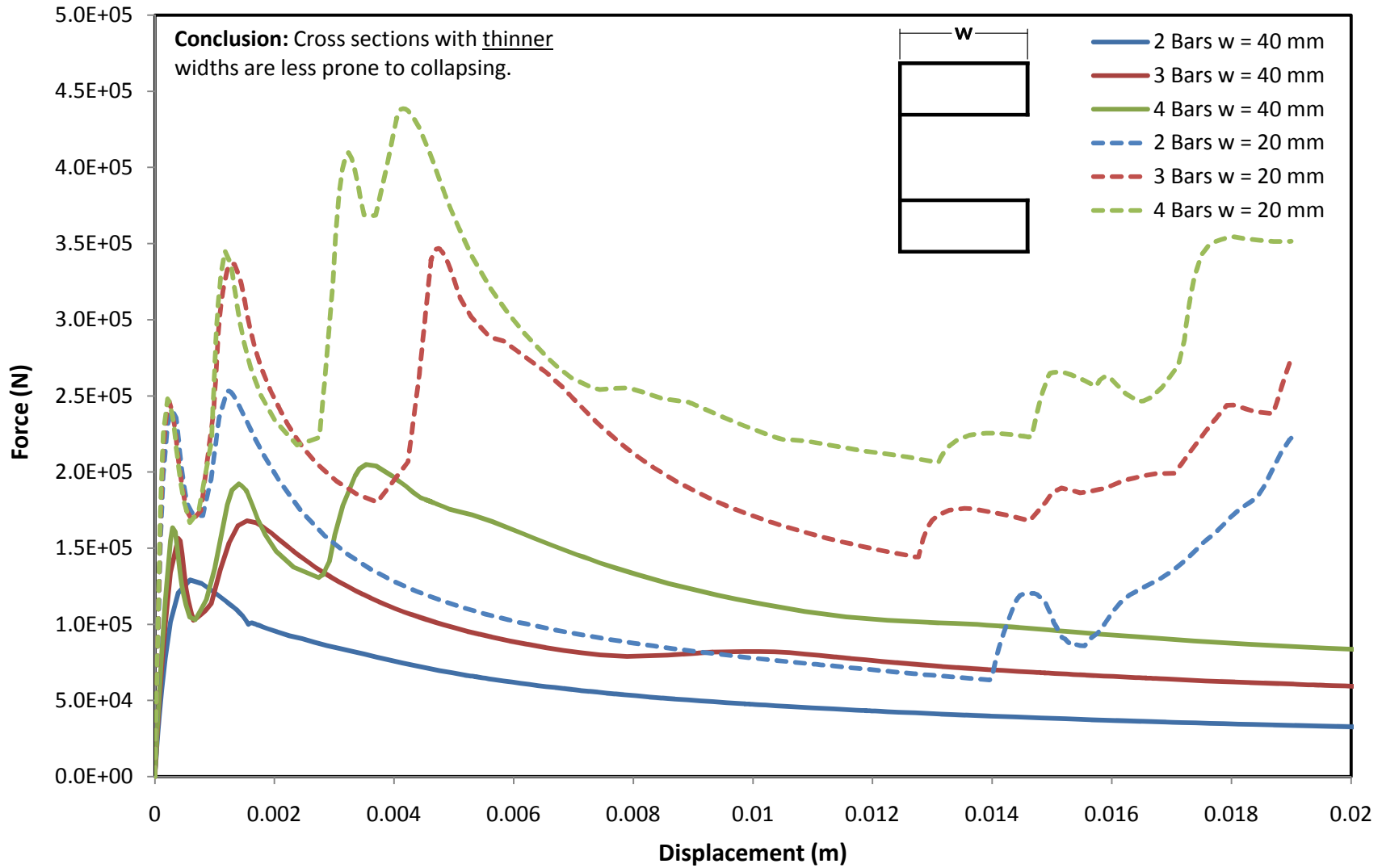


Figure 63. Effect of cross section width variation on energy absorption.

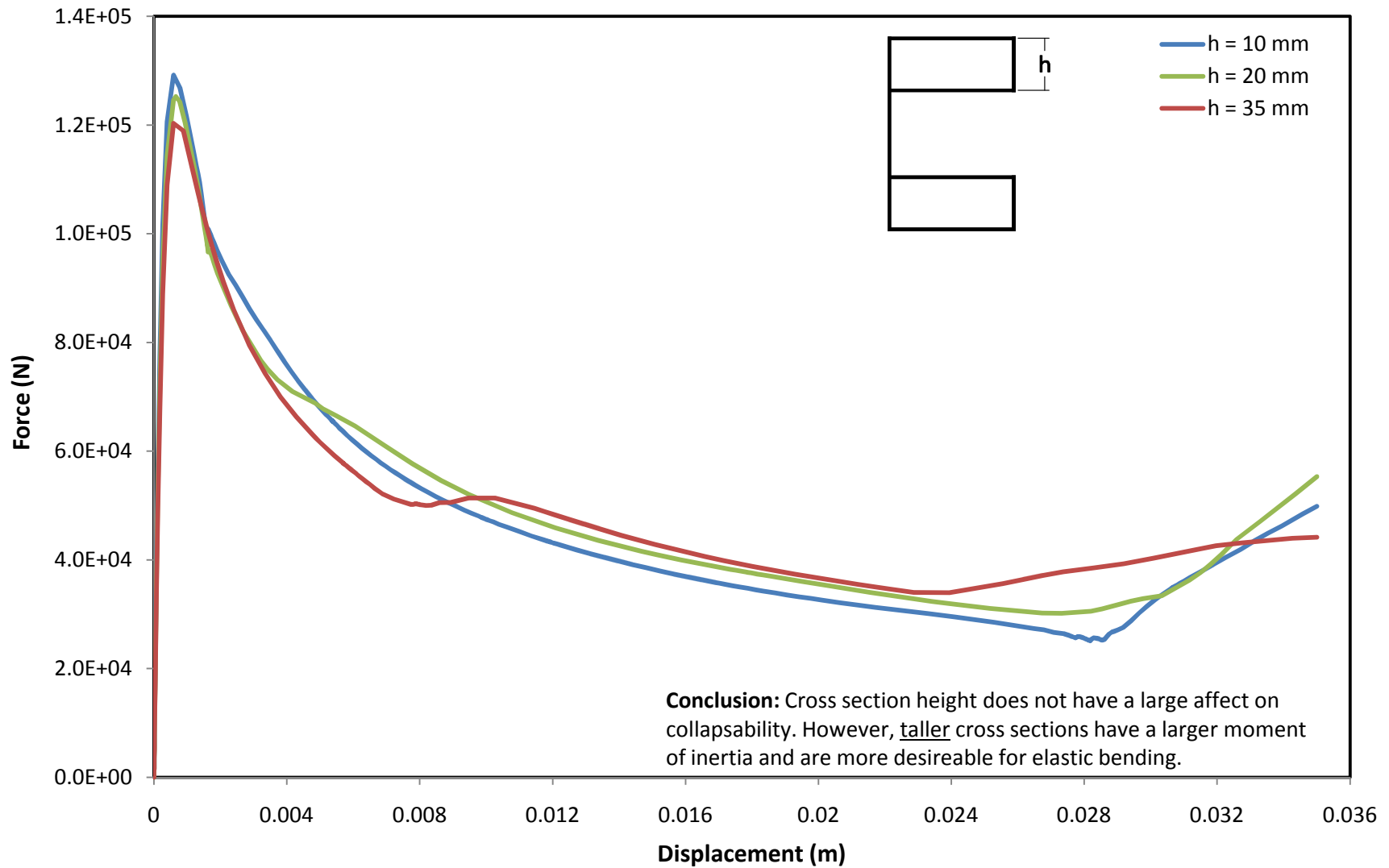


Figure 64. Reinforcement height effects on energy absorption.

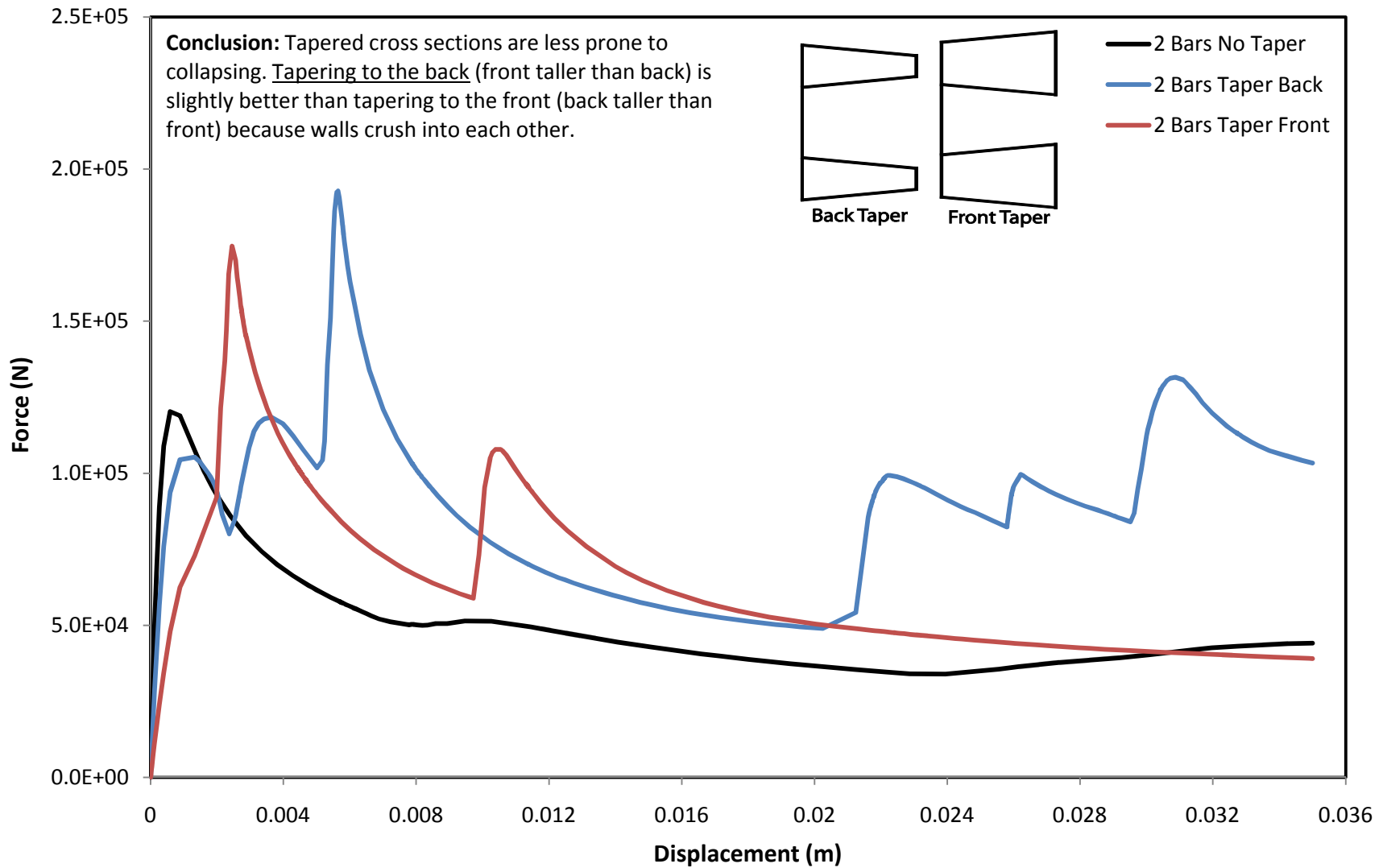


Figure 65. Effect of cross section taper orientation on energy absorption

APPENDIX H: MATERIAL COMPARISON

Table 8. List of AISI recommended materials

| AISI Material List | | Typical Yield Strength (Mpa) | Typical Tensile Strength (Mpa) | Minimum Elongation (%) |
|--------------------|-------------------|------------------------------|--------------------------------|------------------------|
| DR210 (CR) | Dent resistant | 220 | 360 | 40 |
| 1008/1010 (HR) | Low-carbon | 269 | 386 | 35 |
| 35XLF (CR) | Microalloy | 285 | 400 | 35 |
| 1008/1010 (CR) | Low-carbon | 296 | 331 | 35 |
| 40XLF (CR) | Microalloy | 315 | 425 | 33 |
| 10B21(M) | Carbon-Boron | 320 | 480 | 18 |
| 15B21(M) | Carbon-Boron | 330 | 500 | 27 |
| 15B24 (CR) | Carbon-Boron | 330 | 500 | 27 |
| 35XLF (HR) | Microalloy | 331 | 407 | 35 |
| 590T (CR) | Dual Phase | 371 | 634 | 24 |
| 50XLF (CR) | Microalloy | 376 | 475 | 28 |
| 50XLF (HDG-CR) | Microalloy | 379 | 453 | 30 |
| 50XLF (HR) | Microalloy | 403 | 480 | 31 |
| 55XLF (HDG-CR) | Microalloy | 415 | 492 | 28 |
| 55XLF (CR) | Microalloy | 418 | 501 | 27 |
| 55XLF(HR) | Microalloy | 439 | 505 | 29 |
| 60XLF (HDG-CR) | Microalloy | 452 | 531 | 26 |
| 60XLF (CR) | Microalloy | 459 | 527 | 26 |
| 60XLF (HR) | Microalloy | 475 | 531 | 27 |
| 780T (CR) | Dual Phase | 518 | 834 | 18 |
| 70XLF (HR) | Microalloy | 527 | 600 | 26 |
| 70XLF (CR) | Microalloy | 530 | 614 | 20 |
| 80XLF (HR) | Microalloy | 587 | 673 | 22 |
| 80XLF (CR) | Microalloy | 592 | 690 | 19 |
| 140T (CR) | Dual Phase | 634 | 1034 | 13 |
| 80XLF (HDG-CR) | Microalloy | 641 | 662 | 15 |
| 120XF (CR) | Recovery Annealed | 869 | 883 | 12 |
| 120XF (HDG - CR) | Recovery Annealed | 876 | 889 | 11 |
| M130HT (EG-CR) | Martensitic | 923 | 1055 | 5.4 |
| 135XF (CR) | Recovery Annealed | 969 | 985 | 7 |
| 140XF (CR) | Recovery Annealed | 1010 | 1028 | 5.6 |
| M160HT (EG-CR) | Martensitic | 1020 | 1179 | 5.1 |
| M190HT (EG-CR) | Martensitic | 1214 | 1420 | 5.1 |
| M220HT (EG-CR) | Martensitic | 1420 | 1627 | 4.7 |

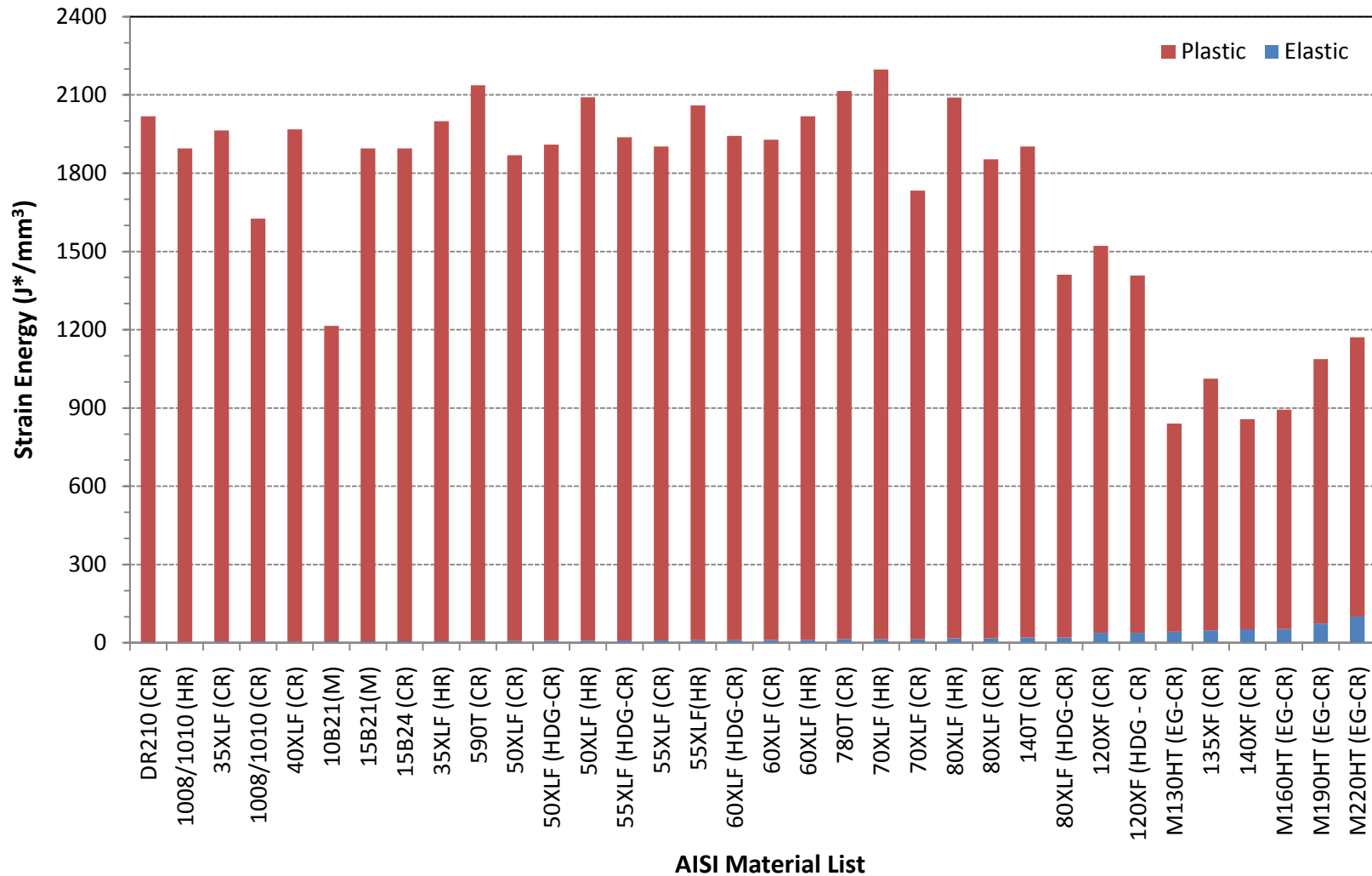


Figure 66. Strain Energy calculated from the approximated stress-strain curve of each metal, assuming 50% efficiency for the elastic deformation and 70% efficiency for plastic deformation

Mittal Steel USA Properties

Properties for all materials considered in the design were provided by Mittal Steel USA. Abaqus input required true stress and plastic strain as material property inputs, and provided formulas to perform conversions from engineering stress and strain.

$$\epsilon^T = \ln(1 + \epsilon_{nom}) \tag{Eq. 1}$$

$$\sigma^T = \sigma_{nom} (1 + \epsilon_{nom}) \tag{Eq. 2}$$

$$\epsilon^{Pl} = \epsilon^T - \frac{\sigma^T}{E} \tag{Eq. 3}$$

Equations 1 and 2 are used to convert Mittal Steel’s engineering stress and strain (σ_{nom} and ϵ_{nom}) to true stress and strain (σ^T and ϵ^T). Equation 3 uses these values to calculate plastic strain (ϵ^{Pl}). Stress and strain values used in Abaqus for HF 60 and M220 are included below.

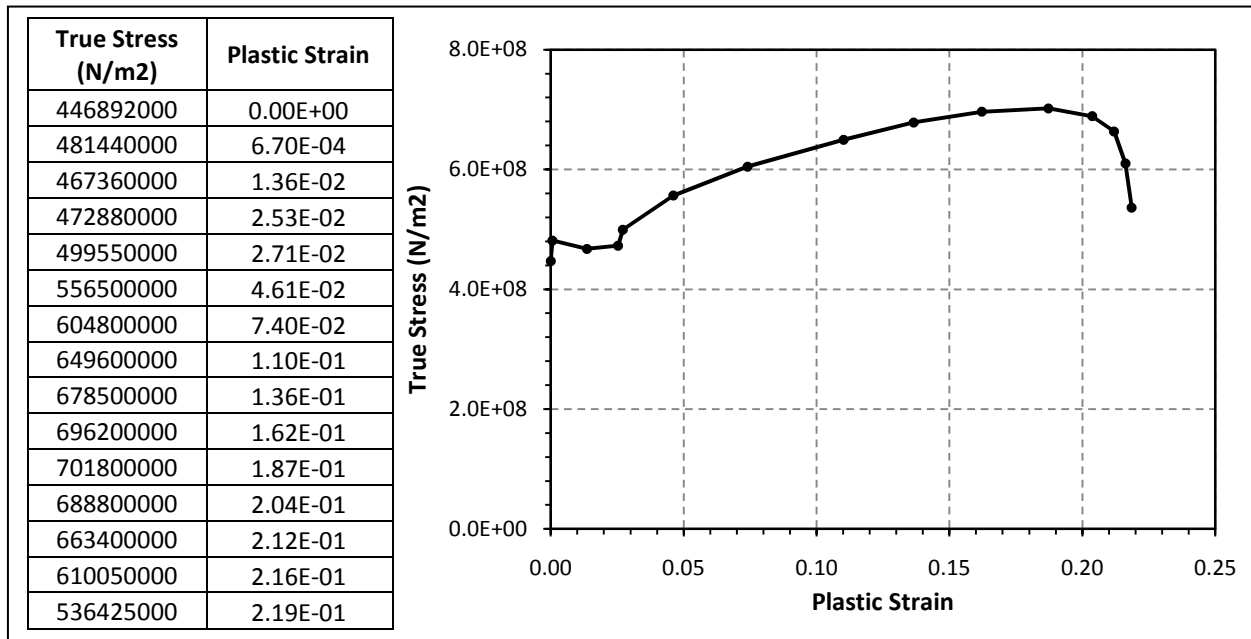


Figure 67. Stress-strain data for HF 60 high strength steel.

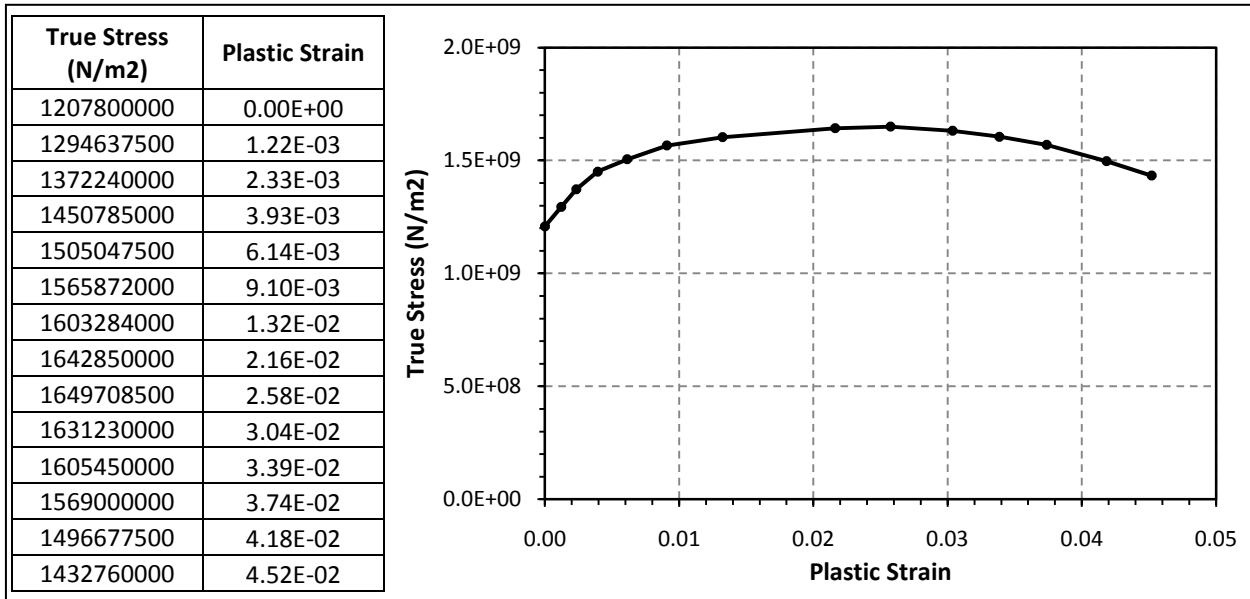


Figure 68. Stress-strain data for M220 Ultra High Strength Steel

APPENDIX I: FEA DATA SHEETS



GB17354-1998

Speed: 0.745 (80% KE with 3 75kg passengers)

Notes: Full frontal test
Crush cans modeled as springs

D6080-1.1 SEA = 2.8 kg
EA Thickness 60 mm

Plate 2 Tapers

| Model # | Beam Geometry | | | | | | | | | | Test Requirements and Results | | | | | | | | Model Description | | | | |
|---------|---------------------|------------------|-------------------|---------------------|-------------------|----------------|------|--------------------------|-------------------------|-------------|-------------------------------|----------------|--------------------------|---------------------------|---------------------------|----------------------------|---------------------|-------------------------|-------------------|---------------|----------|-------|---------------------------------------|
| | Overall Height (mm) | Taper Width (mm) | Taper Height (mm) | Taper Distance (mm) | Taper Angle (deg) | Thickness (mm) | | Sweep (mm ¹) | Area (mm ²) | Weight (kg) | Max Intrusion (mm) | Intrusion (mm) | Left Crush Can Disp (mm) | Right Crush Can Disp (mm) | Left Crush Can Force (kN) | Right Crush Can Force (kN) | Intrusion Pass/Fail | Crush Can Force Pass/Fa | Crush Can Model | Barrier Model | Material | Notes | |
| | | | | | | Plat | Tape | | | | | | | | | | | | | | | | |
| 1 | 110 | 50 | 19 | 6 | 6.843 | 0.7 | 0.7 | 140.7 | 244.6 | 2.8 | 5.6 | 88.9 | 52.6 | 0.2 | 2.6 | 5.2 | 4.9 | Passed by 36.3mm | Pass | Springs/Pin | Curved | M190 | Spacer B, flat plate, & D6080-1.1 SEA |
| 2 | 110 | 0 | 0 | 0 | null | 0.8 | 0 | null | 88 | 1.0 | 3.8 | null | 30.2 | 0.4 | 0.5 | 8 | 7.9 | Pass | Pass | Springs/Areas | Curved | M190 | D6090-1.1 SEA |
| 3 | 110 | 0 | 0 | 0 | null | 0.8 | 0 | null | 88 | 1.0 | 3.8 | null | 50.6 | 0.3 | 0.7 | 5.5 | 5.2 | Pass | Pass | Springs/Pin | Curved | M190 | D6090-1.1 SEA |
| 4 | 120 | 50 | 35 | 6 | 6.843 | 0.7 | 0.7 | 140.7 | 274 | 3.2 | 6.0 | 88.9 | 31.4 | 0.5 | 1.1 | 11.4 | 10.6 | Passed by 57.5mm | Pass | Springs/Pin | Curved | M220 | No SEA |

IIHS Full Frontal

Speed: 2.485 m/ (80% KE)

Notes: Full frontal test
Crush cans modeled as springs D6080-1.1 SEA = 2.8 kg

EA Thickness 60 mm

Plate 2 Tapers (Double Stacked)

| Model # | Beam Geometry | | | | | | | | | | Test Requirements and Results | | | | | | | | Model Description | | | | |
|---------|---------------------|------------------|-------------------|---------------------|-------------------|----------------|------|--------------------------|-------------------------|-------------|-------------------------------|--------------------|----------------|--------------------------|---------------------------|---------------------------|----------------------------|---------------------|-------------------------|-----------------|---------------|----------|---|
| | Overall Height (mm) | Taper Width (mm) | Taper Height (mm) | Taper Distance (mm) | Taper Angle (deg) | Thickness (mm) | | Sweep (mm ¹) | Area (mm ²) | Weight (kg) | Total Weight | Max Intrusion (mm) | Intrusion (mm) | Left Crush Can Disp (mm) | Right Crush Can Disp (mm) | Left Crush Can Force (kN) | Right Crush Can Force (kN) | Intrusion Pass/Fail | Crush Can Force Pass/Fa | Crush Can Model | Barrier Model | Material | Notes |
| | | | | | | Plat | Tape | | | | | | | | | | | | | | | | |
| 1 | 110 | 50 | 19 | 6 | 6.843 | 1 | 2 | 140.7 | 588.87 | 6.83 | 9.63 | 88.9 | 90.0 | - | - | - | - | Failed by 1.1mm | Fail | Pins | Curved | M220 | No EA |
| 2 | 110 | 50 | 19 | 6 | 6.843 | 2.1 | 0.7 | 140.7 | 398.6 | 4.62 | 7.42 | 88.9 | 134.0 | 2.2 | 48.1 | 5 | 34.5 | Failed by 45.1mm | Pass | Pins | Curved | M190 | With inner B section (110,25,25,3) |
| 3 | 120 | 50 | 35 | 6 | 6.843 | 0.7 | 0.7 | 140.7 | 274 | 3.18 | 5.98 | 88.9 | 133.8 | 1.9 | 2.8 | 40.2 | 42.4 | Failed by 44.9mm | Pass | Spring/Pin | Curved | M190 | D6080-1.1 Split EA |
| 4 | 120 | 50 | 35 | 6 | 6.843 | 0.7 | 0.7 | 140.7 | 274 | 3.18 | 5.98 | 88.9 | 109.3 | 1.9 | 2.5 | 20.4 | 19.7 | Failed by 20.4mm | Pass | Spring/Pin | Curved | M190 | D6080-1.1 Split EA larger |
| 5 | 120 | 50 | 35 | 6 | 6.843 | 1.4 | 0.7 | 140.7 | 358 | 4.15 | 6.95 | 88.9 | 168 | 2.7 | 2.7 | 56.3 | 57.3 | Failed by 79.1mm | Pass | Spring/Pin | Curved | M220 | No EA; Plate across back |
| 6 | 120 | 50 | 35 | 6 | 6.843 | ~1.4 | 0.7 | 140.7 | ##### | ##### | ##### | 88.9 | 180.0 | 2.5 | 2.3 | 54 | 50.6 | Failed by 91.1mm | Pass | Spring/Pin | Curved | M220 | No EA; Back plate from crush can to crush can |
| 7 | 120 | 50 | 35 | 6 | 6.843 | 0.7 | 0.7 | 140.7 | 274 | 3.18 | 5.98 | 88.9 | 84.8 | 1.7 | 4.1 | 36.7 | 29.5 | Passed by 4.1mm | Pass | Spring/Pin | Curved | M220 | D6080-0.6 SEA; MISSING CONTACT INTERACTION |
| 8 | 120 | 50 | 40 | 6 | 6.843 | 0.7 | 0.7 | 140.7 | 281 | 3.26 | 6.06 | 88.9 | | | | | | null | null | Spring/Pin | Curved | M220 | |
| 9 | 120 | 50 | 40 | 6 | 6.843 | 0.7 | 1.3 | 140.7 | 449.87 | 5.22 | 8.02 | 88.9 | 87.3 | 1.5 | 3.5 | 31.6 | 30 | Passed by 1.6mm | Pass | Spring/Pin | Curved | M220 | D6080-0.7 |
| 10 | 120 | 50 | 35 | 6 | 6.843 | 0.7 | 0.7 | 140.7 | 274 | 3.18 | 5.98 | 88.9 | 231.0 | 1.9 | 5.2 | 41.2 | 40.7 | Failed by 142.1mm | Pass | Spring/Pin | Curved | M220 | No EA |
| 11 | 120 | 50 | 35 | 6 | 6.843 | | | 140.7 | 0 | 0.00 | | 88.9 | 152.6 | 4.0 | 4.3 | 65 | 64.9 | Failed by 63.7mm | Pass | | | | 10840226 |
| 12 | 120 | 50 | 35 | 6 | 6.843 | 1.4 | 0.7 | 140.7 | 358 | 4.15 | 6.95 | 88.9 | 134.5 | 1.8 | 1.7 | 38.8 | 37.4 | Failed by 45.6mm | Pass | | | | No EA; Plate across back |
| 13 | 120 | 50 | 35 | 6 | 6.843 | 0.7 | 0.7 | 140.7 | 274 | 3.18 | 5.98 | 88.9 | 170.3 | 2.5 | 2.6 | 55.2 | 55.7 | Failed by 81.4mm | Pass | Spring/Pin | Curved | M220 | 110404010.0.7 |
| 14 | 120 | 50 | 35 | 6 | 6.843 | 0.7 | 0.7 | 140.7 | 274 | 3.18 | 5.98 | 88.9 | 95.8 | 1.5 | 5.5 | 30.8 | 35.7 | Failed by 6.9mm | Pass | Spring/Pin | Curved | M220 | 40 reinforcing beam |
| 15 | 120 | 50 | 35 | 6 | 6.843 | 0.7 | 0.7 | 140.7 | 274 | 3.18 | 5.98 | 88.9 | 88.1 | 1.4 | 3.8 | 31.3 | 30.6 | Passed by 0.8mm | Pass | Spring/Pin | Curved | M220 | D6080-0.7 SEA (~1.8kg) |
| 16 | | | | | null | | | | 0 | 0.00 | | null | | | | | | null | null | | | | |
| 17 | | | | | null | | | | 0 | 0.00 | | null | | | | | | null | null | | | | |
| 18 | | | | | null | | | | 0 | 0.00 | | null | | | | | | null | null | | | | |
| 19 | | | | | null | | | | 0 | 0.00 | | null | | | | | | null | null | | | | |
| 20 | | | | | null | | | | 0 | 0.00 | | null | | | | | | null | null | | | | |
| 21 | | | | | null | | | | 0 | 0.00 | | null | | | | | | null | null | | | | |
| 22 | | | | | null | | | | 0 | 0.00 | | null | | | | | | null | null | | | | |
| 23 | | | | | null | | | | 0 | 0.00 | | null | | | | | | null | null | | | | |
| 24 | | | | | null | | | | 0 | 0.00 | | null | | | | | | null | null | | | | |
| 25 | | | | | null | | | | 0 | 0.00 | | null | | | | | | null | null | | | | |
| 26 | | | | | null | | | | 0 | 0.00 | | null | | | | | | null | null | | | | |
| 27 | | | | | null | | | | 0.00 | | | null | | | | | | null | null | | | | |

| IIHS Offset | | | | | | | | | | | | | | | | | | | | | | | |
|--------------|-------------------------------|--|--|--|--|--|--|--|--|--|--|--|--|--|--|--|--|--|--|--|--|--|--|
| Speed: | 1.242 (80% KE) | | | | | | | | | | | | | | | | | | | | | | |
| Notes: | 15% offset test | | | | | | | | | | | | | | | | | | | | | | |
| | Crush cans modeled as springs | | | | | | | | | | | | | | | | | | | | | | |
| | D6080-1.1 SEA = 2.8 kg | | | | | | | | | | | | | | | | | | | | | | |
| EA Thickness | 60 mm | | | | | | | | | | | | | | | | | | | | | | |

| Plate 2 Tapers (Double Stacked) | | | | | | | | | | | | | | | | | | | | | | | |
|---------------------------------|---------------------|------------------|-------------------|---------------------|-------------------|----------------|------------|-------------------------|-------------|--------------|-------------------------------|-----------------------|--------------------------|---------------------------|---------------------------|----------------------------|---------------------|---------------------------|-----------------|---------------|----------|-------|-----------------------|
| Model # | Beam Geometry | | | | | | | | | | Test Requirements and Results | | | | | | Model Description | | | | | | |
| | Overall Height (mm) | Taper Width (mm) | Taper Height (mm) | Taper Distance (mm) | Taper Angle (deg) | Thickness (mm) | Sweep (mm) | Area (mm ²) | Weight (kg) | Total Weight | Max Intrusion (mm) | Corner Intrusion (mm) | Left Crush Can Disp (mm) | Right Crush Can Disp (mm) | Left Crush Can Force (kN) | Right Crush Can Force (kN) | Intrusion Pass/Fail | Crush Can Force Pass/Fail | Crush Can Model | Barrier Model | Material | Notes | |
| 1 | 110 | 50 | 19 | 6 | 6.843 | 0.8 | 0.8 | 140.7 | 279.55 | 3.24 | 6.04 | 10.0 | 63.7 | 0.3 | 2.2 | 7.7 | 32.5 | Failed by 53.7mm | Pass | Spring/Pins | Curved | M190 | No EA |
| 2 | 120 | 50 | 35 | 6 | 6.843 | 0.7 | 0.7 | 140.7 | 274 | 3.18 | 5.98 | 10.0 | 41.7 | 0.3 | 2.1 | 6 | 27.4 | Failed by 31.7mm | Pass | Spring/Pins | Curved | M190 | Chopped D6080-1.1 SEA |
| 3 | 120 | 50 | 35 | 6 | 6.843 | 0.7 | 0.7 | 140.7 | 274 | 3.18 | 5.98 | 10.0 | 30.0 | 0.1 | 1.8 | 2.3 | 38.2 | Failed by 20mm | Pass | Spring/Area | Curved | M190 | Chopped D6080-1.1 SEA |
| 4 | 120 | 50 | 35 | 6 | 6.843 | 0.7 | 0.7 | 140.7 | 274 | 3.18 | 5.98 | 10.0 | | | | | | null | null | Spring/Pins | Curved | M220 | D6080-0.7 SEA |

| RCAR Full Frontal | | | | | | | | | | | | | | | | | | | | | | | |
|-------------------|-------------------------------|--|--|--|--|--|--|--|--|--|--|--|--|--|--|--|--|--|--|--|--|--|--|
| Speed: | 2.485 m/s (80% KE) | | | | | | | | | | | | | | | | | | | | | | |
| Notes: | Full frontal test | | | | | | | | | | | | | | | | | | | | | | |
| | Crush cans modeled as springs | | | | | | | | | | | | | | | | | | | | | | |
| | D6080-1.1 SEA = 2.8 kg | | | | | | | | | | | | | | | | | | | | | | |
| EA Thickness | 60 mm | | | | | | | | | | | | | | | | | | | | | | |

| RCAR Full Frontal | | | | | | | | | | | | | | | | | | | | | | | |
|-------------------|---------------------|------------------|-------------------|---------------------|-------------------|----------------|------------|-------------------------|-------------|--------------|-------------------------------|----------------|--------------------------|---------------------------|---------------------------|----------------------------|---------------------|---------------------------|-----------------|---------------|-------------|-------|--------------------|
| Model # | Beam Geometry | | | | | | | | | | Test Requirements and Results | | | | | | Model Description | | | | | | |
| | Overall Height (mm) | Taper Width (mm) | Taper Height (mm) | Taper Distance (mm) | Taper Angle (deg) | Thickness (mm) | Sweep (mm) | Area (mm ²) | Weight (kg) | Total Weight | Max Intrusion (mm) | Intrusion (mm) | Left Crush Can Disp (mm) | Right Crush Can Disp (mm) | Left Crush Can Force (kN) | Right Crush Can Force (kN) | Intrusion Pass/Fail | Crush Can Force Pass/Fail | Crush Can Model | Barrier Model | Material | Notes | |
| 1 | 110 | 50 | 19 | 6 | 6.843 | 0.7 | 0.7 | 140.7 | 244.6 | 2.84 | 5.64 | 88.9 | 84.2 | 1.5 | 4.6 | 32.4 | 30.7 | Passed by 4.7mm | Pass | | | | |
| 2 | 120 | 50 | 35 | 6 | 6.843 | 0.7 | 0.7 | 140.7 | 274 | 3.18 | 5.98 | 88.9 | 77.4 | 1.5 | 4.1 | 33.1 | 29.6 | Passed by 11.5mm | Pass | Spring/Pin | RCAR offset | M220 | With D6080-1.1 SEA |
| 3 | 120 | 50 | 35 | 6 | 6.843 | 0.7 | 0.7 | 140.7 | 274 | 3.18 | 5.98 | 88.9 | | | | | | null | null | Spring/Pin | RCAR offset | M220 | No EA |

RCAR Offset

Speed: 3.727 (80% KE)

Notes: 40 % offset test

Crush cans modeled as springs D6080-1.1 SEA = 2.8 kg

EA Thickness

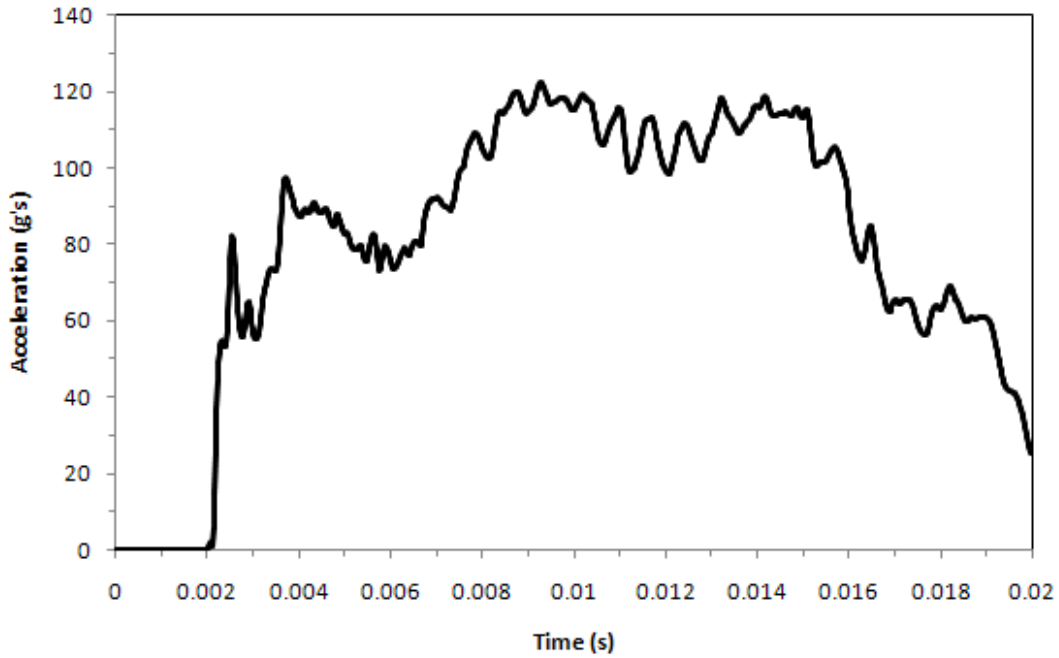
60 mm

Plate 2 Tapers (Double Stacked)

| Model # | Beam Geometry | | | | | | | | | | Test Requirements and Results | | | | | | | | Model Description | | | | |
|---------|---------------------|------------------|-------------------|---------------------|-------------------|----------------|------------|-------------------------|-------------|-------------------|-------------------------------|----------------|--------------------------|---------------------------|---------------------------|----------------------------|---------------------|---------------------------|-------------------|---------------|-------------|-------|--------------------|
| | Overall Height (mm) | Taper Width (mm) | Taper Height (mm) | Taper Distance (mm) | Taper Angle (deg) | Thickness (mm) | Sweep (mm) | Area (mm ²) | Weight (kg) | Total Weight (kg) | Max Intrusion (mm) | Intrusion (mm) | Left Crush Can Disp (mm) | Right Crush Can Disp (mm) | Left Crush Can Force (kN) | Right Crush Can Force (kN) | Intrusion Pass/Fail | Crush Can Force Pass/Fail | Crush Can Model | Barrier Model | Material | Notes | |
| 1 | 110 | 50 | 19 | 6 | 6.843 | 0.7 | 0.7 | 140.7 | 244.6 | 2.84 | 5.64 | 88.9 | 104.9 | 0.6 | 99.3 | 12.1 | 64.4 | Failed by 16mm | Pass | Spring/1Pin | RCAR offset | M190 | With D6080-1.1 SEA |
| 2 | 110 | 50 | 19 | 6 | 6.843 | 0.7 | 0.7 | 140.7 | 244.6 | 2.84 | 5.64 | 88.9 | 94.3 | 0.7 | 85.8 | 15.3 | 64.6 | Failed by 5.4mm | Pass | Spring/Areas | RCAR offset | M190 | With D6080-1.1 SEA |
| 3 | 110 | 50 | 19 | 6 | 6.843 | 0.7 | 0.7 | 140.7 | 244.6 | 2.84 | 5.64 | 88.9 | 102.9 | 0.6 | 99.3 | 13.6 | 65 | Failed by 14mm | Pass | Spring/1Pin | RCAR offset | M220 | With D6080-1.1 SEA |
| 4 | 110 | 50 | 19 | 6 | 6.843 | 0.7 | 0.7 | 140.7 | 244.6 | 2.84 | 5.64 | 88.9 | 92.5 | 0.8 | 86.5 | 16.6 | 65 | Failed by 3.6mm | Pass | Spring/Areas | RCAR offset | M220 | With D6080-1.1 SEA |
| 5 | 110 | 45 | 19 | 6 | 7.595 | 0.7 | 0.7 | 145.7 | 230.72 | 2.68 | 5.48 | 93.9 | 109.1 | 0.5 | 104.0 | 12 | 65 | Failed by 15.2mm | Pass | Spring/1Pin | RCAR offset | M190 | With D6080-1.1 SEA |
| 6 | 110 | 45 | 19 | 6 | 7.595 | 0.7 | 0.7 | 145.7 | 230.72 | 2.68 | 5.48 | 93.9 | 96.1 | 0.7 | 90.2 | 14.2 | 65 | Failed by 2.2mm | Pass | Spring/Areas | RCAR offset | M190 | With D6080-1.1 SEA |
| 7 | 110 | 45 | 19 | 6 | 7.595 | 0.7 | 0.7 | 145.7 | 230.72 | 2.68 | 5.48 | 93.9 | 106.7 | 0.6 | 103.1 | 12.9 | 65 | Failed by 12.8mm | Pass | Spring/1Pin | RCAR offset | M220 | With D6080-1.1 SEA |
| 8 | 110 | 45 | 19 | 6 | 7.595 | 0.7 | 0.7 | 145.7 | 230.72 | 2.68 | 5.48 | 93.9 | 94.7 | 0.8 | 90.5 | 15.9 | 65 | Failed by 0.8mm | Pass | Spring/Areas | RCAR offset | M220 | With D6080-1.1 SEA |
| 9 | 110 | 50 | 30 | 6 | 6.843 | 0.8 | 0.8 | 140.7 | 297.15 | 3.45 | 6.25 | 88.9 | 82.8 | 0.9 | 96.8 | 18.4 | 87.5 | Passed by 6.1mm | Fail | Spring/Areas | RCAR offset | M220 | With D6080-1.1 SEA |
| 10 | 110 | 60 | 19 | 6 | 5.711 | 0.7 | 0.7 | 130.7 | 272.44 | 3.16 | 5.96 | 78.9 | 89.8 | 1.0 | 87.4 | 20 | 65 | Failed by 10.9mm | Pass | Spring/Areas | RCAR offset | M220 | With D6080-1.1 SEA |
| 11 | 110 | 60 | 19 | 6 | 5.711 | 0.8 | 0.8 | 130.7 | 311.36 | 3.61 | 6.41 | 78.9 | 80.5 | 1.0 | 97.0 | 21.6 | 93.1 | Failed by 1.6mm | Fail | Spring/Areas | RCAR offset | M220 | With D6080-1.1 SEA |
| 12 | 110 | 50 | 30 | 6 | 6.843 | 0.8 | 0.8 | 140.7 | 297.15 | 3.45 | 6.25 | 88.9 | 84.4 | 0.8 | 96.3 | 18.1 | 84.9 | Passed by 4.5mm | Fail | Spring/Areas | RCAR offset | M190 | With D6080-1.1 SEA |
| 13 | 110 | 50 | 25 | 6 | 6.843 | 0.8 | 0.8 | 140.7 | 289.15 | 3.35 | 6.15 | 88.9 | 83.8 | 1.0 | 96.2 | 19.7 | 86.1 | Passed by 5.1mm | Fail | Spring/Areas | RCAR offset | M190 | With D6080-1.1 SEA |
| 14 | 120 | 50 | 35 | 6 | 6.843 | 0.7 | 0.7 | 140.7 | 274 | 3.18 | 5.98 | 88.9 | 87.7 | 0.8 | 85.1 | 17.9 | 65 | Passed by 1.2mm | Pass | Spring/Areas | RCAR offset | M220 | With D6080-1.1 SEA |
| 15 | 120 | 50 | 30 | 6 | 6.843 | 0.7 | 0.7 | 140.7 | 267 | 3.10 | 5.90 | 88.9 | 89.4 | 0.9 | 85.7 | 18.6 | 65 | Failed by 0.5mm | Pass | Spring/Areas | RCAR offset | M220 | With D6080-1.1 SEA |
| 16 | 110 | 50 | 40 | 6 | 6.843 | 0.7 | 0.7 | 140.7 | 274 | 3.18 | 5.98 | 88.9 | 85.6 | 0.9 | 84.4 | 18.8 | 65 | Passed by 3.3mm | Pass | Spring/Areas | RCAR offset | M220 | With D6080-1.1 SEA |
| 17 | 120 | 50 | 40 | 6 | 6.843 | 0.7 | 0.7 | 140.7 | 281 | 3.26 | 6.06 | 88.9 | 85.5 | 0.8 | 84.0 | 18.1 | 65 | Passed by 3.4mm | Pass | Spring/Areas | RCAR offset | M220 | With D6080-1.1 SEA |
| 18 | 120 | 50 | 35 | 4 | 4.574 | 0.7 | 0.7 | 140.7 | 273.45 | 3.17 | 5.97 | 88.9 | 86.9 | 0.9 | 83.8 | 18.5 | 65 | Passed by 2mm | Pass | Spring/Areas | RCAR offset | M220 | With D6080-1.1 SEA |
| 19 | 120 | 50 | 35 | 8 | 9.090 | 0.7 | 0.7 | 140.7 | 274.78 | 3.19 | 5.99 | 88.9 | 88.1 | 0.8 | 86.2 | 17.5 | 64.7 | Passed by 0.8mm | Pass | Spring/Areas | RCAR offset | M220 | With D6080-1.1 SEA |

Pedestrian Protection

Max acceleration must be under 150 G's

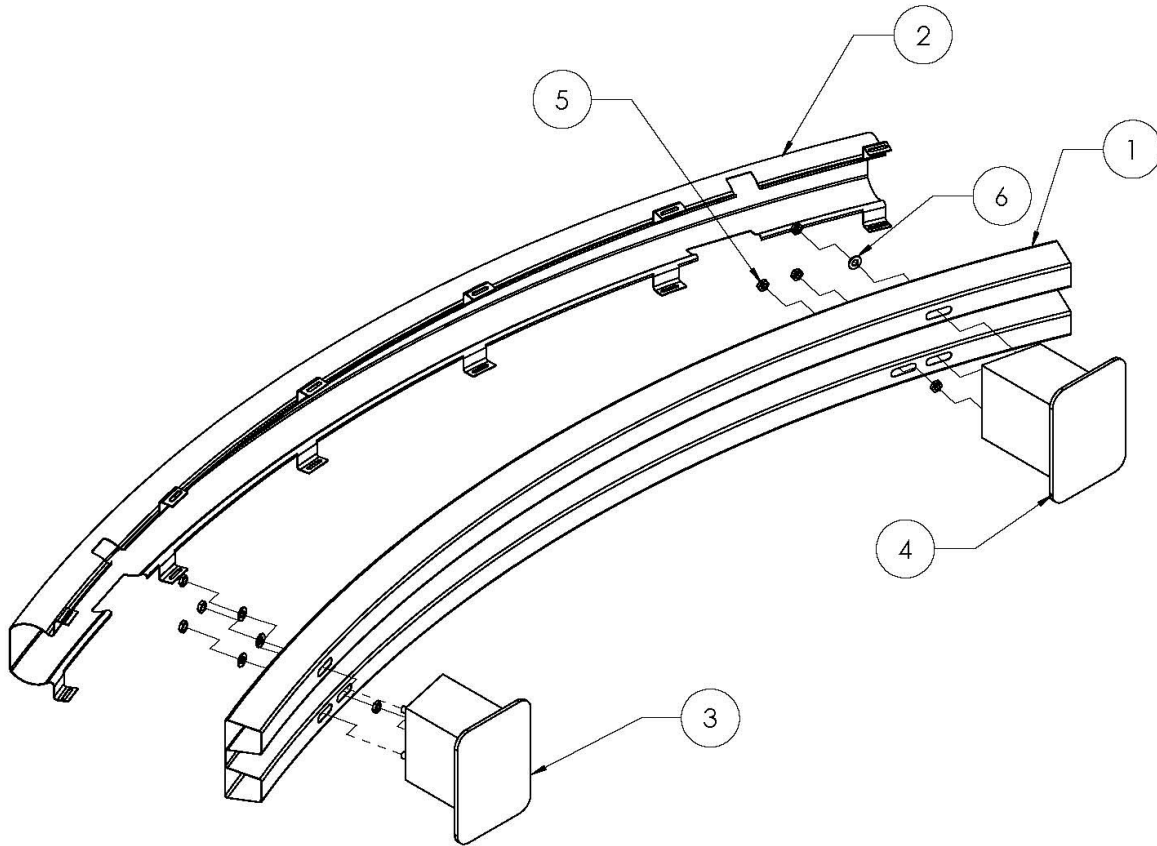


| | | | |
|-----------|--------|---------------|----------|
| Pass/Fail | Pass | Weight of Leg | Material |
| Max Accel | 122.55 | 13.4 kg | HF 60 |
| | | Specs | |
| | | 1.1 mm thick | |
| | | 60 mm deep | |
| | | 100 mm height | |

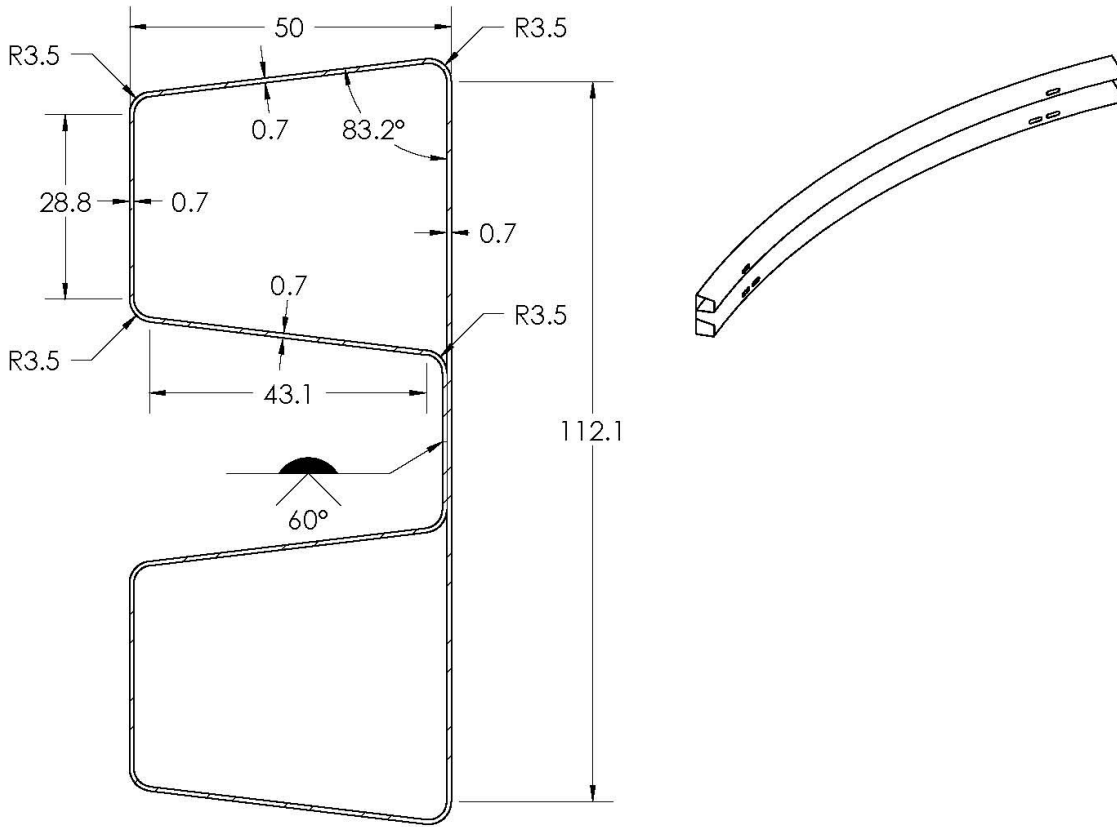
Note: This SEA was analyzed using filleted edges

APPENDIX J: DETAILED DRAWINGS

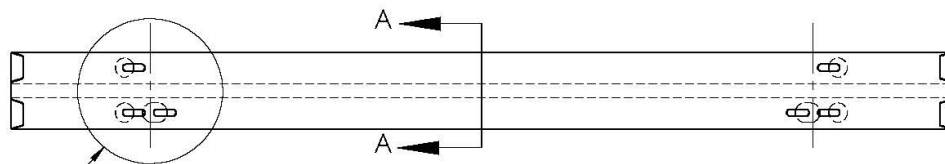
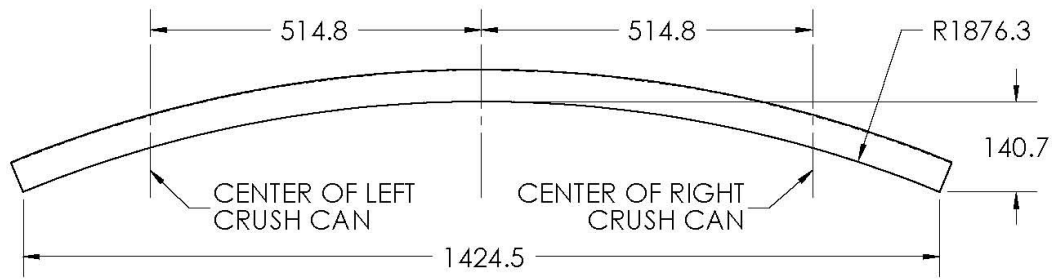
| ITEM NO. | PART NUMBER | DESCRIPTION | QTY. |
|----------|---------------------------|---------------------------------|------|
| 1 | Base 120-50-35-6-07 | M220, roll formed | 1 |
| 2 | Steel Energy Absorber | HF 60, stamped | 1 |
| 3 | Crush Can left | Provided by Shape Corp. | 1 |
| 4 | Crush Can right | Provided by Shape Corp. | 1 |
| 5 | M8 Steel bolt | McMaster-Carr Part #: 90695A040 | 8 |
| 6 | M8 Stainless Steel Washer | McMaster-Carr Part #: 93849A105 | 6 |



| | | | | | |
|---|---------|---|---|-------------------------------|---|
| <p>PROPRIETARY AND CONFIDENTIAL THE INFORMATION CONTAINED IN THIS DRAWING IS THE SOLE PROPERTY OF CAL POLY REVHEADS. ANY REPRODUCTION IN PART OR AS A WHOLE WITHOUT THE WRITTEN PERMISSION OF CAL POLY REVHEADS IS PROHIBITED.</p> | | DIMENSIONS ARE IN MM TOLERANCES: FRACTIONAL ± ANGULAR: MACH ± BEND ± TWO PLACE DECIMAL ± THREE PLACE DECIMAL ± | | NAME CAH DATE 6/8/09 | CAL POLY REVHEADS BUMPER REINFORCEMENT BEAM ASSEMBLY |
| | | MATERIAL | | CHECKED GAB 6/8/09 | |
| NEXT ASSY | USED ON | FINISH | COMMENTS: BASE BUMPER REINFORCEMENT BEAM FOR GB17354-199B, IHS, & FCAR | | SIZE A |
| APPLICATION | | DO NOT SCALE DRAWING | | DWG. NO. ASM 001 | REV. 1 |
| | | | SCALE: 1:10 | WEIGHT: | SHEET 1 OF 1 |



SECTION A-A
SCALE 1 : 1



REFER TO
B002

PROPRIETARY AND CONFIDENTIAL
THE INFORMATION CONTAINED IN THIS DRAWING IS THE SOLE PROPERTY OF CAL POLY REVHEADS. ANY REPRODUCTION IN PART OR AS A WHOLE WITHOUT THE WRITTEN PERMISSION OF CAL POLY REVHEADS IS PROHIBITED.

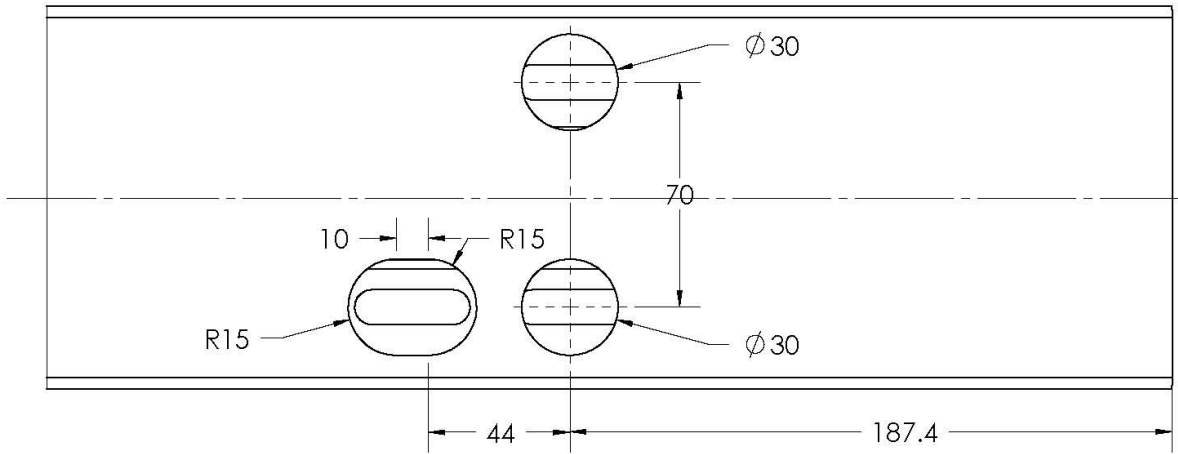
| | | | | | |
|-------------|---------|---|--|------------------|----------------|
| ASM001 | | DIMENSIONS ARE IN MM TOLERANCES: FRACTIONAL ± ANGULAR: MACH ± BEND ± TWO PLACE DECIMAL ± THREE PLACE DECIMAL ± | DRAWN GAB 6/8/09 | NAME GAB | DATE 6/8/09 |
| | | MATERIAL ELECTROSITE M220 | CHECKED BRT 6/8/09 | ENG APPR. | |
| | | FINISH | MFG APPR. | Q.A. | |
| NEXT ASSY | USED ON | | COMMENTS: BASE BUMPER REINFORCEMENT BEAM FOR GB17354-1998, IHS, & PCAR | | |
| APPLICATION | | DO NOT SCALE DRAWING | SIZE A | DWG. NO. B001 | REV. 1 |

CAL POLY REVHEADS
BASE BUMPER
REINFORCEMENT
BEAM

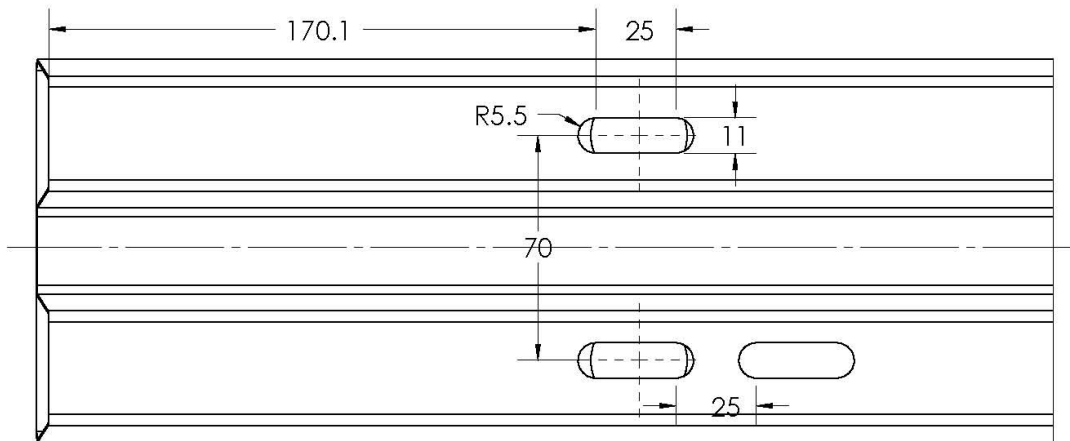
| | | |
|-------------|-----------------|--------------|
| SCALE: 1:10 | WEIGHT: 3.26 kg | SHEET 1 OF 1 |
|-------------|-----------------|--------------|

LEFT SIDE OF BUMPER - DETAIL B-B

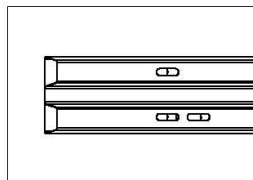
FRONT FACE



BACK FACE

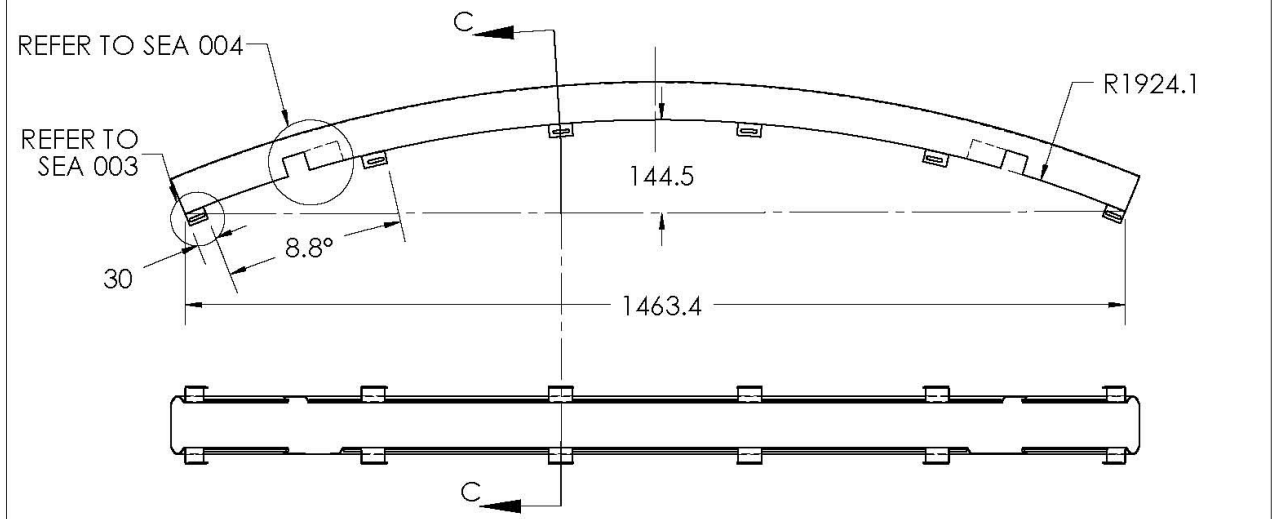
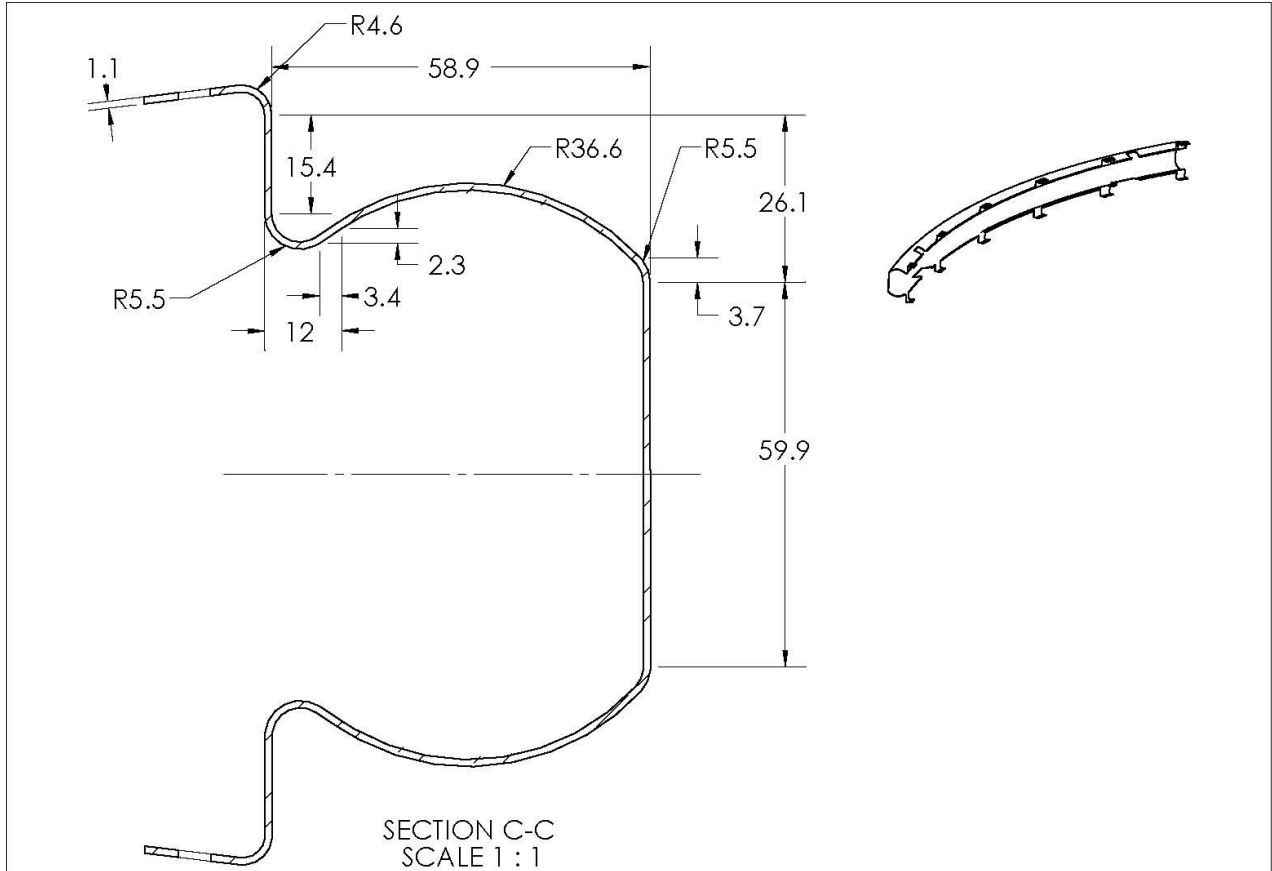


NOTE: ALL BACK CUT OUTS ARE THE SAME SHAPE

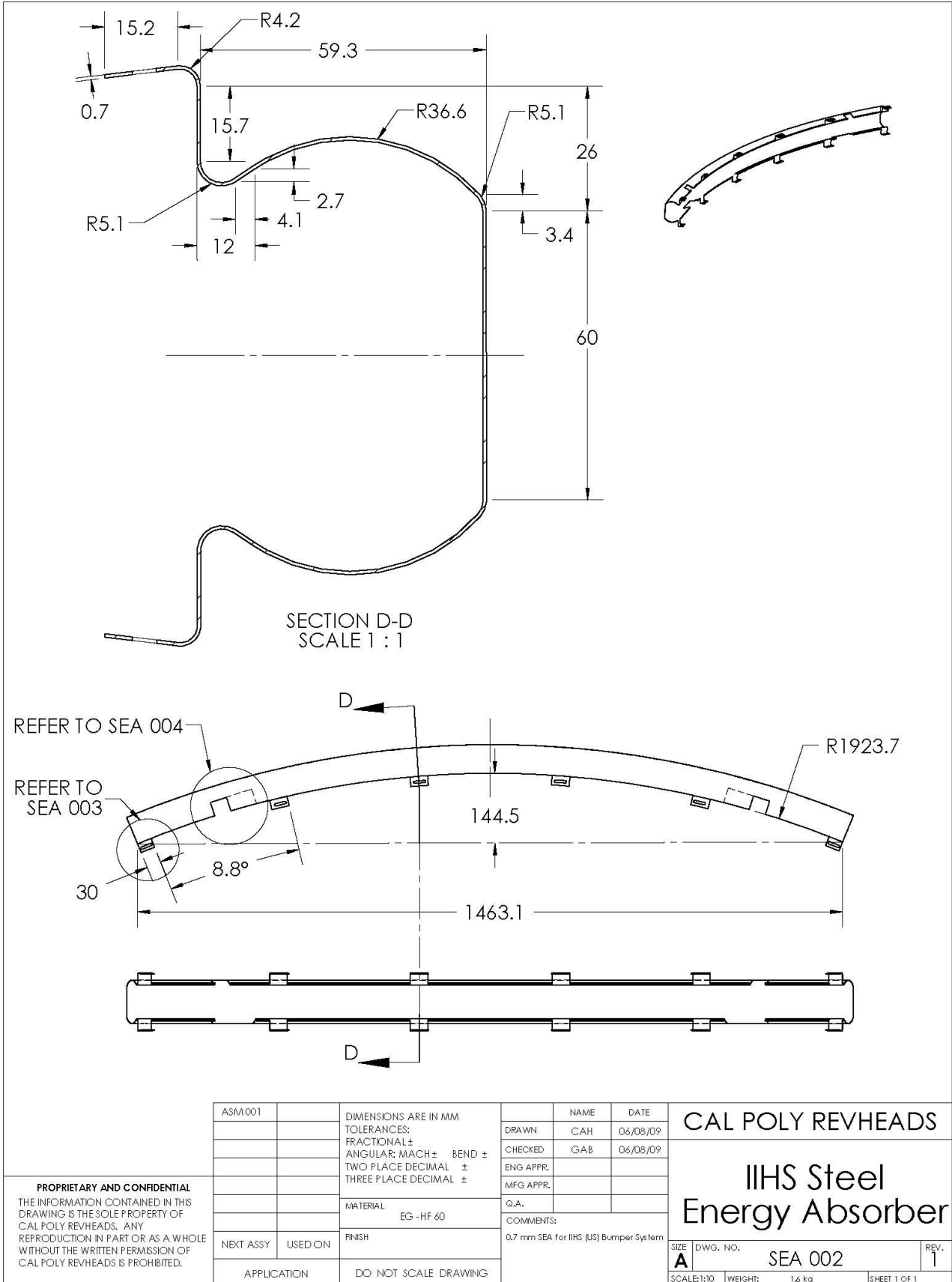


DETAIL B-B

| | | | | | | | |
|---|-------------|---------|---|---|-------------|--|--------|
| <p>PROPRIETARY AND CONFIDENTIAL THE INFORMATION CONTAINED IN THIS DRAWING IS THE SOLE PROPERTY OF CAL POLY REVHEADS. ANY REPRODUCTION IN PART OR AS A WHOLE WITHOUT THE WRITTEN PERMISSION OF CAL POLY REVHEADS IS PROHIBITED.</p> | ASM 001 | | <p>DIMENSIONS ARE IN MM TOLERANCES: FRACTIONAL ± ANGULAR: MACH ± BEND ± TWO PLACE DECIMAL ± THREE PLACE DECIMAL ±</p> | NAME | DATE | <p>CAL POLY REVHEADS</p> <p>BASE BEAM DETAIL DRAWING</p> | |
| | | | | DRAWN | CAH | | 6/8/09 |
| | | | | CHECKED | GAB | | 6/8/09 |
| | | | | ENG APPR. | | | |
| | | | | MFG APPR. | | | |
| | | | | Q.A. | | | |
| | | | | COMMENTS: | | | |
| | | | | <p>BASE BUMPER REINFORCEMENT BEAM FOR GB17354-199B, IHS, & RCAR</p> | | | |
| | NEXT ASSY | USED ON | FINISH | SIZE | DWG. NO. | REV. | |
| | | | | A | B002 | 1 | |
| | APPLICATION | | DO NOT SCALE DRAWING | SCALE:1:10 | WEIGHT: | SHEET 1 OF 1 | |



| | | | | | | | |
|---|-------------|---------|---|--|----------------|--|----------|
| <p>PROPRIETARY AND CONFIDENTIAL THE INFORMATION CONTAINED IN THIS DRAWING IS THE SOLE PROPERTY OF CAL POLY REVHEADS. ANY REPRODUCTION IN PART OR AS A WHOLE WITHOUT THE WRITTEN PERMISSION OF CAL POLY REVHEADS IS PROHIBITED.</p> | ASM 001 | | <p>DIMENSIONS ARE IN MM TOLERANCES: FRACTIONAL ± ANGULAR: MACH ± BEND ± TWO PLACE DECIMAL ± THREE PLACE DECIMAL ±</p> | NAME | DATE | <p>CAL POLY REVHEADS RCAR Steel Energy Absorber</p> | |
| | | | | DRAWN | CAH 06/08/09 | | |
| | | | | CHECKED | GAB 06/08/09 | | |
| | | | | ENG APPR. | | | |
| | | | | MFG APPR. | | | |
| | | | MATERIAL | EG - HF 60 | | Q.A. | |
| | | | FINISH | | | COMMENTS: | |
| | NEXT ASSY | USED ON | | 1.1 mm SEA for RCAR (European) Bumper System | | SIZE | DWG. NO. |
| | APPLICATION | | DO NOT SCALE DRAWING | | | A | SEA 001 |
| | | | | SCALE:1:10 | WEIGHT: 2.4 kg | SHEET 1 OF 1 | REV. 1 |



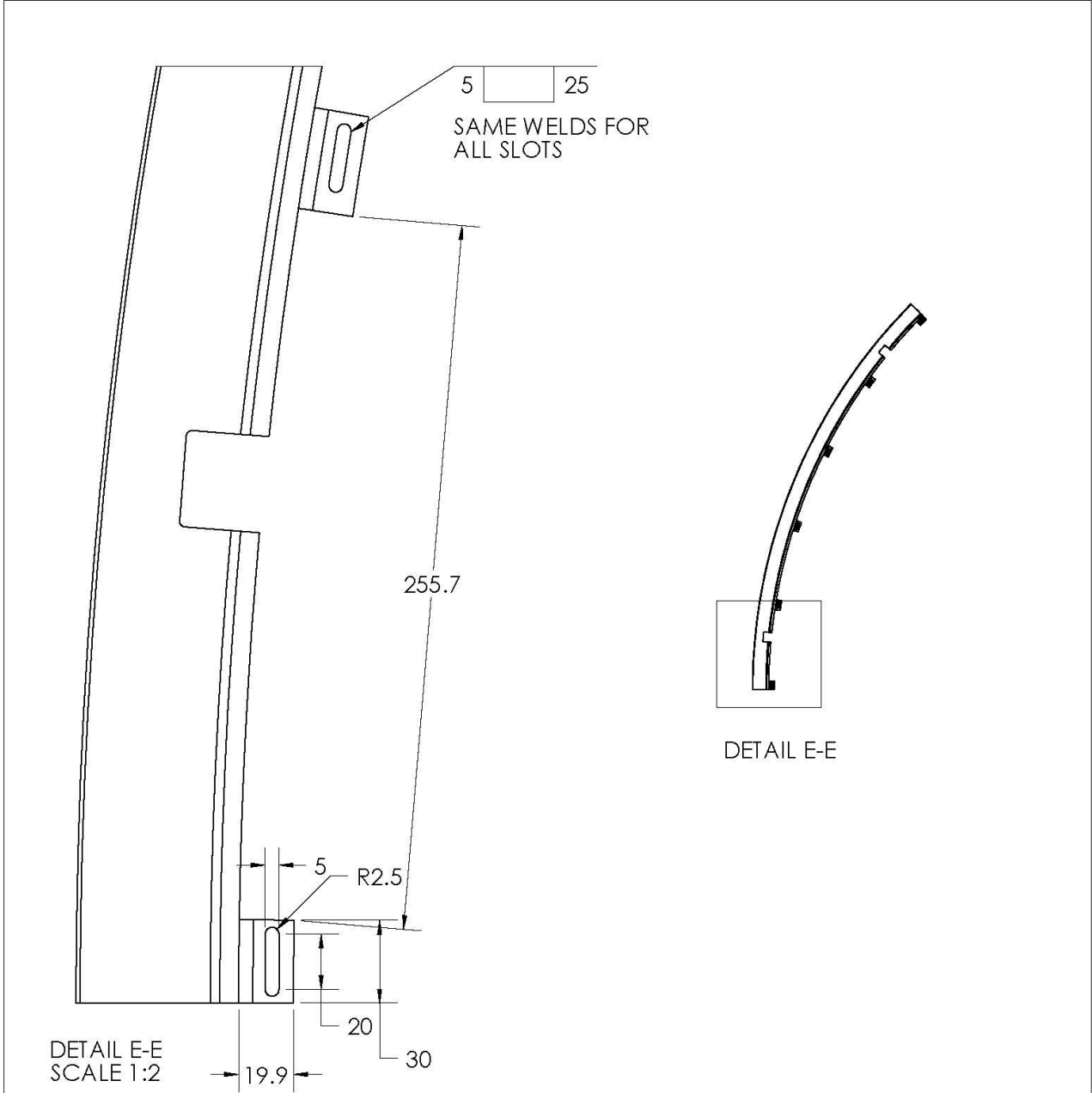
| | | | | |
|---------|-------------|---|-----------|---------------------------------------|
| ASM 001 | | DIMENSIONS ARE IN MM TOLERANCES: FRACTIONAL ± ANGULAR: MACH ± BEND ± TWO PLACE DECIMAL ± THREE PLACE DECIMAL ± | NAME | DATE |
| | | | DRAWN | C.AH 06/08/09 |
| | | | CHECKED | GAB 06/08/09 |
| | | | ENG APPR. | |
| | | | MFG APPR. | |
| | | | Q.A. | |
| | | | COMMENTS: | 0.7 mm SEA for IHS (US) Bumper System |
| | NEXT ASSY | USED ON | | |
| | APPLICATION | DO NOT SCALE DRAWING | | |

CAL POLY REVHEADS

IHS Steel
Energy Absorber

| | | |
|-------------|----------------|--------------|
| SIZE | DWG. NO. | REV. |
| A | SEA 002 | 1 |
| SCALE: 1:10 | WEIGHT: 1.6 kg | SHEET 1 OF 1 |

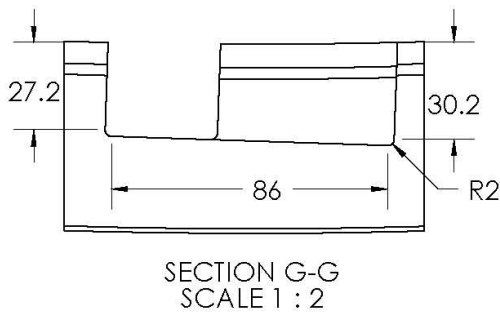
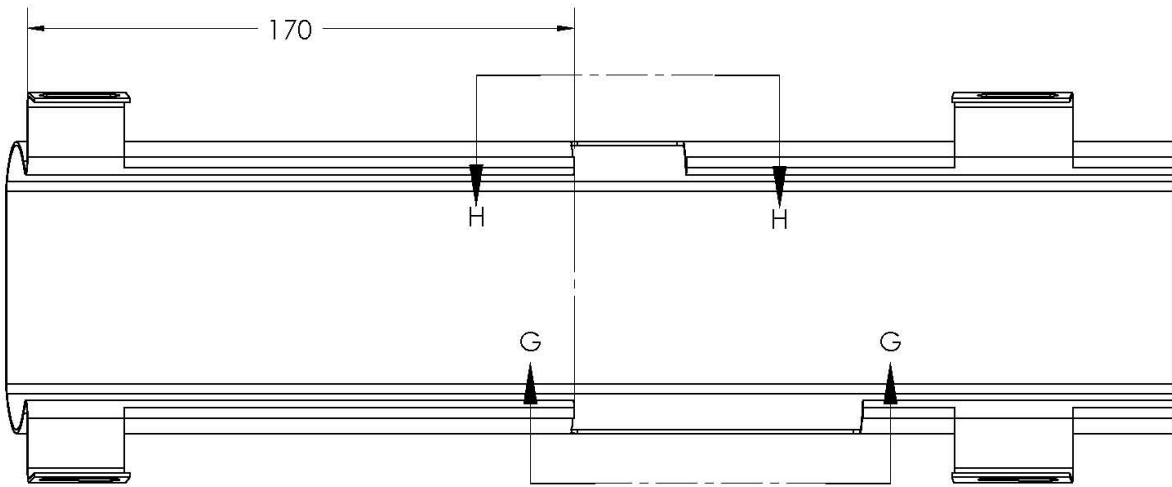
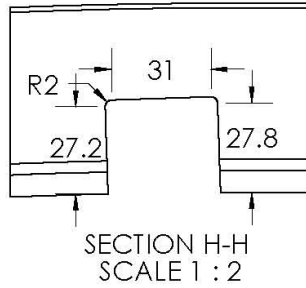
PROPRIETARY AND CONFIDENTIAL
THE INFORMATION CONTAINED IN THIS DRAWING IS THE SOLE PROPERTY OF CAL POLY REVHEADS. ANY REPRODUCTION IN PART OR AS A WHOLE WITHOUT THE WRITTEN PERMISSION OF CAL POLY REVHEADS IS PROHIBITED.



6 EQUALLY SPACED TABS AS DESCRIBED ABOVE

| | | | | | | | | |
|---|-------------|---------|---|------------|-----------|--|--------------|--------------|
| <p>PROPRIETARY AND CONFIDENTIAL THE INFORMATION CONTAINED IN THIS DRAWING IS THE SOLE PROPERTY OF CAL POLY REVHEADS. ANY REPRODUCTION IN PART OR AS A WHOLE WITHOUT THE WRITTEN PERMISSION OF CAL POLY REVHEADS IS PROHIBITED.</p> | ASM 001 | | DIMENSIONS ARE IN MM TOLERANCES: FRACTIONAL ± ANGULAR: MACH ± BEND ± TWO PLACE DECIMAL ± THREE PLACE DECIMAL ± | NAME | DATE | <p>CAL POLY REVHEADS</p> <p>Steel Energy Absorber Tabs</p> | | |
| | | | MATERIAL | EG - HF 60 | DRAWN | | CAH 06/08/09 | |
| | | | FINISH | | CHECKED | | GAB 06/08/09 | |
| | NEXT ASSY | USED ON | | | ENG APPR. | | | |
| | APPLICATION | | DO NOT SCALE DRAWING | | MFG APPR. | | | |
| | | | | Q.A. | | SIZE | DWG. NO. | REV. |
| | | | | COMMENTS: | | A | SEA 003 | 1 |
| | | | | | | SCALE:1:10 | WEIGHT: | SHEET 1 OF 1 |

LEFT SIDE OF STEEL ENERGY ABSORBER



| | | | | | | | |
|---|-------------|---------|---|------------|---------|--------|---|
| <p>PROPRIETARY AND CONFIDENTIAL THE INFORMATION CONTAINED IN THIS DRAWING IS THE SOLE PROPERTY OF CAL POLY REVHEADS. ANY REPRODUCTION IN PART OR AS A WHOLE WITHOUT THE WRITTEN PERMISSION OF CAL POLY REVHEADS IS PROHIBITED.</p> | ASM 001 | | <p>DIMENSIONS ARE IN MM TOLERANCES: FRACTIONAL ± ANGULAR: MACH ± BEND ± TWO PLACE DECIMAL ± THREE PLACE DECIMAL ±</p> | DRAWN | NAME | DATE | <p>CAL POLY REVHEADS Steel Energy Absorber Assembly Notches</p> |
| | | | | CHECKED | CAH | 6/8/09 | |
| | | | | ENG APPR. | GAB | 6/8/09 | |
| | | | | MFG APPR. | | | |
| | | | | Q.A. | | | |
| | | | COMMENTS: | | | | |
| | NEXT ASSY | USED ON | MATERIAL | | | | SIZE |
| | | | EG-HF 60 | | | | DWG. NO. |
| | | | FINISH | | | | SEA 004 |
| | APPLICATION | | DO NOT SCALE DRAWING | | | | REV. |
| | | | | | | | 1 |
| | | | | SCALE:1:10 | WEIGHT: | | SHEET 1 OF 1 |

APPENDIX K: PEDESTRIAN TEST PLAN

TEST PLAN

EuroNCAP Pedestrian Leg Drop

MATERIALS:

1. Model leg with accelerometer
2. Bumper test specimen
3. Test fixture
4. Data acquisition system with laptop
5. 25-ft BNC cable
6. Tape measure
7. Scale
8. High speed camera and laptop
9. Portable hard drive

TEST PROCEDURE:

SET UP & INITIAL MEASUREMENTS

1. Measure and record the mass of the model leg.
2. Attach leg to drop platform with rope.
3. Attach accelerometer and BNC cable to leg and wind cable around rope.
4. Tape cable around rope making sure there is enough slack to prevent damage to cable.
5. Set up test fixture and bumper specimen in drop zone.
6. Rope off drop zone with caution tape.
7. Set up high speed camera and data acquisition equipment at a safe distance away from the drop zone.
8. Perform practice leg drop to ensure correct operation and settings of high speed camera and data acquisition.
9. Position leg above drop zone.
10. Measure and record leg drop height.

DROP TEST

11. Set high speed camera to record data.
12. Ensure drop zone is clear.
13. Begin drop countdown and start data acquisition system.
14. Drop leg onto bumper specimen.
15. Trigger high speed camera.

DATA STORAGE & CLEAN UP

16. Save high speed camera footage and acceleration data to a portable hard drive.
17. Disconnect high speed camera and data acquisition equipment.
18. Clean up all equipment.